FABRICATION OF METALLIC GLASS $Fe_{81}B_{13.5}Si_{3.5}C_2$ RIBBONS AND STUDY OF ITS THERMAL STABILITY

A Thesis Submitted
in Partial Fulfilment of the Requirements
for the Degree of
MASTER OF TECHNOLOGY

by

PRATAP KUMAR ROY

to the
MATERIALS SCIENCE PROGRAM
INDIAN INSTITUTE OF TECHNOLOGY KANPUR
August 1986

MSP-1986-M-ROY-FAB

BAPI, MA ''!

জ্ঞানের ভোজ শেষ নাই,

আমার চেষ্টা বৃথা তাই।।

'হীরক রাজার দেশে'

সত্যজিৎ রায়

Source of Knowledge will Never be Dry

No Point Giving it a Useless Try

' Hirak Rajar Deshey '

Satyajit Ray

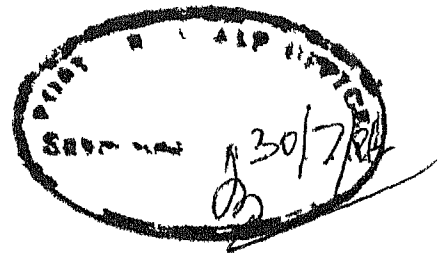

CERTIFICATE

Certified that this work on 'FABRICATION OF METALLIC GLASS $Fe_{81}B_{13.5}Si_{3.5}C_2$ RIBBONS AND STUDY OF ITS THERMAL STABILITY' has been carried out under our supervision and that it has not been submitted elsewhere for a degree

D C Agarwal
Assistant Professor
Material Science Program
I I T Kanpur

K.P Gupta
Professor
Material Science Program
I I T Kanpur

Date July 30, 1986

ACKNOWLEDGEMENT

I sincerely thank Dr K P Gupta not only for his individual and personal guidance but particularly for creating an aura of freedom and unmatched enthusiasm I am at a loss to understand how Dr D C Agarwal could maintain a close watch even from a faraway place like Cornel University U S A

I am grateful to all the staff of MSP and ACMS for the instant and close attention paid all through Special thanks are due to Mr R S Sharma for helping me in experimental set up I can never express my gratitude to Mr Satya Narayan Pradhan whose work spilled well beyond of his duties of producing an excellently typed thesis

I will always remember my friends, the intimate bonds grew out of both the dark as well as sunny days of my stay here in I I T Kanpur Particularly I remember the quarrels with Mr D Bandyopadhyay, the memory of which is becoming sweeter and sweeter with the passage of time

Finally the trees and the vast meadowland with their nonhuman inhabitants of I I T Kanpur will never erase out of my memory wherever the destiny takes me away I can never forget them

PRATAP ROY

LIST OF FIGURES

LIST OF TABLES

ABSTRACT

Fe-B-Si-C metallic glasses are both scientifically and technologically important However the research as well as the use are often handicapped by already processed material received from other sources without known previous thermal history or the very narrow ribbons prepared in the laboratory

In the present study, reasonably wide ribbons have been produced using an existing single roller melt spinning aparatus and the process has been standardized The range of different process parameters have been identified The time and temperature path difference between the state of molten metal and the final amorphous state seems to be important in achieving an amorphous state The jet turbulence of the molten metal, on the other hand affects the physical properties of the prepared ribbons

The prepared ribbons have been tested with X-ray and TEM to confirm their amorphous nature.

The prepared ribbons have been subjected to both isothermal and dynamic heat treatments They have been tested by both calorimetric and electrical resistance vs temperature experiments It has been found that the crystallization process is passing through a series of multistep,

overlapping reactions The melt spun ribbons have not been found to be crystallized even after annealing well beyond crystallization temperature for several minutes Contrary to general belief, structural relaxation has been found to enhance the crystallization temperature It also affects the crystallization process itself Relaxed samples show up either some old intermediate reactions already present but are camouflaged by structural disorder or are passing through new intermediate reactions It has also been found that even after a high annealing to 310oC for 25 minutes the relaxation of the as melt spun sample is negligible On the contrary a 60 minuite anneal at the same temperature almos relaxes the sample Moreover even a single thermal cycle through a temperature near but below crystallization start temperature relaxes the sample completely The samples, subjected to different heat treatments do not loose the ductility The structural relaxation helps in increasing the magnetization process as well as increass the Curie temperatur

Two and most probably a third fine, reversible chan similar to CSRO, have been found below crystallization temperature

LIST OF CONTENTS

PAGE

CHAPTER I

INTRODUCTION

To enquire the limits of non-equilibrium crystallization, Paul Duez and his co-workers first started the technology of metallic glass preparation in 1960 in a rudimentary way After this, it went into hybernation till 1973, when commercial production of metallic glasses started in pilot plants in U S A and Japan The advent of technology started the curiosity of both technologists and scientists and it reached skyhigh limits during the later part of '70s and early '80s, as is evident from the number of personnel involved in research and the number of conferences organised From a technologist's stand point, the presence of high hardness coupled with high tensile strength, remarkable resistance to corrosion makes this class of materials an important conter der for future use Particularly in case of magnetic metallic glasses, the easy and high magnetization, coupled with low magnetic loss, makes it and ideal and potential candidate in all the spheres where soft magnetic properties are useful Future use, among others, envisages the miniaturization of airborne transformers and lucrative space use. From scientific point of view, the field holds intellectual challanges to find out the nature of magnetization processes involved in amorphous systems, the process of work hardening, the nature

of structural and internal disorders and provides an opportunity to test whether all the laws developed for crystalline materials, particularly the age old concept of dislocation movement, hold good for amorphous systems too Or in other words, the study of amorphous state opens up the possibility of finding out the fundamental nature of these laws and if not, developed a more unified and fundamental concept

Even though the most common and favourite process of metallic glass formation, the single roller melt spinning process, seems to be a relatively simple one, the number of process parameters involved, the short time of fabrication, the achievement of severe quenching rate of more than 10^6oC/ minute, till now makes it extremely difficult to produce standard, continuous and wide metallic glass ribbons Hence the field still offers enough challenge to produce standardized glasses as well as enquire the effects of different process parameters The extreme thinness, of the order of 25 to 80 microns and the severe quenching rate produce in the amorphous metallic material inherent instability and throws up interesting effects in the properties For any practical use the nature and the limits of such instabilities and the ways to overcome them cannot be over emphasized These structural relaxation can produce important changes in the properties and behaviour of the material For example, all the literature involving the crystallization behaviour of metallic glasses, assumes a structurally relaxed state just prior to crystallization. It is important to investigate whether this is really

so and if not whether the structural relaxation affect the crystallization and to what extent During such structural relaxation, changes involving topological short range order (TSRO) and chemical short range order (CSRO) have been observed for many metallic glasses

In this work, first it has been tried to produce reasonably wide, continuous and uniform metallic glass ribbons of $Fe_{81}B_{13.5}Si_{3.5}C_2$ equivalent to Allied Chemical's Metglas 2605Sc Secondly crystallization as well as structural relaxation behaviour, the effect of latter on the former, have been studied with as melt spun metallic glasses with or without different types of heat treatment The instability and consequent structural relaxation of the metallic glass ribbons, have been studied using DSC and electrical resistance techniques Magnetic properties namely Curie temperature and magnetization have been studied using the Vibrating Sample Magnetometer And of course the amorphous nature has been confirmed by TEM and X-ray analysis

Chapter II deals with the literature survey involving metallic glass preparation, the crystallization behaviour and structural relaxation involving TSRO and CSRO Chapter III deals with the experimental conditions used Chapter IV gives the experimental observation and finally Chapter V discusses the results obtained.

CHAPTER II

LITERATURE SURVEY

II 1 Fabrication of Metallic Glass Ribbo

There are several ways to melt spin an alloy to produce amorphous metallic ribbons One of the most common methods employs a single roller chill block on which a jet of molten metal is made to impinge Generally the material is heated to or above the liquidous temperature in a quartz or ceramic crucible having a suitable orifice at its end The molten metal is forced through the orifice of the crucible on to a rotating chill block, generally made of copper or steel Under appropriate process conditions a glassy metallic ribbon is formed by the solidification of jet at the rotating substrate Fig 1 describes the essential process

The broad principles of glass formation appear to be as follows The fabrication technique should cool the glass forming melt at a rate faster than its'critical quenching rate' so that crystallization can be avoided It also should cool the melt to a final temperature which should be at least lower than its crystallization temperature or preferably below its glass transition temperature(T_g) The first principle ensures that an amorphous state is achived The second ensures that the glass is recoverable at room temperature Several attempts have been made to explain the modes

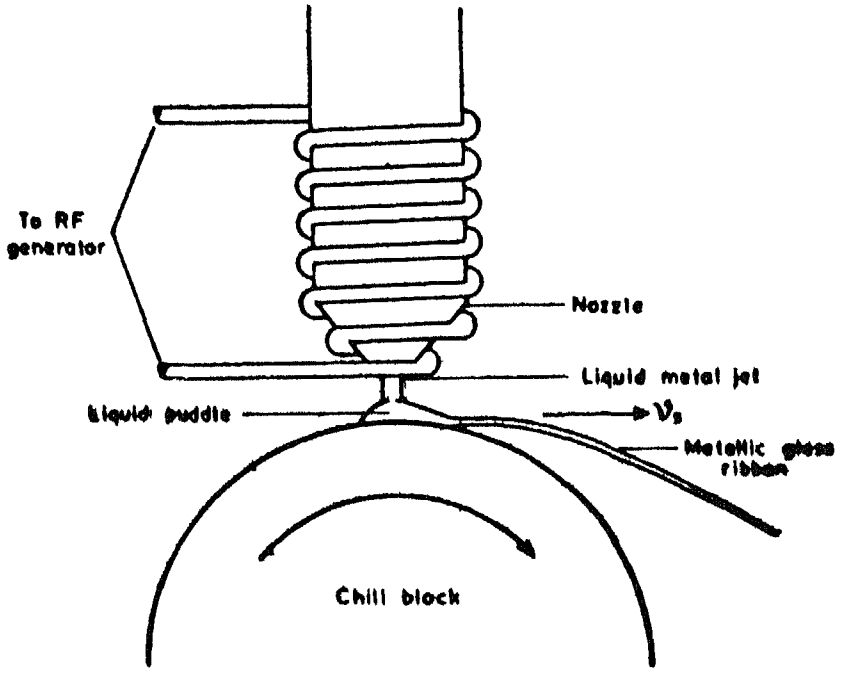

Figure 1 Schematic view of melt spinning apparatus

of ribbon formation and their correlation with the available experimental data [1] Kavesh [2] has described two possible modes of ribbon formation, namely, (i) transport dominated ribbon formation and (ii) energy equilibrium ribbon formation In transport dominated ribbon formation two limiting cases and a mixed case have been distinguished These are (a) thermal transport being the controlling factor (b) momentum transport being the controlling factor and(c) a coupled thermal and hydrodynamic regime controlling the ribbon formation If thermal transport is much faster than momentum transport, a solid boundary layer will form adjacent to the chill surface and propagate into the melt puddle to form the ribbon In this case the materials within the frozen layer will be in motion with the chill surface Outside the frozen layer a sharp velocity transition zone will exist Finally in the outer zone, there will be a slight momentum transpor If momentum transport from the chill sufface is much faster than thermal transport, a liquid boundary layer will be dragged out of the melt puddle by the moving substrate to solidify further downstream The velocity gradient will be continuous across the depth of the puddle

In energy equilibrium mode the ribbon is formed by the wetting of the substrate The dimensions of the molten puddle and therefore the ribbon dimensions, are determined by the equilibrium of kinetic energy, surface energy and viscous dissipition of the jet, puddle, chill surface

and the air boundary layer in motion with the chill surface

In the laboratory scale, the formation of glassy metal and the ribbon geometry depend mainly on the material parameters and process parameters In the material parameters, the selection of suitable alloy system is the most important criterion for metallic glass formation A single parameter which is shown to be useful in expressing the glass forming Fendency (GFI) of an alloy system is the reduced glass transition temperature(T_{gr} which is the ratio of the glass transition temperature T_g and melting point T_m Davis [3] has shown that the alloy which has a T_{gr} > O 45 can be cast to metallic glass successfully Pure metals with T_{gr} < O 25 can not be quenched to glassy state under the usually achieved cooling rates (10^4-10^8oC/ second) Davis [4 and 5] reported that at a cooling rate of more than 10^{10} oC/ second, partly glassy Ni foils can be produced only if Ni has a trace of oxygen in it Glass formation in the case of alloys appears to be favoured if the compositions are near eutectic compositions Glass forming binary alloys, mainly transition or noble metals, containing 15 to 30/ semimetals or alloys of inter-transition metals such as Nb-Ni and Cu-Zr have been studied extensively All the glass forming alloys seem to have two common features, a negative heat of mixing indicating a strong interaction between constituent atoms and relatively low melting temperature In case of binary alloys the critical quenching rate seems to be around 10^6oC/ second or higher Addition of a third of a fourth alloying

element, which exibits different crystalline symmetry, enhances to a great extent the ease of formation of glasses mainly by lowering the melting point (Table 1). For example Pd-Cu-Si, Pd-Ni-P, Pt-Ni-P alloys having a critical cooling rate of 10^2oC/ second [6] can be cast in glassy rod form of 1 to 3mm diameter Table 1 lists some of the glass forming alloys

In the process level, the important parameters which control the formation of glassy state seem to be the cooling rate, the decree of supercooling (i e , the initial temperature of molten jet and the final temperature of the substrate) and heterogenious nucleation rate. These factors in turn are governed by the volumetric flow rate of the melt through the nozzle, length of the nozzle, distence between chill surface and nozzle tip, surface velocity of the chill block, polish and cleanness of the chill surface [7-9] Libermann [7] has given an emperical relationship Q=Wts applicable for a low value of volumetric flow rate upto $4x10^3$mm/ second where W is the width of the ribbon (mm), t is the thickness of the ribbon (mm), s is the linear speed of rotating chill block (mm/second) and Q is the volumetric flow rate (mm^3/ second) At higher values of Q, upto $7x10^3$ mm^3/second, the relationship between ribbon dimension and casting conditions can be best explained by Kavesh's [2] energy equilibrium model Q is varied by varying orifice length Pavuna [1] and Libermann [7] have shown that the relationship of W and Q is linear This linearity has been

TABLE 1

Metallic glass forming systems

Group	Representative system	Typical composition (atom /)	Typical system	T_m (oC)	T_g (oC)	T_x (oC)	$r_{A,B}$
Early transition metal/ noble metal + metalloid	Pd-Si, Co-P, Fe-P-C, Ni-P-B, Au-Si,	15-25 metalloid	$Au_{81}Si_{19}$	1336	290	280	0 92
Early transition metal + late transition metal/ Cu	Zr-Cu, Y-Cu, Ti-Ni, Nb-Ni, Ta-Ni,	30-65 Cu 40-65 Ni 30-40 late transition metal	$Cu_{60}Zr_{40}$	1800	740	760	1 23
Early transition +Li, Mg group	(Ti Zr) Be	20-60 Be	Zr-Be	2050	-	-	0 73
Actinide +early transition metal	U-V, V-Cr	20-40 (early transition metal	-	-	-	-	-
Ternary systems	-	-	$Au_{78}Ge_{14}Si_8$	632	297	305	-
	-	-	$Pd_{77}Cu_6Si_{17}$	1009	636	675	-
	-	-	$Pt_{56}Ni_{24}P_{20}$	770	485	642	-
	-	-	$Fe_{80}P_{13}C_7$	1220	720	710	-

T_x = Crystalization temperature oC

$r_{A,B}$ = Ratio of the diameter of the bigger atom to that of the smaller atom

verified(Fig 2) by Agarwal and Chal achary [10] Pavuna [1] also noted that Q has to be kept constant in a given melt spinning run so that the ribbon edges do not become uneven

Fig 3 shows the effect of ejection pressure on the glass formation for the $Fe_{14}B_5Si_3C_1$ alloy system [11] The figure indicates that the square root of ejection pressure is directly proportional to ribbon thickness and ribbon surface finish and after a limiting value, which is dependent on nozzle slot breadth, the ribbon thickness is maximum and the pressure has no further effect on the formation of glass The ejection pressure is generally applied just after the required heating of the melt Agarwal and Chakachary [10] have found that with a circular orifice diameter greater than 1 mm the ejection of melt takes place before the pressure is applied

During practical experiment to produce metallic glass ribbons, the problem of oxidation during melt spinning in air is very important. As pointed out by Agarwal and Chakachary [10], the major factor which governs the oxidation of melt spun ribbon is the distance between the chill block and the nozzle They hold the view that the above mentioned distance at the upper bound is limited by the chance of melt oxidation and freezing during the flow of the molten metal from nozzle to substrate At the lower bound, the distance is limited by the chance of nozzle end hitting the

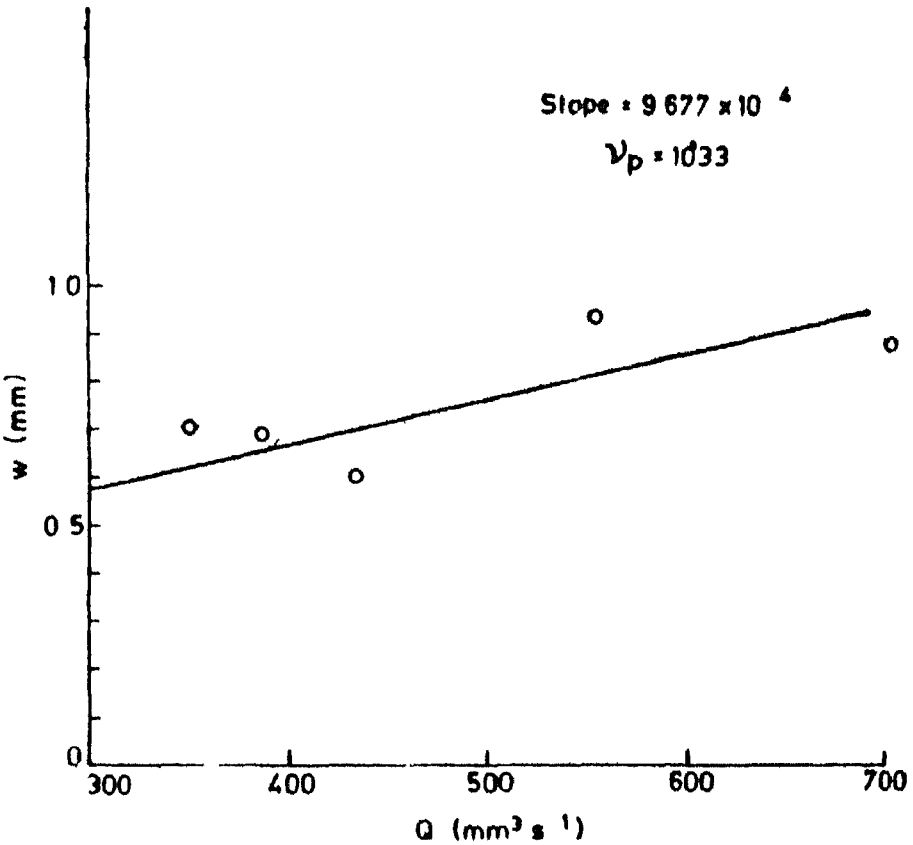

Figure 2 Effect of the volumetric flow rate on the width of the ribbon

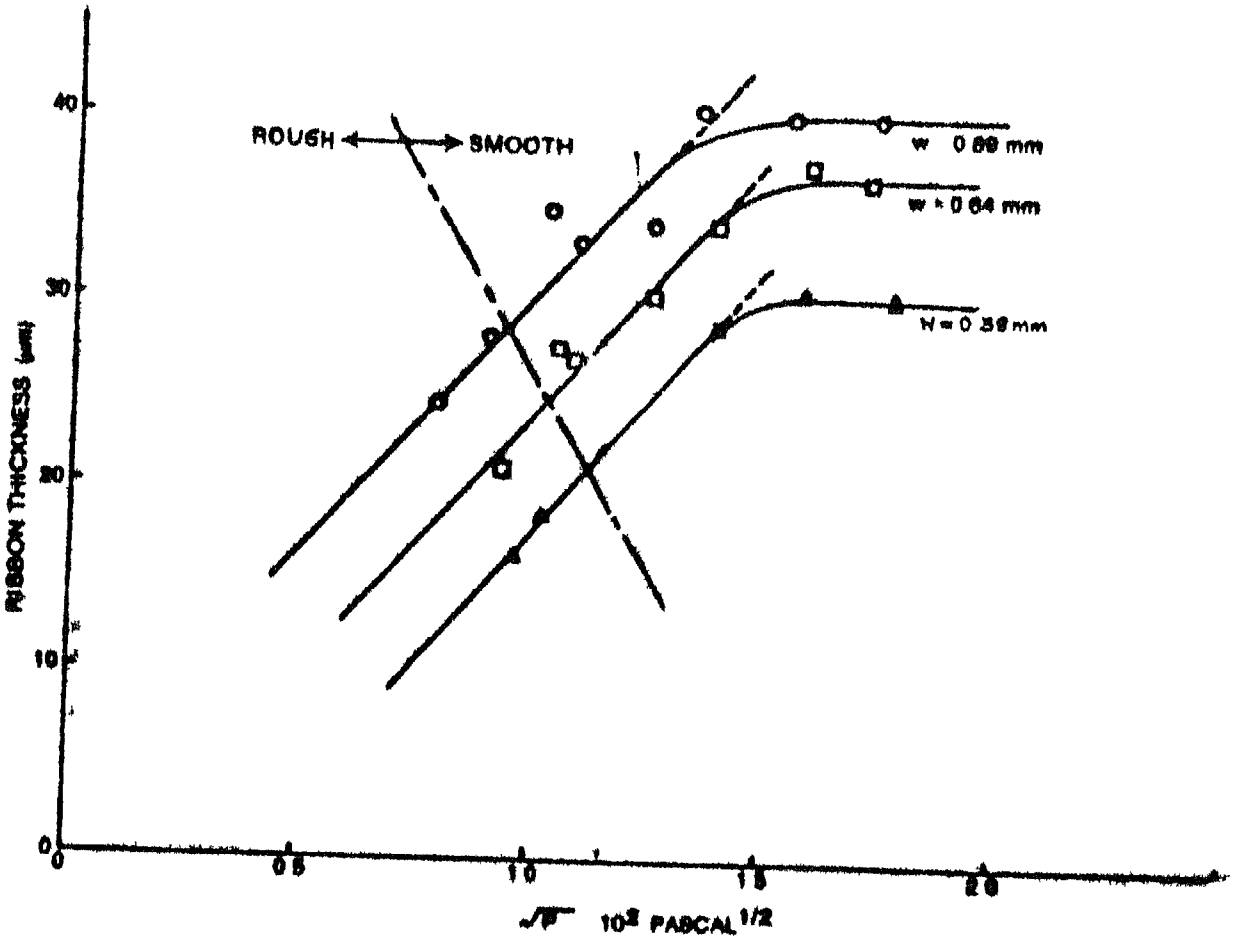

Fig 3 Ribbon thickness and ribbon surface finish as a function of the squared root of ejection pressure P, measured in three nozzle slot breadth w

substrate because of the vibrations present in the wheel On the basis of the above observation, Agarwal and Chakachary [10] have recommended an optimum distance of 1 mm between the nozzle tip and the rotating substrate For circular nozzles,Pavuna [1] has given a thumb rule for optimum distance to be equal to four times the diameter of the orifice of the nozzle

The jet impingement angle or more specifically the angle of the nozzle to the wheel surface is maintained at 90o Libermann [7] has shown that if the angle is changed, it only results in the reduction of the width of the ribbon without any other compensating advantage Pavuna [1] has shown that the chill surface has to be clean in order to avoid the possibilities of heterogeneous nucleation This observation of Pavuna has been supported by Agarwal and Chakachary [

II 2 Crystallisation

From a technological standpoint, thermal stability of metallic glasses is an important parameter for their use More recently the interesting properties of microcrystalline alloys have also focussed the attention on crystallization of amorphous metallic alloys There is also the fundamental interest in developing a uniform theory of amorphous and crystalline states All these have generated an interest in the study of amorphous to crystalline transformation of metallic glasses

Experimental evidence points to the fact that amorphous to crystalline transformation occurs through nucleation and growth and is essentially a diffusion controlled process Depending on the amount of chemical species present, the transition from amorphous to crystalline state can occur in any of the three modes 1) Polymorphic 2) Eutectic or Eutectoid and 3) Primary [12,13] The nature of the diffusion can be short range, intermediate or long range [13]

Polymorphic transition In the Fe-B system, for B concentration more than 16 atomic percent, the transformation of amorphous $Fe_{75}B_{25}$ to Fe_3B is a Polymorphic transformation (Fig 4c) [14] In these cases the parent amorphous phase $Fe_{75}B_{25}$ is transforming to Fe_3B without a marked change in concentration The product, in general, may be in a supersaturated stable or metastable state The

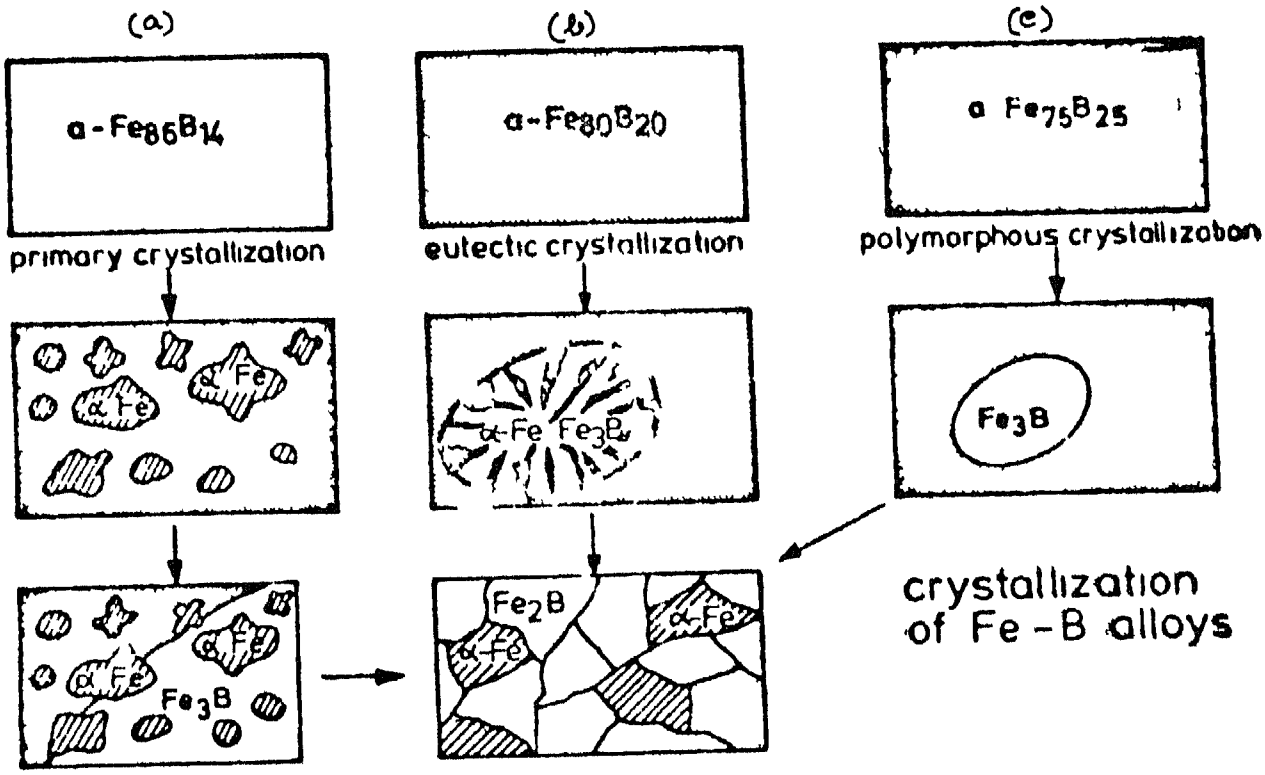

Figure 4 Schematic diagram of typical crystallization modes in Fe-B metallic glass alloys depending on chemical composition on the parent amorphous phase

diffusional atoms are jumping across the transformation front Hence, a short range diffusion is taking place In general the polymorphic type of transformation occurs in the concentration range of pure elements or stoichiometric compounds

Eutectic/ Eutectoid transformation In Fe-B system with B concentration 17-20 atomic percent, α-Fe and Fe_3B precipitate out simultaneously from amorphous matrix at 500oC [14] At higher temperatures, further breakdown of Fe_3B occurs In analogy to the transformation of crystalline material into two product phases simultaneously, the transformation of an amorphous phase $Fe_{80}B_{20}$ into two product phases α Fe and Fe_3B (Fig 4b) is called a Eutectoid or Eutectic type of transformation Here an intermediate range diffusion of atoms is taking place Hence, this process is slower than polymorphic transformation

) Primary transformation In Fe-B system, with B concentration less than 16 atomic percent, the crystallization behaviour can be explained by primary crystallization The amorphous $Fe_{86}B_{14}$ alloy initially precipitates α-Fe between 300oC to 450oC [14] (Fig 4a) At a higher temperature of 550oC, Fe_3B starts to crystallize from B enriched matrix At a still higher temperature, the Fe_3B crystals decompose into α-Fe and Fe_2B In general, in this type of transformation, the product crystalline phase is

substantially different from the parent amorphous phase

In the as produced amorphous metallic state, it is expected that the material is highly unstable and on heating it should go through some changes and finally crystallization should occur In considering the crystallization process, an ideal metastable state i e a state of complete structural relaxation is generally assumed to have been achieved before reaching the crystallization temperature Hence, at least, theoratically, the effect of quenching rate, state of stiess etc ,are not expected to influence crystallization behaviour When the amorphous materials are subjected to dynamic tests such as DTA,DSC and measurement of change in electrical resistance with change in temperature etc , the factors like state of stress, effect of quenching rate etc,, however are expected to influence crystallization The time elapsed before crystallization, which depends on the heating rate employed, may not be sufficient to take the specimen to an ideal metastable state before crystallization It has been observed that in majority of the cases, the investigators work with specimens obtained from sources like Allied Chemicals, U S A Depending on the manufacturing conditions such as quenching rate, superheating etc and storage time, the specimens of the same composition may show somewhat different crystallization characteristics The effect of the above mentioned parameters on the crystallization process as well as on the structure and stability of metallic glasses have

not been thoroughly investigated Higher quenching rate and higher superheat are expected to increase the level of thermal stress as well as chemical and structural disorders Hence, an acceleration in crystallization is to be expected Contary to this expectation, however, crystallization in $Fe_{40}Ni_{40}B_{20}$ glasses do not start from the ribbon surface which was in contact with the cold substrate [15] In this case, crystallization starts from the free surface which is less severely quenched than the surface in contact with rotating substrate This somewhat unexpected recrystallization behaviour obtained in $Fe_{40}Ni_{40}B_{20}$ metallic glass ribbon has been suggested to be due to the lack of critical size and number of quenched in nuclei This state of quenched in nuclei is important since these act as a trigger in the crystallization process

The crystallization of amorphous $Fe_{81}B_{13\ 5}Si_{3\ 5}C_2$ (Metglas 2605Sc) has been studied extensively [16 to 19] since it is an important material from engineering point of view. The Fig 5 illustrates the DSC data obtained by Swartz et al [16] on Metglas 2605Sc The heating rate used in this experiment is 10oC/ minute The dip in the DSC trace near 377oC has been interpreted to be due to Curie temperature The two distinct exothermic peaks, at 497oC and 532oC indicate at least a two stage crystallization in this material The X-ray diffraction results of Swartz et al [16] are shown in Fig 6 The X-ray patterns are obtained with several

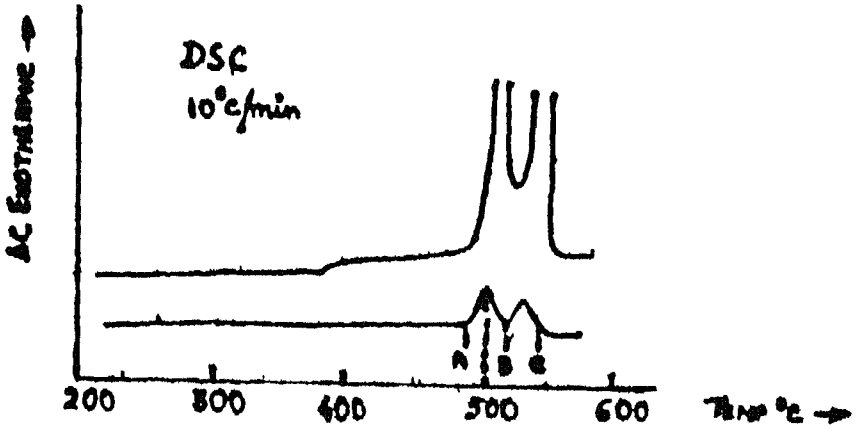

Figure 5 DSC recording of as received Metglas 2605 Sc (The upper trace is a 10 fold expansion of lower one)

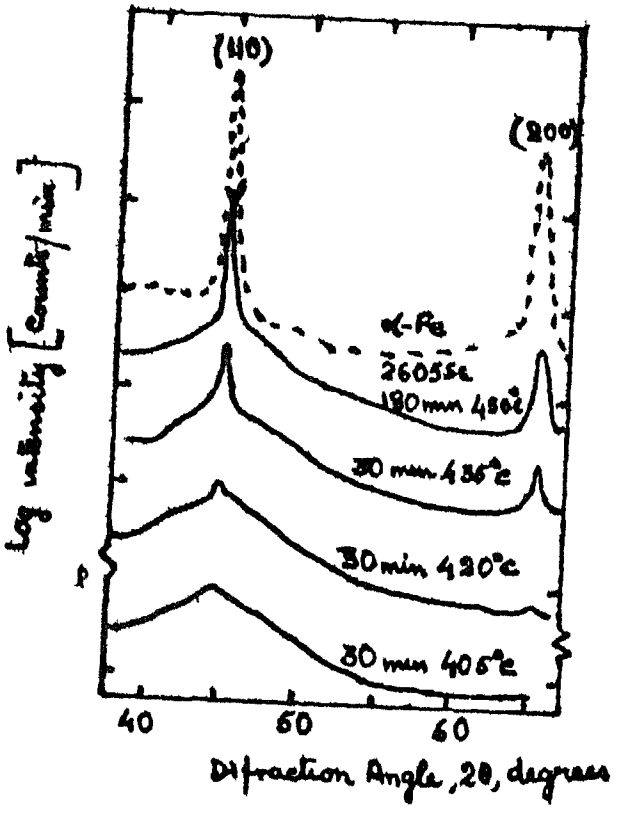

Figure 6 X- ray diffraction spectra of isothermally annealed samples of 2605 Sc along with an α-Fe pattern for comparison

Metglas 2605Sc specimens annealed for 30 minutes at different temperatures Fig 6 also indicates an X-ray diffraction pattern of pure α Fe The amorphous state of the as obtained material is characterized by the appearence of a broad intensity maximum between 40o to 50o diffraction angles (2θ) The results indicate that on 30 minute annealing α Fe peaks begin to appear and even after 3 hours annealing at 450oC, the broad peak due to amorphous state does not completely vanish However, after 7 hours of annealing at 450oC, the diffraction pattern show complete crystallization with the appearance of only α Fe and Fe_3B diffraction lines On the basis of DSC and XRD data, alongwith TEM and coercivity data Swartz et al [16] proposed that α Fe is the first phase to crystallize , Then Fe_3B nucleates heterogeneously and consumes the remaining amorphous matrix Saegusa and Moris [17,18] studied Metglas 2605Sc, using Mossbauer technique after isochronally annealing the specimens from room temperature to 487oC (20 minutes to reach 487oC from room temperature) and upto 722oC (50 minutes to reach 722oC) Their results can be summerized as follows The Curie temperature is reported to be 397oC (397± 2oC) At 417oC, the first crystallization product, Fe and 4 atomic percent Si precipitates out Between 432oC and 437oC, a quasistable amorphous phase, with composition $Fe_{75\ 2}B_{18\ 2}Si_{3\ 2}C_{2\ 4}$ has been reported At 442oC, the second crystallization of Fe_2B starts and the amorphous

Metglas 2605Sc specimens annealed for 30 minutes at different temperatures Fig 6 also indicates an X-ray diffraction pattern of pure α Fe The amorphous state of the as obtained material is characterized by the appearence of a broad intensity maximum between 40o to 50o diffraction angles (2θ) The results indicate that on 30 minute annealing α Fe peaks begin to appear and even after 3 hours annealing at 450oC, the broad peal due to amorphous state does not completely vanish However, after 7 hours of annealing at 450oC, the diffraction pattern show complete crystallization with the appearance of only α Fe and Fe_3B diffraction lines On the basis of DSC and XRD data, alongwith TEM and coercivity data Swartz et al [16] proposed that α Fe is the first phase to crystallize , Then Fe_3B nucleates heterogeneously and consumes the remaining amorphous matrix Saegusa and Moris [17,18] studied Metglas 2605Sc, using Mossbauer technique after isochronally annealing the specimens from room temperature to 487oC (20 minutes to reach 487oC from room temperature) and upto 722oC (50 minutes to reach 722oC) Their results can be summerized as follows The Curie temperature is reported to be 397oC (397± 2oC) At 417oC, the first crystallization product, Fe and 4 atomic percent Si precipitates out Between 432oC and 437oC, a quasistable amorphous phase, with composition $Fe_{75\ 2}B_{18\ 2}Si_{3\ 2}C_{2\ 4}$ has been reported At 442oC, the second crystallization of Fe_2B starts and the amorphous

matrix, within the temperature range of 442oC to 457oC, assumes another quasistable state The composition of this quasistable state is somewhat uncertain but it has been suggested to be $Fe_{76.0}B_{17.3}Si_{3.0}C_{3.7}$ In the event of complete precipitation of C as Fe_3C, the composition of the quasistable state may also be $Fe_{16}B_{20.3}Si_{3.8}$ The amount of Fe_3C however, is too small to be detected Above 457oC, the crystallization continues till it is completed at 507oC Above 527oC, an ordering transformation in the crystallized Fe + 4 atomic percent Si occurs The final crystallized product have been suggested to be Fe + 7 atomic percent Si, Fe_2B and Fe_3C, the amount of Fe_3C being too small Bhanu Prasad and Bhatnagar [19] have studied the crystallization behaviour of Metglas 2605Sc, employing DTA, electrical resistivity with change in temperature and Mossbauer studies DTA results(Fig 7)show that crystallization occurs at around 452oC, in agreement with what has been observed by Swartz et al (Fig 5) But unlike Swartz et al Bhanu Prasad et al find that crystallization process give rise to three thermal effects between 452oC to 627oC The first two peaks at 487oC and 507oC are the most prominent ones and a third peak is at 577oC The first two peaks appear at slightly lower temperatures than what has been found by Swartz et al [16 Fig 8 shows the dependence of electrical resistivity relative to ρ_{20C} Initially electrical resistivity increases linearly with temperature At 452oC, the temperature around which

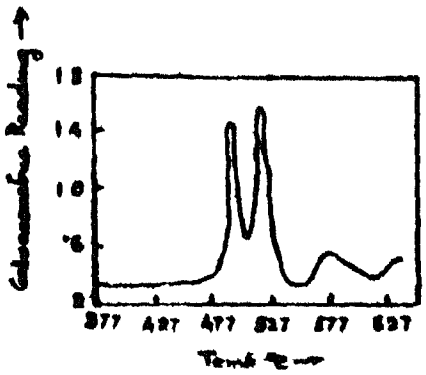

Figure 7 DTA of Metglas 2605Sc over temperature range of 377oC to 627oC

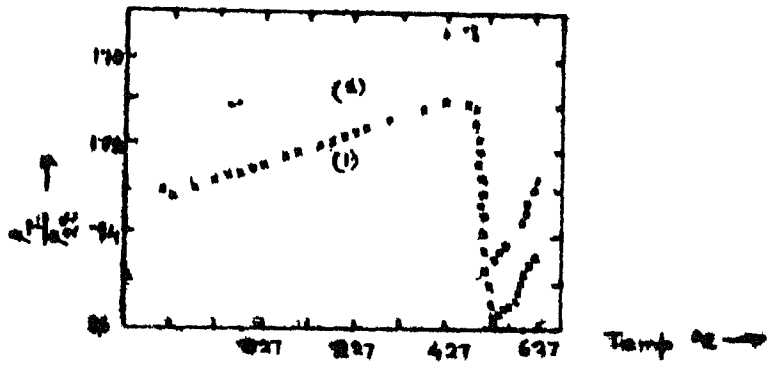

Figure 8 Resistivity ratio (T)/ (2) vs temperature(oC) of Metglas 2605Sc
(Curve (b) represents the reproducibility of curve (a) when repeated with a fresh sample).

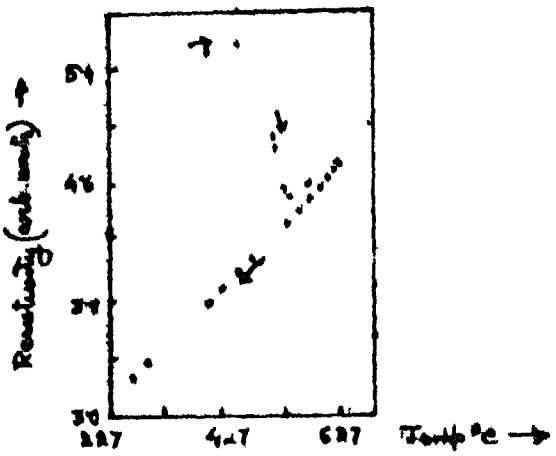

Figure 9 Electrical resistivity as a function of temperature for Metglas2605Sc between 227oC to627oC.

crystallization begins, a rapid change of slope occurs and from about 477oC, relative resistivity decreases very rapidly with increase in temperature At around 535oC, the temperature at which the second peak in DTA occurs, the relative resistivity again begins to increase A further change in slope of relative resistivity vs temperature occurs at ~ 552oC which corresponds to the temperature at which the third DTA peak begings After crystallization, when the specimen is cooled, ρ(T) follows a different path as shown in Fig 9 which is typical of crystallized samples Through Mossbauer studies and XRD work Bhanu Prasad et al have tried to interpret the observed thermal effects and electrical resistivity changes in terms of formation of specific products during crystallization process The thermal effect in the temperature range of 452 to 507oC has been attributed to the precipitation of pure α-Fe phase till a compositionally stable amorphous phase is achieved (The α phase, in the terminology of Sageusa and Moris [17] as well as Bhanu Prasad et al [19] means almost pure α Fe [20]. The second peak in DTA trace, approximately between 507o and 537oC is attributed to crystallization of the compositionally stable amorphous phase It is observed that the two DTA peaks almost overlap each other This may be interpreted in the following way As soon as pure α-Fe is precipitated the remaining amorphous phase starts crystallizing which is completed at 537oC The third peak at 577oC is possibly due to the precipitation of pure α-Fe or a new

Fe_{100-X} Si_X phase The final crystallization products are given to be α Fe, Fe_2B and a magnetic $Fe_{23}(CB)_6$ or an alloy of $Fe_{100-X}Si_X$ alongwith a small amount of Fe_3C. The Curie temperature for Metglas 2605Sc has been given to be 425oC (±1) which is comparatively higher than that determined by Swartz et al [17]

II.3 Structural Relaxation

A very high quenching rate, generally of the order of 10^4oC per second or more is employed in preparing metallic glasses This high quenching rate enables the alloy to bypass crystallization and attain an amorphous state During quenching, the atoms have insufficient time to relieve the high temperature atomic configurations As a result, the as quenched alloy remains in a highly metastable state When this highly metastable amorphous alloy is heat treated, the quenched in structure will tend to relax to a more stable state Several concepts to describe the features of atomic process involved in structural relaxation have been proposed [21-25]

The concept of excess free volume is a very well known and common concept to describe structural relaxation in polymorphic glasses [21-23] The free volume in glassy state is analogous to the concept of vacancy in crystalline state The equilibrium free volume present in glassy state is directly proportional to temperature and is related to viscosity As the liquid is cooled, the free volume is

decreased with an increase in viscosity However the decrease in free volume requires time as the 'excess free volume' somehow has to reach the surface [21-22] Hence the rate of change of viscosity, which is dependent on diffusivity, determines the rate of annealing out of the excess free volume If the temperature is dropped quickly to or below glass transition temperature (T_g), a high viscosity, usually 10^3 poise at T_g, is reached Because of the high viscosity and insufficient time, all the free volume can not reach the surface As a result, excess free volume will remain trapped in the structure During structural relaxation, the excess free volume is expected to anneal out

Egami [24], however has disputed the above concept of structural relaxation of metallic glasses through 'annealing out of excess free volume' process proposed by Turnbull and Cohen [25] In a study of $Fe_{40}Ni_{40}P_{14}B_6$ glass, Egami has shown that well below T_g, a rather extensive atomic rearrangement, involving collective movement of a large number of atoms, takes place Inspite of this large rearrangement of atoms, the corresponding change in volume is very small [24] On the basis of the above consideration, Egami has introduced the concept of structural defects, more or less analogous to crystalline metals, to explain structural relaxation In this concept it has been assumed that below T_g, the excess free volume captured in the glassy system collapses leaving internal strains around it. The centre

of these strains is considered equivalent to defects in crystalline materials For structural relaxation, the mechanism proposed assumes that the defects go on transforming and redistributing themselves to more stable low energy configurations, probably by splitting up into smaller and more stable defects Ultimately they become a part of the stable amorphous structure This change is an irreversible and exothermic change

Using energy dispersive X-ray diffraction (EDXD) analysis of $Fe_{40}Ni_{40}P_{14}B_6$ glasses, Egami [24] has shown that the structural relaxation involves an extensive change in short range order of basic structural units which are considered to remain unaffected themselves except for some slight distortions The change in short range order thus involves only change in relative configuration of these units with respect to each other It is not dependent on the chemical identities of the atoms in each structural unit Hence this type of short range order has been called topological short range order (TSRO)] Available information [24-29] suggests that the relaxation due to TSRO is slow and occurs over a wide range of temperature TSRO results in the reduction of creep and stress relaxation rates [26-27], decrease in internal friction [28] as well as densification of the alloy [29]

In amorphous metallic alloys, another kind of change in short range order with change in temperature is

observed This is due to a change in short range correlation of different chemical species In contrast to the irreversible, relatively slow relaxation characteristics of TSRO, the chemical short range order (CSRO) is found to be reversible, and relatively fast It usually occurs within a relatively narrow temperature range [30,31] However, the existance of CSRO, has not been proved directly since the conventional X-ray diffraction techniques are rather difficult to use for this purpose [24] The evidence of the presence of CSRO is through indirect means such as property changes observed during magnetic transition, electrical resistivity, and elastic modulus measurements For example, it has been found that if $Fe_{27}Ni_{53}P_{14}B_6$ is cyclically annealed for 60 minutes at 250oC and 30 minutes at 300oC, a change in Curie temperature (T_c) is observed [32] The change in T_c is totally reversible for eight annealing cycles (Fig 10) [32]. Electrical resistance measurements as a function of temperature has been done for a large number of systems These are classified in three groups, namely metal-metal system, multimetal-metalloid system and monometal-metalloid system The electrical resistance change with temperature is shown in Fig 11 [33] for a large number of metal-metal systems Similarly the electrical resistance change with temperature is shown for a large number of multimetal-metalloid systems, in Fig 12 [33] In all the systems studied (Figs 11 and 12) a variation of relative resistance with

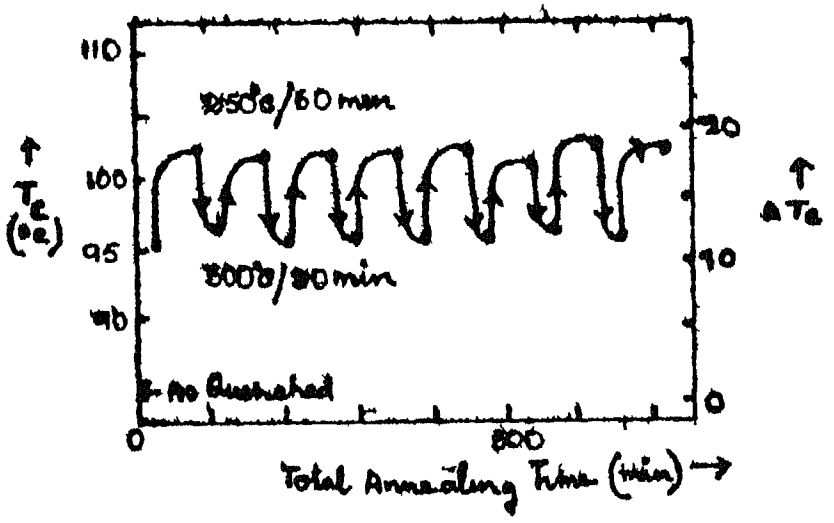

Figure 10 Changes in Curie temperature of $Fe_{27}Ni_{53}P_{14}B_6$ during cyclic annealing at 300°C for 30 minutes and 250°C for 120 minutes over eight cycle indicating that the changes are totally reversible
(Curves connecting data points are guides for the eye and does not represent the true kinetics of change)

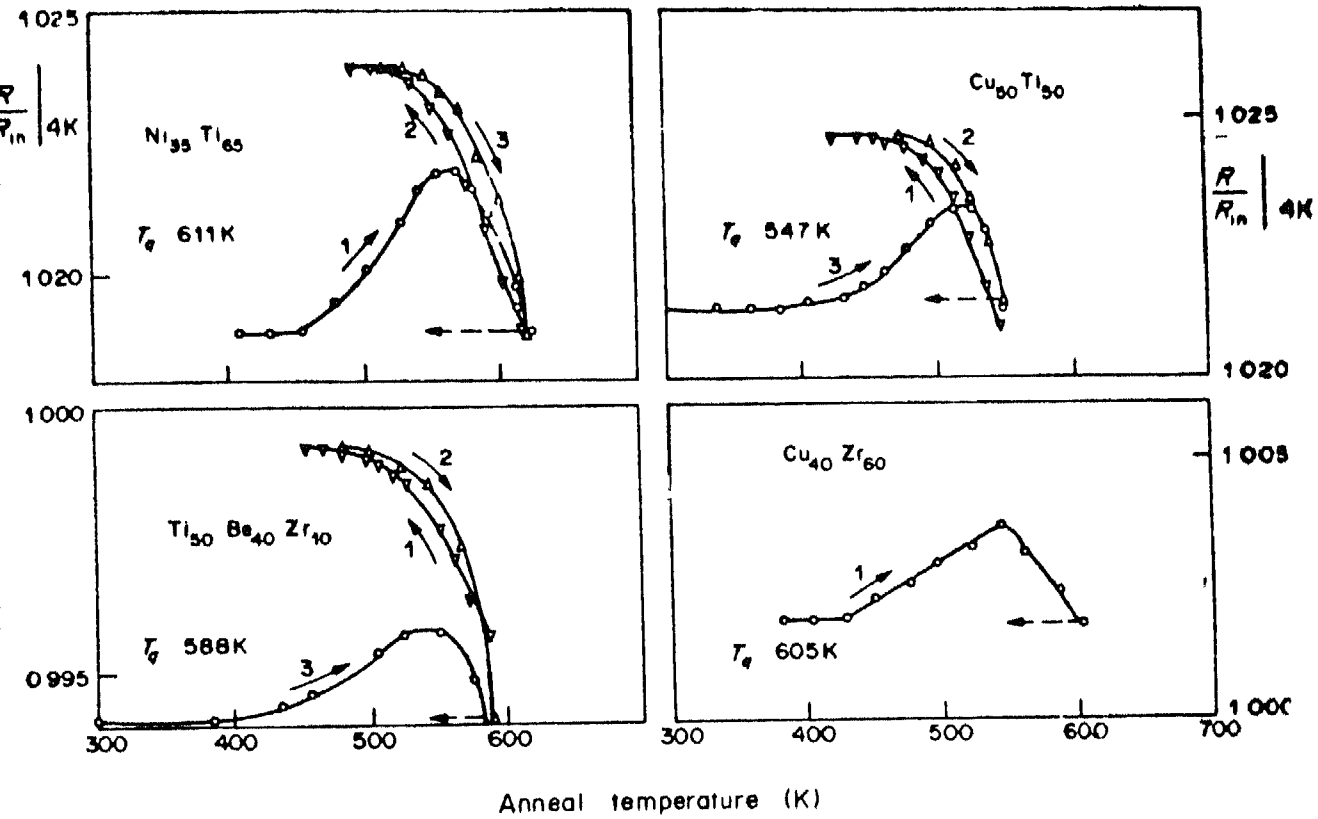

Fig. 11 Evolution of the electrical resistance during isochronal up and down temperature cycles or heat up anneals after a quench from the maximum temperature preceded by a ten minute anneal at this temperature (All curves were normalised with respect to the initial resistance in the as received condition The duration of every anneal is 10 min The symbols ∇ and Δ are for anneals conducted at decreasing and increasing temperatures respectively in this figure)

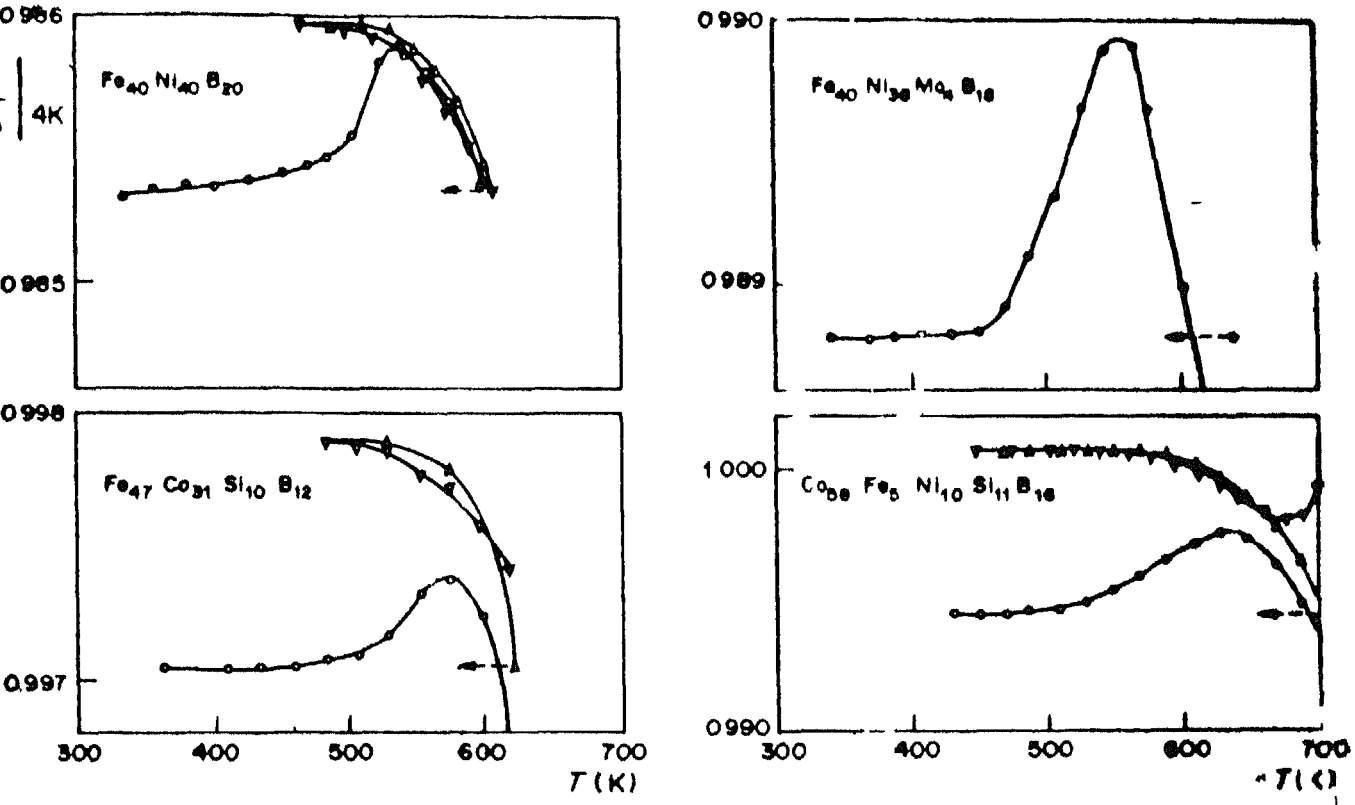

Fig 12 Evolution of the 4 K resistance of some metal–metalloid glasses during 10 min isochronal anneals conducted after a prestabilization (10 or 30 min) treatment at the maximum temperature indicated on the figure

temperature on isochronal annealing of the alloys is observed Clearly a reversible effect is found for both metal-metal and multimetal- metalloid systems On the basis of above experiments, Balanjat et al [33] have surmised the following In case of systems which show reversible effect, the common factor is the presence of two metal species regardless of whether a metalloid is present or not The Faber-Ziemann theory [34] also postulates a change in electrical resistivity with CSRO in amorphous alloys On the basis of above observations,the presence of a CSRO in amorphous metallic alloys have been accepted Egami [35] proposed a two process model to account for CSRO-TSRO change in amorphous alloys Chen [36] proposed a one process model to account for both reversible and irreversible change in amorphous alloys

In the case of monometal-metalloid alloys, there is no basis for a common factor to explain the reversible changes For example, $Fe_{80}B_{20}$ does not show a reversible effect whereas $Fe_{81.5}B_{14.5}Si_4$ shows it [33] Similarly, $Pd_{82}Si_{18}$ shows a reversible effect [37] whereas $Pd_{80}Si_{20}$ does not [33]. However, one thing is common for the alloys which show a reversible effect in monometal-metalloid systems The reversible effect is found to be very small in magnitude [33]. Another important conclusion is that all the monometal - metalloid systems showing reversible effect deviate from the 80 atomic percent metal-20 atomic percent metalloid compositions For example, $Fe_{80}B_{20}$ and $Pd_{20}Si_{20}$ do not show a

reversible effect whereas $Pd_{82}Si_{18}$ shows it Balanjat et al [33] have postulated that in metallic glasses, the available interstitial sites are around O 2 atomic fraction The metalloid atoms occupy the interstitial position Hence not much atomic rearrangement will be possible at 20 atomic percent metalloid composition All the interstitial sites will be occupied Some authors [33] have also suggested that in certain system the reversible change may be insensitive to electrical resistivity Hence they have stressed the need for further experimentation with calorimetric and other tests In general CSRO causes a change in Curie temperature, seggregation [38] and change in field induced magnetic anisotropy [39] However some of these property changes may be affected by TSRO too and vice versa [24,32,35,40]

TSRO and CSRO may be superimposed on each other. This makes their detection difficult Fig 13 and Fig 14 show the electrical resistance change for two systems when subjected to several heating and cooling cycles The reversible effects are shown by a bump in the resistivity curve of Fig 13 The vertical shift of the curves also shows that TSRO is changing for each cycle If the equilibrium state of CSRO was highly sensitive to TSRO, then it would not have been possible to realize a reversible process

When amorphous alloys are subjected to the effect of time and temperature, another kind of internal

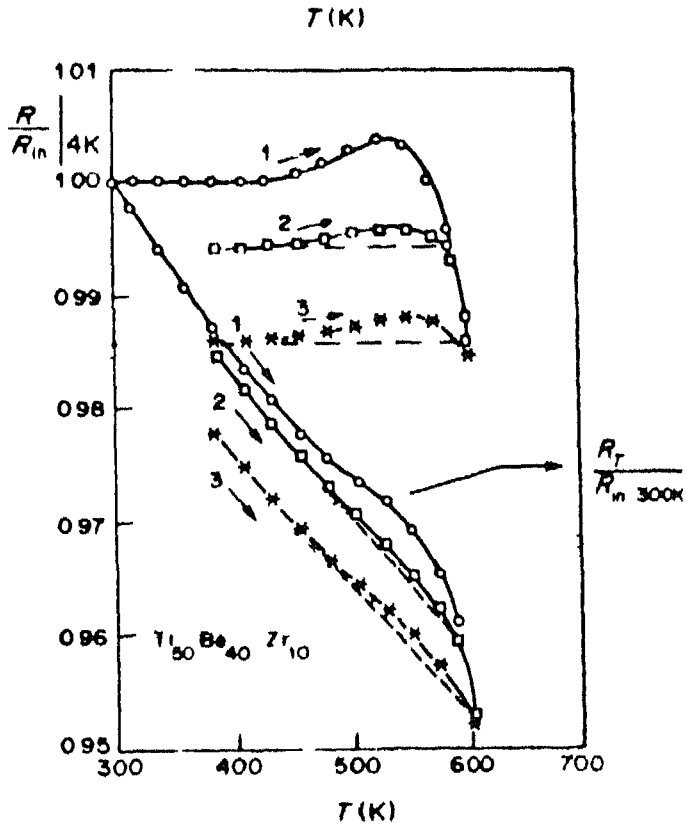

Figure 10 Temperature dependence of the electrical resistance of $Cu_{50}Ti_{50}$ and $Ti_{50}Be_{40}Zr_{10}$ measured at the end of every isochronal anneal during the first heat up sequence of specimens originally in the as received condition (The short range (reversible) ordering manifests itself by a bump in the $R(T)$ curves)

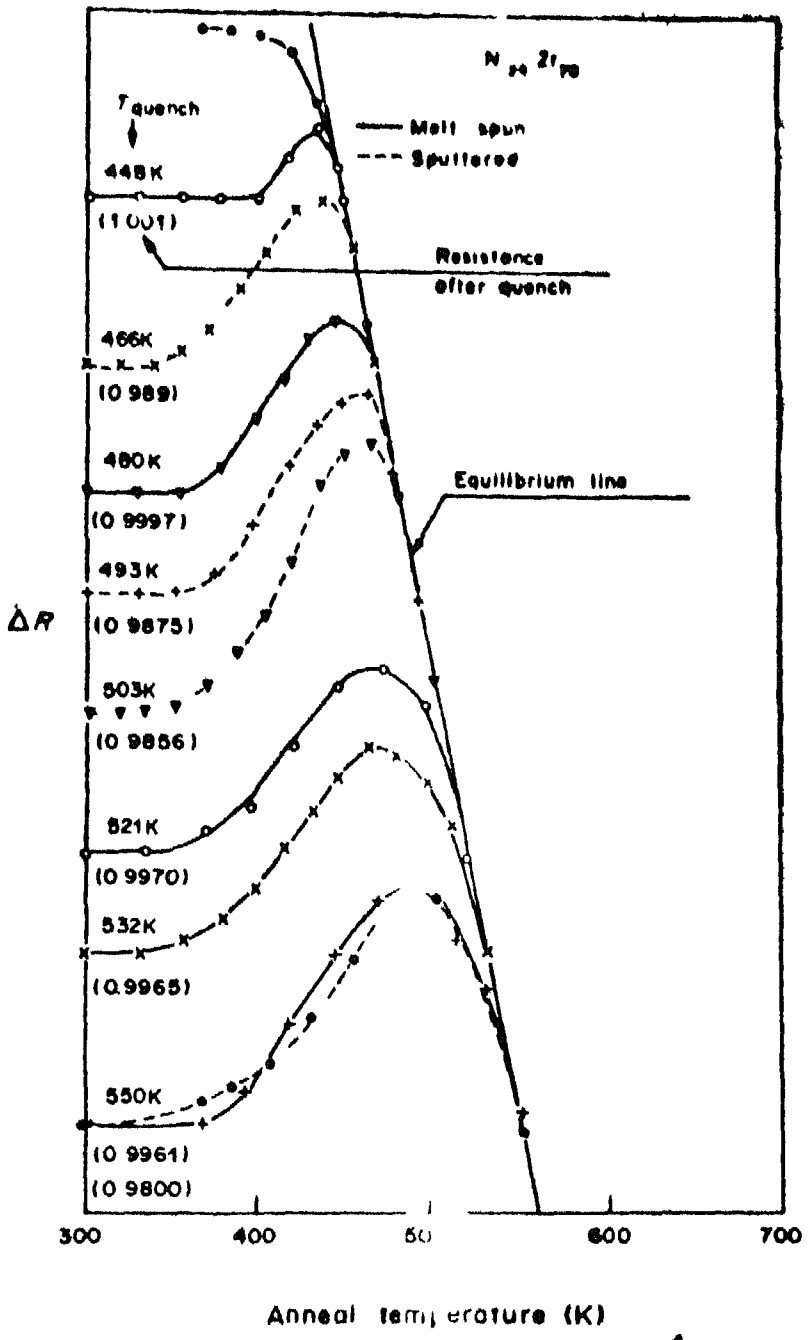

Fig. 14 Reversible resistance effects in $Ni_{24}Zr_{76}$ (There is obviously an irreversible decrease in resistance super imposed on the reversible effect as indicated by the resistance values reported on the figure In the figure the curves for the various annealing cycles have been shifted upwards to compensate for the irreversible resistance decrease)

stress relevıng may take place If the as quenched amorphous alloy ıs subjected to mechanıcal workıng, internal stresses are stored ın the alloy The resıdual stresses at low temperature annealıng get relıved by the dıffusıon of structural defects [32]. These resıdual stress effects result ın change ın stress ınduced magnetıc anısotropy and stress relaxatıon [41] Sometımes they affect the magnetıc propertıes too Lubrosky et al [42] have shown a remarkable change ın remanance, Curıc temperature and decrease ın saturatıon fıeld by relıevıng stresses at a temperature slıghtly below T_g

A harmful effect of heat treatment ıs that ın some cases [43] the alloy bocomes brıttle Davıs group [44] has shown thal the embrıttlement occurs ın those cases where the fınal product after crystallızatıon ıs B C C or H C P When the fınal crystallızed product ıs FCC, the embrıttlement does not occur The relatıonshıp between the fınal crystallızed phase and the relaxed amorphous phase ıs not well understood at present But the ınvestıgatıon shows that there probably ıs a relatıon

Structural relaxatıon behavıour of Metglas 2605Sc has been studıed by Mossbauerspectroscopy by Sageusa and Morıs [18] Metglas 2605Sc was ısochronically annealed at varıous temperatures usıng dıfferent heatıng rates The Mossbauerspectra were recorded On these basıs, the authors suggested that structural relaxatıon ın Metglas 2605Sc to

take place in three different stages Annealing before crystallization of the as melt spun sample appears to produce no substantial change upto 127oC In the temperature range of 127oC and 347oC an increase in short range ordering has been observed This may be topological or chemical In interpreting magnetic properties of $Fe_{27}Ni_{53}P_{14}B_6$ glass, Egami [32] has proposed a pairing of Fe-Fe atoms Sageusa and Moris [18] concluded that for a similar pairing to opeiate in 2605Sc, an increase in the average Fe^{57} hyperfine field is expected in Mossbauerstudy They observed the required increase in the Metglas 2605Sc This led to the conclusion that enhancement of short range Fe-Fe pair ordering is taking place in the temperature range of 127oC to 347oC. However they are not sure of this observation In the r@gion of 347oC to 417oC, a different kind of ordering has been observed The crystallization studies of Metglas 2605Sc suggested [18] that thc first crystalline product precipitating out at 417oC is α phase containing 4 atomic percent Si This observation led them to conclude that in the temperature range between 347oC and 417oC atomic rearrangement may be producing atomic clusters which later help the formation of nuclei1 containing Fe- with 4 atomic persent Si A two step structural relaxation doesnot appear to bc peculiar to Metglas 2605Sc $Fe_{40}Ni_{40}P_{14}B_6$ glass also appears to show two stage relaxation process [45]

CHAPTER III

EXPERIMENTAL PROCEDURE

III.1 Fabrication of Metallic Glass Ribbon

Fabrication of metallic glass ribbon involves the following steps

i) Preparation of nozzle

ii) Preparation of the alloy and

iii) Melt spinning

Each of these steps are discussed in detail in the following section

i) Preparation of the nozzle For preparing nozzles to inject molten metal onto a rotating substrate quartz tubes are utilized The induction coil of the melt spinning set up was suitable for holding only 10 mm internal diameter and 12 mm outer diameter quartz tubes One end of the quartz tubes is to be sealed and formed into a suitably shaped nozzle For this a graphite die is needed into which the sealed end of the quartz tube can be blown to form the nozzle shape An orifice is then cut at the closed end of the quartz tube to produce the nozzle suitable for melt spinning

The die is hard fabricated using a graphite block The one end open die cavity is shaped using

jewellers file and the die cavity surface is polished Different dies are prepared to give differ nt nozzles as given in the results One end of a 12 mm O D quartz tube is sealed in oxyhydrogen flame The closed end of the quartz tube is then heated to its softening temperature, pressed vertically in the die cavity and Argon gas pressure is applied at its open end so that the softened quartz glass fill the die cavity providing uniform wall thickness. For proper filling of the die cavity the pressure of Argon gas used is O 3 Kg/cm^2. The tip of the closed end of the nozzle where orifice is to be made is thinned slowly by rubbing it against belt surfacer and 4/O emery paper, taking care that the nozzle does not break due to vibration The flatte i- ning of the nozzle tip as well as its thinning is continued till a hole is about to develope. The nozzle is then mounted on the bed of a circular diamond saw cutting m/c (Microslice 2, Metals Research Ltd , Cambridge, U K) The line joining the two opposite walls of the quartz tube is kept parallal to the cutting surface With few rotation of the cutting wheel a rectangular orificc is made. The sharp edges ofthe nozzle are polished with a 4/O emery paper Then the nozzle are finally stressrelivevd by annealing This procedure produce serration free orifice The alternate procedure of orifice making, namely,first cutting the orifice followed by thinning the nozzle by emery polishing usually produce undesirable serrations at the orifice The nozzles produced

are of approximately 6 mm in orifice length

ii) Preparation of the alloy Preparation of $Fe_{81}B_{13.5}Si_{3.5}C_2$ alloy is done in two steps a) First a master alloy of Fe and C is prepared by induction melting and b) Then the Fe-B-Si-C alloy is prepared by arc melting Fe,Fe-C alloy, B and Si The materials used for alloy preparation are 99 999/ pure Fe 99/ B, 99 9/ Si (all from Alpha Products USA) and C powder obtained from graphite rod trimmings

a) Preparation of Fe-C alloy An alloy to contain ultimately 2 at/ C is prepared by induction melting of weighed quantities (50 gm or 100 gm) of Fe and baked graphite powder taken in a recrystallized alumina crucible Weighed quantities of Fe and C are induction melted in Argon atmosphere using a graphite crucible as a suscepter and is homogenized just below the melting point of the alloy for 30 minutes The prepared Fe-C alloy is cut into pieces and is inspected under an optical microscope at a magnification of 500X It ensures that there is no undissolved C present in the alloy The alloy is cleaned by polishing with emery paper and cut in small pieces

b) Preparation of Fe-B-Si-C alloy Appropriate amounts of pure B, Si and Fe-C alloy are weighed to produce about 20 gms of $Fe_{81}B_{13.5}Si_{3.5}C_2$ alloy Each batch of alloy is melted thrice in an arc furnace in Argon atmosphere to ensure proper homogenization The pellets from arc melting

are polished clean and broken by a pneumatic hammer. 10 to 15 gms of the above alloy is cleaned by using a mild solution of 1 0 part by volume of hydrochloric acid and 2 parts by volume of water The cleaned alloy pieces are then taken in an one end sealed quartz tube of 10 mm O D to premelt the alloy pieces to form a single cylindrical specimen of 8 mm O D This is done to have maximum amount of material for melt spinning using the existing apparatus and to prevent possibility of cracking of the quartz nozzle The quartz tube along with the charge is then successively evacuated and flushed with high purity Argon (IOL grade Iolar -2) three times to ensure complete removal of oxygen from quartz tube The alloy is then melted in the same induction heater used for final melt spinning by keeping the variac control of the generator at 68 divisions The melting and the solidification is done thrice to ensure complete homogenization The power input corresponding to the melting becomes fixed in second and third melting The quartz tube is then broken to remove the cylindrical alloy rod of about 8 mm O D The alloy rod is cleaned successively with hydrochloric acid, distilled water and methanol just before using for melt spinning.

iii) Melt spinning The experimental set up for melt spinning is schematically shown in Fig 15 A rolled copper disc of 10 cm diameter and a rim width of 2 5 cm is mounted on a 'Wolf' lathe grinder assembly it serve the

Figure 15 Experimental Meltspinning set up

purpose of the rotating cold substrate The lathe grinder is mounted on a X-Y control table for easy and accurate placement of the substrate below the nozzle The speed of the copper disc can be varied by using an autotransformer and adjusting the AC input voltage The motor speed is calibrated using a tachometer against the applied voltage Before each run the copper disc is cleaned by 4/0 emery paper to give it a matte finish The connection at the other end of the silica tube is so that it can be connected either to a rotary vacuum pump (Precivac Engineering Co , Calcutta) or to a high purity Argon gas cylinder connected with a gas purifying train (Fig 15) It should be mentioned that the vacuum pump is used only for alloy preparation described before and not during actual melt spinning A 3KW, 450KHz R_f generator (Pal Industries, Ghaziabad) is connected with a custom made transformer to provide a high current at low voltage output The induction coil is locally made The coil characteristics are as follows

Diameters of tube = 2 mm

Coil diameter= 15mm

Coil height=20 mm

Number of turns/length = 3

Coil material=refrigeration Cu tube

Gap of coil and quartz tube =0 5 mm

The power and hence the temperature of the charge in the R_f coil is varied by controlling a variable voltage

transformer Since there is no power meter provided with the equipment, the standardization of melting and melt spinning process has been done in turns of the dials reading (maximum reading 100) of the adjustable transformer

The nozzle is cleaned with distilled water and methanol and dried in hot air The prepared charge, weighing 10 to 15 gms as described in the material preparation, is taken in the nozzle The open end of the nozzle is connected with Argon and the whole system is flushed with pure dry Argon for few minutes A weak flow of Argon is maintained till ejection of the melt to prevent chances of oxidation of the charge The nozzle is placed inside R_f coil vertically above the rotating surface of the copper wheel The distance of the nozzle tip to the surface of the copper wheel is varied from less than 1mm upto 2 mm, even though the smaller gap is generally preferred Care is taken to see that the R_f coil does not touch the nozzle and a uniform gap between the nozzle tip and the R_f coil is maintained The nozzle is so placed in the R_f coil that the lowest end of the nozzle tip, with a small fraction of the sample, is kept slightly outside the R_f coil at the chilled block end The maximum part of the sample at the other end, is kept inside the R_f coil The above arrangement has important consequences which will be discussed later The loaded nozzle is then heated up, slowly at first increasing by 2 divisions of the adjustable

transformer upto 30 divisions After 30 divisions the charge is heated up quickly Near about 60 divisions the alloy reaches its melting temperature While the charge is heated to 40 divisions of the adjustable transformer the chill block is set in motion The temperature is raised quickly at this point,transformer adjusted at the rate of 30 divisions per second to reach the desired superheat value of 75 divisions of the transformer At this point the melt is held for 1 second and the ejection pressure, which is preset between 0 6 to 1 2 Kgf/cm^2 , is applied The molten metal ejects out on the rotating Cu substrate to produce the ribbons Five to six metre long, six to seven milimeter wide ribbon of average thickness 30 micron can be obtained

III 2 Characterisation

The metallic glass $Fe_{81}B_{13.5}Si_{3.5}C_2$ produced by melt spinning technique is subjected to two different types of physical studies (i) Study of the melt spun ribbon from the process point of view and (ii) studies related to thermal stability of amorphous ribbons. For the first kind of studies metrological, X-ray and TEM techniques are used to study the macroscopic as well as microscopic nature of the material Whereas for the latter kind of studies change in electrical resistance with temperature and differential seanning calonimetry (DSC) are used Since the alloys are

useful for their magnetic properties, to a limited extent magnetic properties are tested using a vibrating sample magnetometer

1) Study of melt spun ribbons from process point of view The metallic glass ribbons produced in laboratories are generally not much wide. Hence for precise measurement of dimensions, a Carl-Zeuiss MP-320 shodowgraph is used It is essentially an optical projector with 100X magnification and is fitted with a micrometer to read the dimensions directly from the enlarged shadow of the sample Thickness is measured using a micrometer screw gauge Both X-ray TEM are used to determine whether the melt spun ribbons are crystalline or amorphous

A Phillips Transmission Electron Microscope EM 301, operated at 100 KV is used The samples are first cleaned successively in trichloroethylene (TCE) for degreasing, followed by acetone to remove TCE and finally washed in methanol The samples are then thinned by electrochemical thinning A bath of 5/ perchloric acid + 95/ methanol is prepared The solution is explosive above 20oC Hence it is cooled by an ice bath to keep it at a temperature below 10oC Platinum is used as a cathode and the sample as anode The thinning conditions are 30V at 8o -12oC for 4 to 5 seconds Apperance of small holes on the immersed part of the sample indicates completion of sample thinning The prepared sample is kept immersed in methanol, till putting in TEM,

to prevent oxidation

A Rich-Seifert Isodebyflex 2002 twin tube diffractometer fitted with Cr target tube is used for X-ray diffraction The specimen is prepared by cutting the melt spun ribbons in 2 54 cm long pieces The cut pieces of the ribbon are cleaned successively in trichloroethylene, acetone and methonol These are attached to a computer card/piece of 2 54 cm x 2 54 cm size using quickfix The whole card board space is completely covered with two layers of ribbons The two layers of ribbon pieces are found necessary to complectly cut off the diffraction pattern due to computer card The prepared specimen is mounted on the diffractometer stage and a diffraction pattern is recorded using the following diffractometer conditions-

Slit size = 2 mm
Receiving slit = 0 3 mm
Voltage = 40 KV
Current = 30 mA
Scanning speed =9/min
Chart speed = 3 cm/min
Time constant = 2 sec
Range = 10 K counts/min
Angles scanned (2θ) =10o to120

ii) Study related to thermal stability a) Sample preparation Sample preparation procedure for thermal stability tests and magnetic tests are the same The melt spun Fe-B-Si-C ribbon seemsto have a fine layer of oxide forming very soon after its formation So these oxide layers are cleaned by lightly polishing the surface with 4/O emery paper, followed by successively cleaning with trichloroethyline acetone and methanol After cleaning some of the

specimens are given specific heat treatments before testing The tests carried out along with specific heat treatment given to the specimens are detailed out below

Test type I - A single run of the melt spun specimen to crystallization

Test type II- A specimen is continuously heated from room temperature to a fixed temperature below the crystallization temperature and then furnace cooled to room temperature This heat treatment cycle (called 'runs' in latter part of the discussions) is repeated several times for some specimens This is followed by a final run to crystallization

Test type III- A specimen is given an isothermal treatment at a fixed temperature of 100oC,310oC,600oC for fixed times e g 10 minutes,25 minutes and 60 minutes for stabilizing the material A stabilized sample is then subjected to either of the following tests- Test type III a) The stabilized specimen is taken to crystallization from room temperature at a fixed rate of heating via single run or test type III b) The stabilized specimen is heated to a fixed temperature below crystallization at a fixed rate of heating followed by furnace cooling This heating and cooling cycle is repeated several times followed by a final run to crystallization

In measuring electrical resistance,either of the test types I and II are employed The sample used is

of uniform width and having no pores or oxide scale An existing apparatus to measure electrical resistance as a function of temperature has been made use of A thermally insulated furnace controlled by a programmable temperature controller is heated at a fixed rate of 1oC or 2oC /minute A standard four probe method of electrical resistance measurement is used The current passed through the sample is kept constant by a HP constant current source A differential method of potential measurement is utilized to make use of high sensitivity ranges of a Keithley microvoltmeter A balance potential is provided by a L and N potentiometer The unbalanced emf is continuously recorded by a two pen strip chart recorder which also simultaneously record the temperature of the specimen A sensitive range of 30μV full scale is used to detect very small changes in electrical resistance Balancing emf of the potentiometer is to be changed frequently to keep the recorder pen within chart span Each time the balancing emf is adjusted and noted so that the potential drop across the specimen can be calculated A Pt vs Pt + 10/ Rh thermocouple is used to measure the specimen temperature

Before starting the electrical resistance measurement the sample chamber is flushed with purified Argon gas Standard Argon gas is passed through a gas purification train containing gas drying columns and hot Cu and Ti chips to remove moisture, Oxygen and Nitrogen

The purified gas is passed through the sample chamber at a rate of 2 to 3 bubbles per minute The programmable controller is turned on and the difference emf is continuously traced on the chart paper In this apparatus the specimen can not be cooled at any desired rate because of heavy thermal insulation of the furnace The typical testing conditions for electrical resistance measurement with increasing temperature are as follows

Chart speed = 0 3 cm/min

μV meter range = 30μV,100μV or 300μV

Heating rate = 2oC/min

Measuring Current = 1 milliamp

Argon gas flow = 2 bubbles/min

A dupont 910 DSC is used for thermal analysis of the ribbons for DSC work Test types I,II and III are employed small pieces of cleaned ribbon weighing approximately 15 to 25 miligrams are put in small aluminium pans provided by the manufacturer for use as crucibles A second empty aluminium pan is used as a reference To protect the sample from oxidation, pure Iolar - 2 Argon gas is passed through the DSC cell The gas inlet of the DSC cell is connected to the gas cylinder fitted with a sensitive pressure regulator and needle valve The outlet is connected to an oil bubbler so that the flow rate can be controlled as well as monitored. A gas flow rate of 2 to 3 bubbles per minute is used throughout the experiment. The heating

cycle is programmed The specimen is first heated to 500C at a rapid rate and the DSC is brought to a standby position No DSC data are recorded below 500C. From this temperature the specimen is heated to the desired temperature as required in different test types at a heating rate of 100C / min. The measurement are made at different sensitivity levels of the DSC and the recorder On the DSC, two sensitivity ranges 1X and 10X are available The chart recorder sensitivity can be chosen from 0 01, to 10V full scale The measurements are made in 'DSC Calibrated' mode of the equipment Base line adjustment are made at the start of a set of experiments but no adjustments are made in between runs to avoid the change in DSC peak characteristics In the highest sensitivity ranges, namely combination of DSC 10X and chart 01V full scale, the base line is found to change slightly after 3 or 4 runs and it is nonlinear Hence from time to time base line traces are made A two pen strip chart recorder is used to record against time Q, the heat evolved or absorbed,and dQ/dT, the latter is found very helpful in detecting small thermal effects Specimen temperature is displayed by a digital mV meter and noted manually on the strip chart recorder One typical experiment for example uses the following conditions

Heating rate = 100C/min

Argon flow rate = 2 to 3 bubbles/min

Initial temperature = 500C

Final temperature = 333oC

Range for Q = 0 1 mV full scale

Range for dQ/dT = 0 01 mV full scale

DSC sensitivity = 10X

DSC in calibrated mode

The cleaned samples are used in the high temperature assembly of a vibiating sample magnetometer (VSM) to measure magnetic moment as a function of temperature in the residual field of a Varian electromagnet The residual field is 40 Oe The specimen is heated at a slow rate approximately at 5oC/minute The magnetic moment vs temperature curve is used to determine the Curie temperature The saturation magnetization of the cleaned specimen is determined at room temperature by keeping the long axis of the specimen parallal to the field

CHAPTER IV

RESULTS

IV 1 Fabrication of Metallic Glass Ribbon

Metallic glass ribbons are prepared in the laboratory using an existing single roller melt spinning apparatus The effect of different process parameters both on ribbon formation and the quality of the ribbons produced are investigated This section gives the result of different process parameters and their effects

Nozzle length The Fig 16 shows the meaning of different terms used Quartz tubes of outside diameter 12 mm and inside diameter 10 mm are taken and nozzles are made The orifice lengths are kept same but the angle with horizontal is varied The other conditions during melt spinning are kept constant Table 2 gives the results obtained with different nozzles The best results are obtained with nozzle C

Ejection pressure Keeping the other conditions fixed, ejection pressure is varied The results are given in Table 3

Distance between chill block and nozzle Table 4 describes the effect of this distance on ribbon formation and characteristics In all the experiments described in Table 4 a pressure of 1 Kgf/cm^2 to 1 2 Kgf/cm^2 is applied

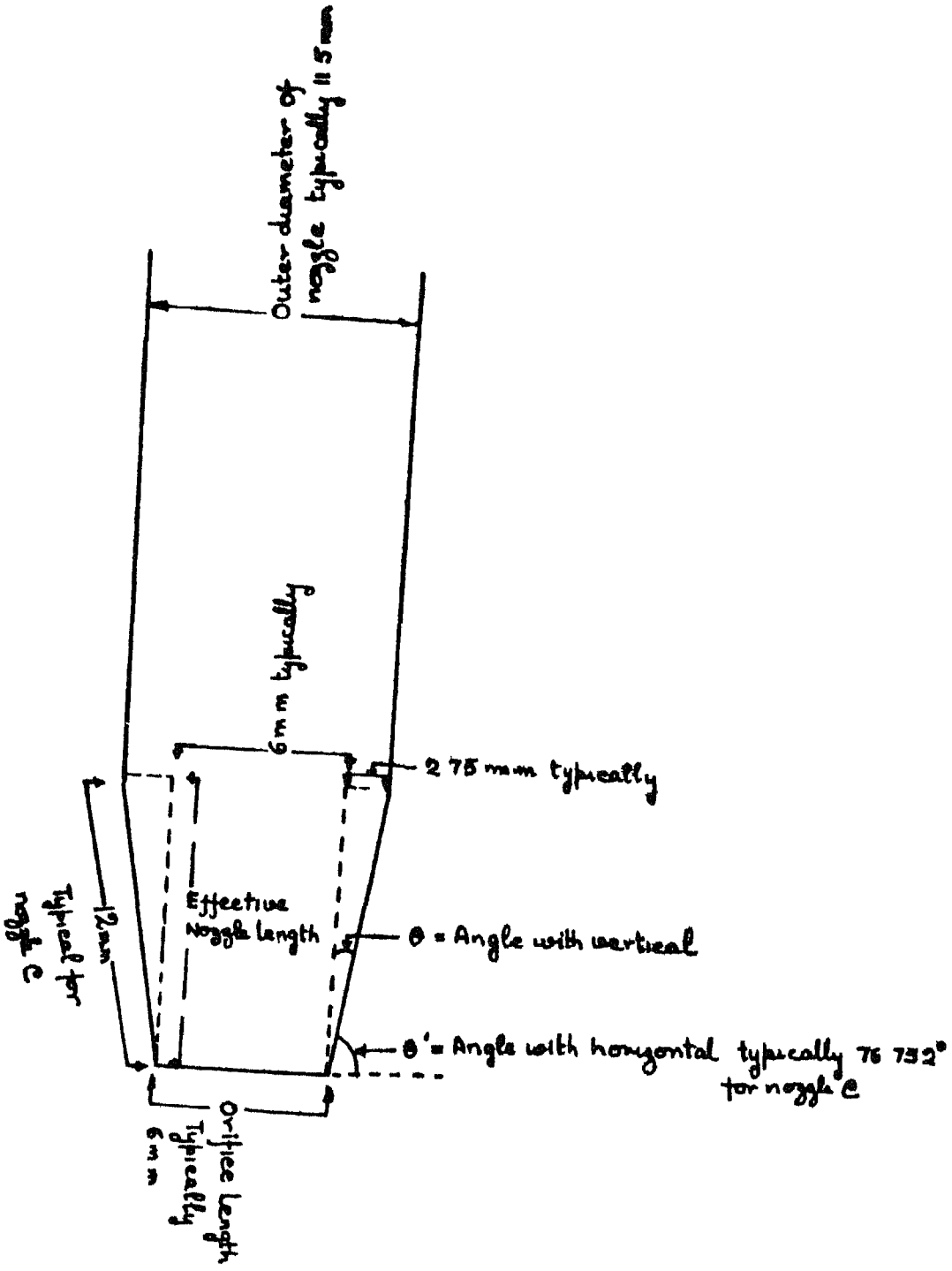

Figure 16 Quartz nozzles for meltspinning

TABLE 2

The effect of nozzle length on ribbon formation

Nozzle	Orifice length (mm)	Angle with horizontal (θ°)	Effective nozzle length (mm)	Ribbon Characteristics
A	6	89	85 7	Uneven and discontinuous ribbons
B	6	80	15 8	Even edge, continuous ribbons
C	6	76	11 6	Even edge, continuous ribbons
D	6	60	4 8	Even edge, continuous ribbons
E	6	35	1.9	Uneven and discontinuous ribbons

TABLE 3

The effect of ejection pressure on ribbon formation

Ejection pressure (kgf/cm^2)	Ribbon characteristics
0 05	Uneven, discontinuous ribbon formation
0 1	Uneven, discontinuous ribbon formation
0 6	Uniform, continuous ribbon formation
0 8	Uniform, continuous ribbon formation
1 0	Uniform, continuous ribbon formation
2 0	Quartz nozzle bursts

TABLE 4

The effect of distance between chillblock and nozzle on ribbon formation

Distance between chillblock and nozzle (mm)	Ribbon characteristics
0 5	Uniform and continuous ribbons
1 0	Uniform and continuous ribbons
2 0	Uniform and continuous ribbons But ribbons show occational brittleness
4 0	Discontinuous and brittle ribbons often having pores
5 0	Bits of ribbons, almost completely brittle

Degree of super heating The number of turns of the input power of the transformer in the induction furnace versus ribbon characteristics is given in Table 5 The ribbons are best produced within the range of 68 to 80 divisions of the input power

Surface velocity of the substrate Four velocities are tried keeping the other experimental conditions fixed and the surface velocity vs the ribbon characteristics are shown in Table 6

Orific geometry The orifice is a rectangular hole with the length being controlled and the width the same as that of the cutting wheel

Several sketches of the good and bad nozzles with different orifice geometry are shown in Fig 17 In nozzle (1) , serration occur when the nozzle is first cut in the cutting wheel and then thinned during preparation . In nozzle (2), the orifice is extended to both the sides of the nozzle In nozzle (3), the width of the nozzle is more than the cutting wheel thickness In nozzle (4), the orifice is not extended throughout the length of the nozzle Nozzle (5) is the best nozzle

Summery of important parameters to produce best metallic glass ribbons under the existing conditions and one particular value to produce continuous and reasonably wide (six to seven milimeters) ribbons are given in Table 7

TABLE 5

The effect of supperheating on ribbon formation

Superheating Number of turns of the divisions power (divisions)	Ribbon characteristics
60-64 (melting point)	Partially crystalline ribbons
62-68	Completely glassy ribbons, edges sometimes brittle
68-80	Completely glassy ribbons, edges not brittle
85-95	Partly crystalline, and sometimes oxidized ribbons
90-100	Mostly crystalline, often burnt out and sometimes metal globule formation

TABLE 6

The effect of chillblock surface velocity on ribbon formation

Voltage (V)	Linear speed (m/minute)	Thickness of the ribbon (micron)	Ribbon characteristics
120	297 0	30-40	Crystallized and brittle
200	480 8	30-35	Uniform and continuous
210	514 3	25-35	Uniform and continuous
270	-	-	Burnt out and semi crystallized

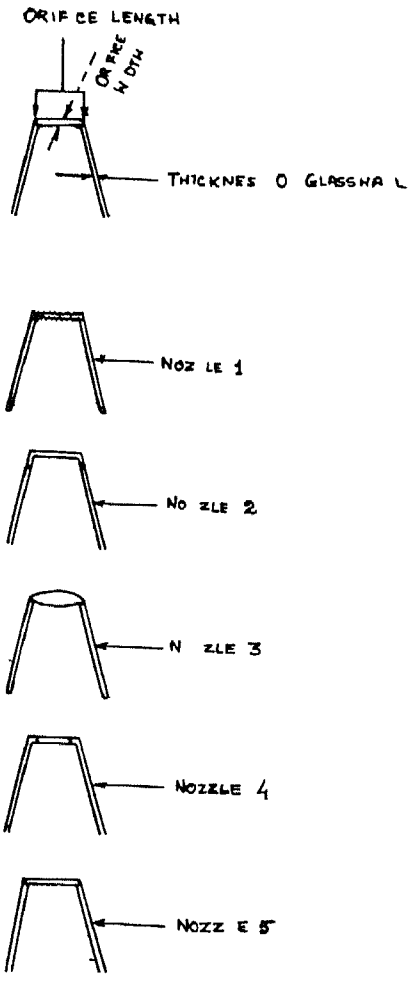

Figure 17 Examples of some nozzles having good or bad orifice

TABLE 7

A summar of inportant parameters to produce continuous four to five meters of metallic glass ribbons of six to seven milimeter width and twenty five to thirty five microns thickness

Parameter	Description	Range	One particular convenient value	Remark
Material	Single nozzle shaped pellets without any oxidized layer or undissolved impurity	Nozzle outside diameter 12 mm, inside diameter 10 mm sample weight 10 to 15 gms	-	The higher the amount of material melt spun better is the product.
Nozzle dimension for 6 mm orifice	Fusedsilica tube for nozzle material	Angle with horizontal -exact range unknown but $60^o > \angle > 80^o$	76 12 mm outside diameter nozzle and 6 mm orifice length	-
Orifice geometry	-	As of Figure 17	-	-
Ejection pressure	-	Not less than 0 6 Kgf/cm^2	0 6 Kgf/cm^2	-
Distance between chill block and nozzle	-	Less than 2mm in upper limit, lower limit in the used set up is 0 3 mm	1 mm	-
Nozzle position	-	Vertical	-	-
Super heating	-	68 div of input power to 80 div of input power	75turns of input power	-
Velocity of substrate	-	See Table 6	480 8	-
Polish and cleanness of the substrate	-	Matte finish	Matte finish	-

IV 2 Characterization

The metallic glass ribbons so produced are studied to see whether the amorphous nature has been achived by X-ray and TEM X-ray results are given in Fig 49 and TEM results are given in Fig 50 given at end

The ribbons are then studied by electrical resistance vs temperature measurements with or without different types of heat treatment The crystallization studies have been given in Fig 18 and 19 The structural relaxation behaviour is given in Fig 20 and Fig 21 The Table 8 correlates the Figure numbers with the experiment and describes for each experiment the conditions and other relevent facts No figures are plotted below 60oC as the initial stabilization of the samples may show spurious effects at the start of the experiment

Similarly Fig. 44 to 48 give the Curie temperature and magnetization/ demagnetization measurements for the prepared samples And Table 11 correlates the Figure number with the experiments performed

Fig 22 to Fig 43 describes the results obtained by DSC measurements for samples with different types of heat treatments Table 10 correlates the Figure number with the corresponding experiment number And Table 9 correlates the experiment number with the corresponding experimental conditions Hence to find the necessary

experimental conditions for a particular figure, say Fig 23, we have to go to Table 10 to find the experimental number, i e experiment 8, and then from Table 9, find out the experimental conditions corresponding to say experiment 8

In DSC it is found that because of some equipment problems, the temperature axis is not uniform giving rise to unequal divisions in temperature Hence the temperatures are plotted manually and are recorded

In all the experiments, the samples are described by the nature of previous heat treatments For example in DSC, a sample refered to as, say 310oC/25 min/ 1st run means an as melt spun sample previously isothermally annealed at 310oC for 25 minutes is cooled to room temperature after annealing and is then dynamically heated in the DSC furnace A 100oC/25 min/ 2nd run sample means a 100oC and 25 minute annealed sample is given a dynamic thermal cycling through a temperature below the crystallization temperature and is then again dynamically heated up in the DSC at a fixed rate of heating Similarly for all the other tests, sometimes the samples are so referred

TABLE 8

Electrical resistance test for various samples with various heat treatments

Experiment Number	Sample condition	Experiment	Equipment and experimental conditions	Figure number	Figure characteristics
Crystallization studies					
1	As melt spun	Sample is heated up from room temperature to 556oC followed by furnace cooling	Chart speed=20/60 cm/minute Heating rate=2oC/minute Measuring current = 1 milliamp Argon gasflow=2 bubbles/minute μV meter sensitivity =100μV	18	X axis=Temperature in oC Y axis=Resistance at the temperature of measurement, R_T $\frac{\text{Resistance at 27oC, } R_T}{\text{Resistance at 27oC, } R_{27}}$ Range= 240oC to 548oC
2a)	As melt spun	Sample is heated from room temperature to 300oC followed by furnace cooling	Chart speed #4/10 cm/minute Heating rate = 2oC/minute Measuring current =1 milliamp Argon gas flow = 2 bubbles/minute μV meter sensitivity = 30μV	-	-

Contd

2b)	As after 2a)	ample is heated from room temperature to 550oC	Chart speed = 4/10 cm/ minute Heating rate = 2oC/ minute Measuring current = 1 milliamp Argon gas flow = 2 bubbles/ minute µV meter sensitivity =30µV upto 350oC 300µV after 350oC	19	Y and Y axis same as above Range =200oC to526oC
Structural relaxation studies					
3a)	As melt spun	Sample is heated up from room temperature to 300oC followed by furnace cooling	Chart speed =8/60cm/ minute Heating rate=2oC/ minute Measuring current =1 milliamp Argon gas flow =2 bubbles/minute µV meter sensitivity = 30µV	20	X and Y axis same as above Range = 60oC to296oC
3b)	As after 3a)	Sample is heated from room temperature to 300oC, followed by furnace cooling	same as above	21	same as above

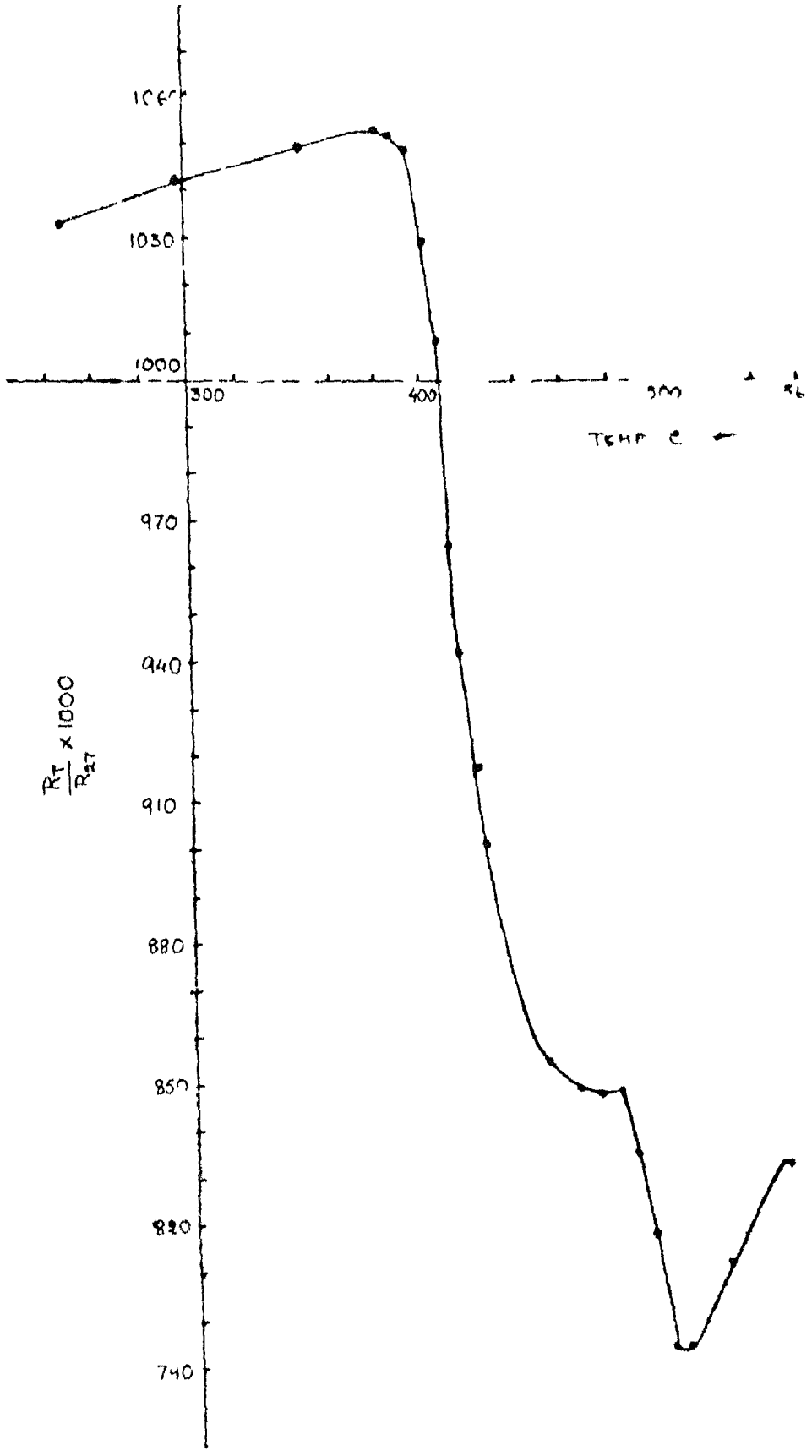

FIGURE 1E Cast film t[illegible] resistance
first [illegible]

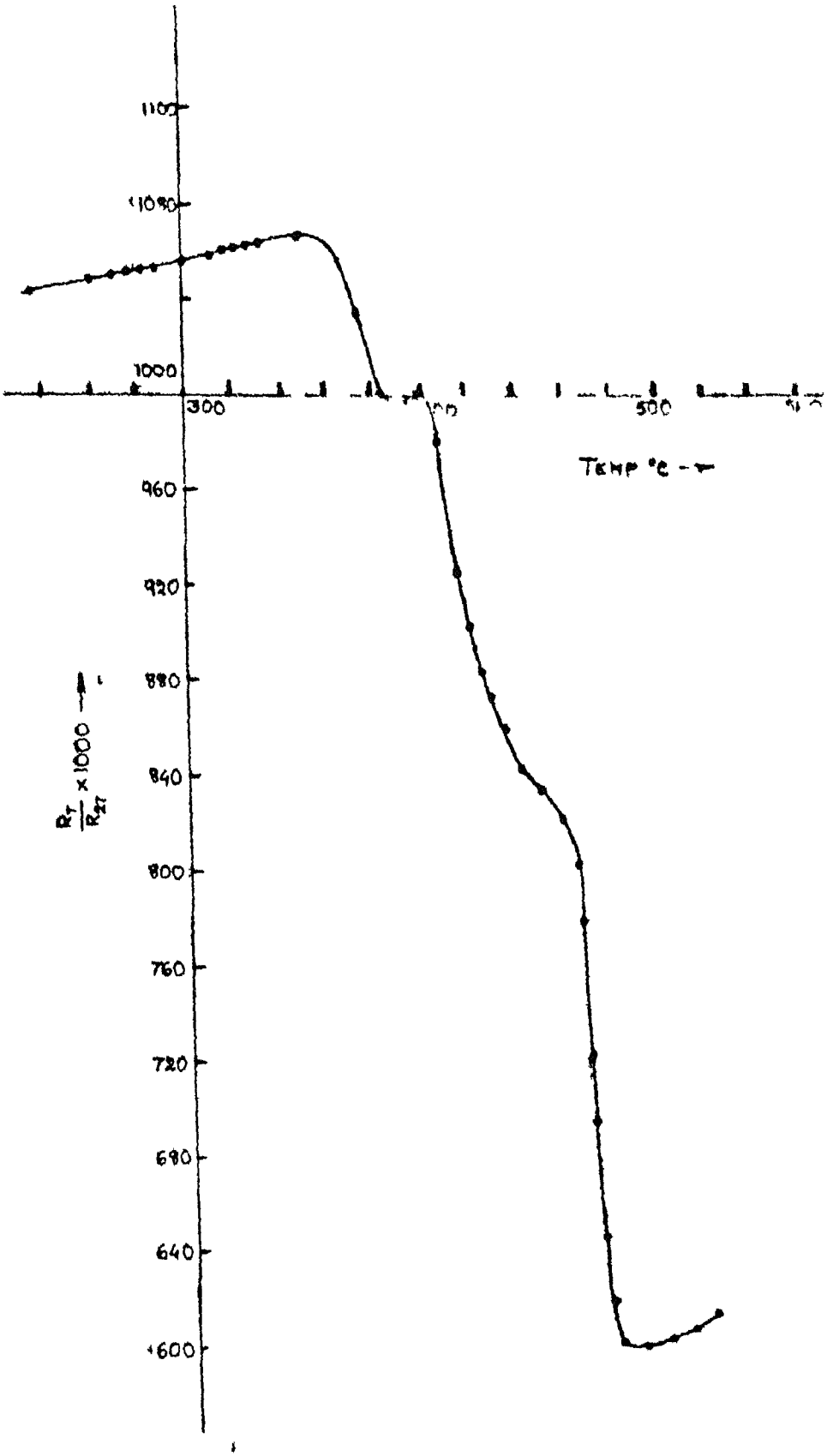

Figure 19 Crystallization studies of 'as melt spun/ second run' sample by electrical resistance

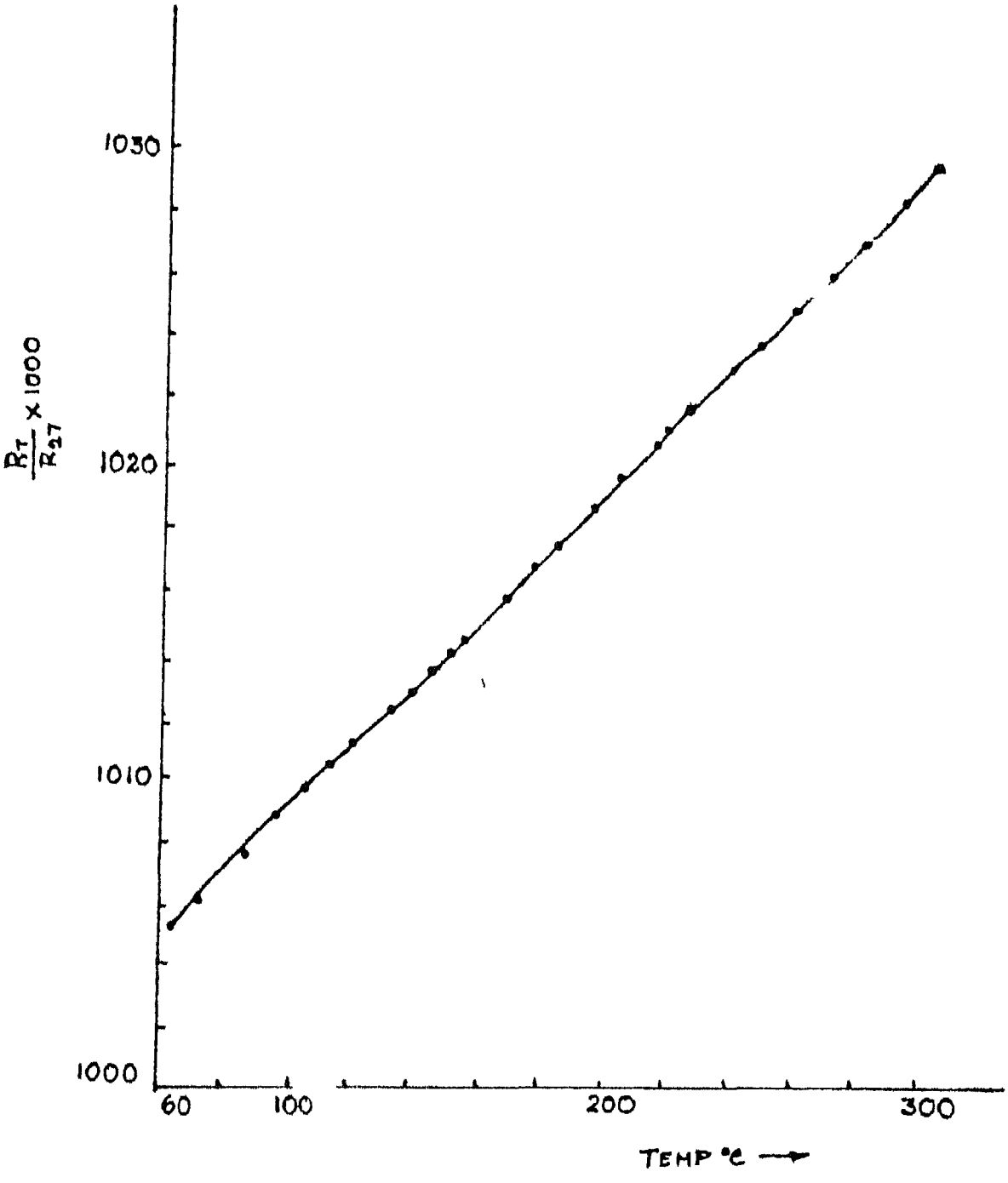

Figure 20 Structural relaxation studies of ' as melt spun/ first run' sample by electric l resistance.

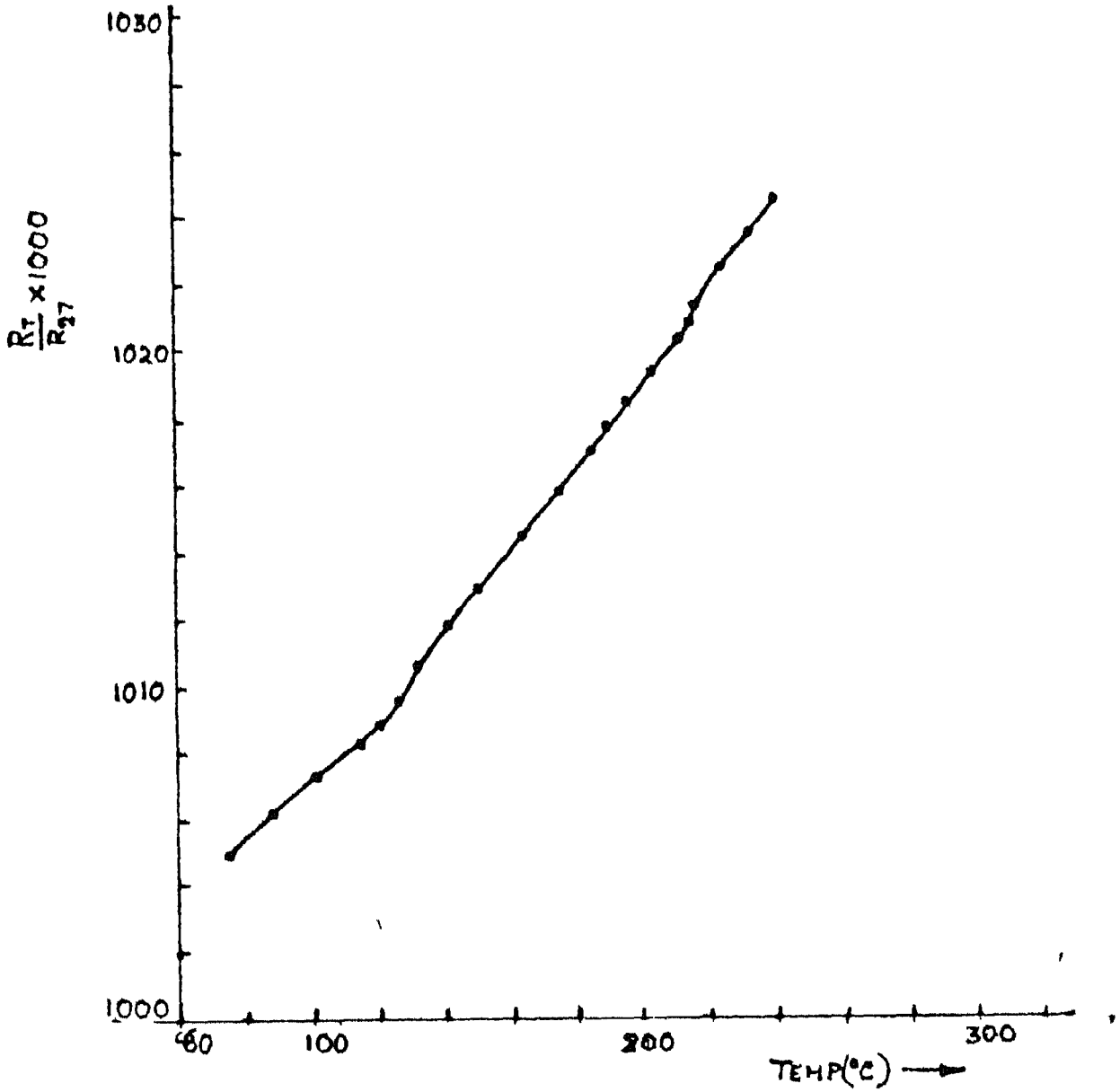

Figure 21 Structural relaxation studies of 'as melt spun/second run' sample by electrical resistance

DSC tests of various samples with various treatments

Experiment No	Sample conditions	Experiment	Equipment sensitivity		
			DSC sensitivity (xX)	Recorder sensitivity Q (V)	Recorder sensitivity dQ/dT (V)
1	As melt spun in air	In single run upto 610oC	10X upto 333oC 1X upto 610oC	1	0 1
2	As melt spun in Argon	a)1st run upto 317oC followed by furnace cooling	10	1	0 1
	As after 2 a)	b) 2nd run upto 322oC followed by furnace cooling	10	1	0 1
	As after 2 b)	c)3rd run upto 317oC followed by furnace cooling	10	1	0 1
3	As melt spun	a)1st run upto 331oC followed by furnace cooling	10	1	0 1
	As after 3 a)	b)2nd run upto 331oC followed by furnace cooling	10	1	0 1
	As after 3 b)	c)3rd run upto 331oC followed by furnace cooling	10	1	0 1
	As after 3 c)	d)4th run upto 610oC	10	1	0 1(upto 331oC) 1 0(from 331oC-610oC)

Contd

4	As melt spun sample heated rapidly to 310oC in vaccun atmosphere in an annealing furnace and kept for 25 minutes followed by uniform cooling to room temperature in 24 hours	a) 1st run upto 331oC furnace cooling	10	O 1	C 1
	As after 4 a)	b) 2nd run upto 331oC followed by furnace cooling	10	O 1	O 1
	As after 4 b)	c) 3rd run upto 331oC followed by furnace cooling	10	O 1	O 1
	As after 4 c)	d) 4th run upto 331oC followed by furnace cooling	10	O 1	O 1
	As after 4 d)	e) 5th run upto 610oC	10	O 1 (upto 331oC) 10 (331oC -610oC)	O 1 (upto 331oC) 10 (331oC-610oC)

Contd

5	As melt spun sample heted rapidly ın vaccum to 31CoC ın an annealıng furnace and kept for 25 minutes foll-owed by unıform cooling to room temperature ın 24 hours	a) 1st run upto 350oC followed by furnace cooling	1	0 1	0 1
	As after 5 a)	b) 2nd run to 610oC	1	1	0 1
6	As melt spun sample heated rapidly to 310oC ın vaccum atmos-phere ın DSC furnace and kept for 60 minutes followed by unıform cooling to room temperature	a) 1st run upto 331oC followed by furnace cooling	1	0 1	0 01
	As after 6 a)	b) 2nd run upto 331oC followed by furnace cooling	1	0 1	0 01
	As after 6 b)	c) 3rd run upto 331oC followed by furnace cooling	1	0 1	0 01

Contd

	As after 6 c)	d) 4th run upto 610oC	1	0 1	0 01 (upto 331oC) 0 1 (331oC-610oC)
7	As melt spun	1st run upto 610oC	1	1	0 1
8	As melt spun heated in furnace rapidly to 310oC in vaccum and kept for 25 minutes followed by uniform cooling to room temperature in 24 hours	a) 1st run upto 610oC followed by furnace cooling	1	1	0 1
	As after 8 a)	b) 2md run upto 295oC	1	1	0 1
9	As melt spun heated rapidly in DSC furnace to 100oC, kept for 25 minutes followed by uniform cooling to room temperature in 45 minutes	1st run upto 610oC	1	1	0 1
10	As melt spun	1st run to 610oC	1	0 1	0 01

Contd

11	As melt spun heated rapidly to 600oC in DSC furnace in Argon atmosphere, kept for 10 minutes followed by uniform cooling to room temperature in 45 minutes	1st run to 500oC	1	0 1	0 01
12	As melt spun heated rapidly to 310oC in DSC furnace in Argon atmosphere, kept for 60 minutes followed by uniform cooling to room temperature in 45 minutes	1st run to 452oC	1	0 1	0 01

In 3rd column of the Table the DSC furnace is used, in 2nd column except where specifically mentioned the experiments are done in an annealing furnace, in DSC experiments heating rate of 10oC / minute is used

TABLE 10

DSC figures representing DSC experiments mentioned in Table 9

Figure No	Experiment No
General Curves	
22	10
23	8
24	6
25	11
26	8,9,7
Crystallization Studies	
27	8,4
28	10,3
29	9
30	5
31	12
Relaxation Studies	
32	3
33	4
34	6
35	3
36	4
37	6
38	3
39	4

Contd .

Contd TABLE 10

Figure No	Experiment No
40	6
41	3
42	4
43	6

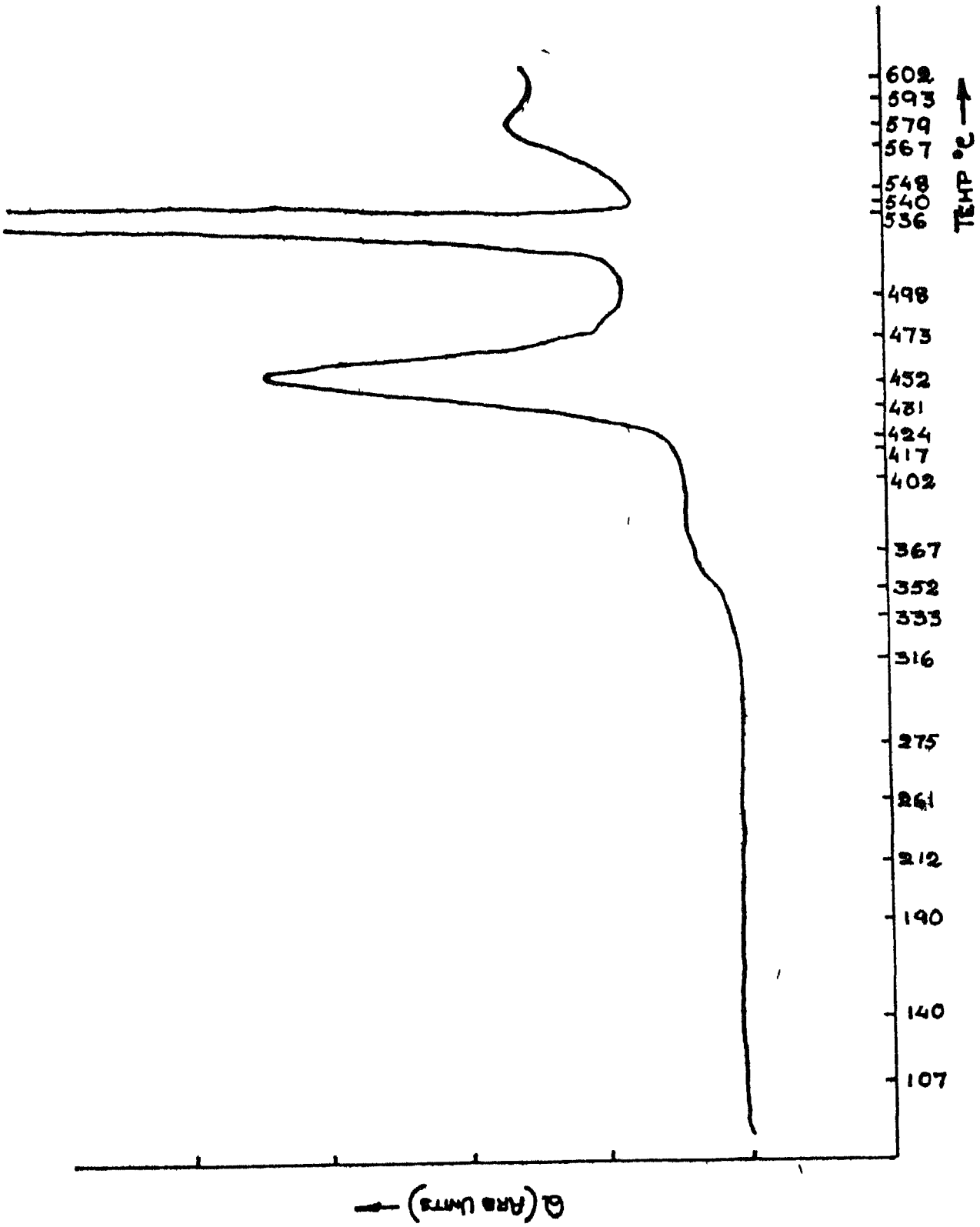

Figure 22 General DSC curve for 'as melt spun first run' sample

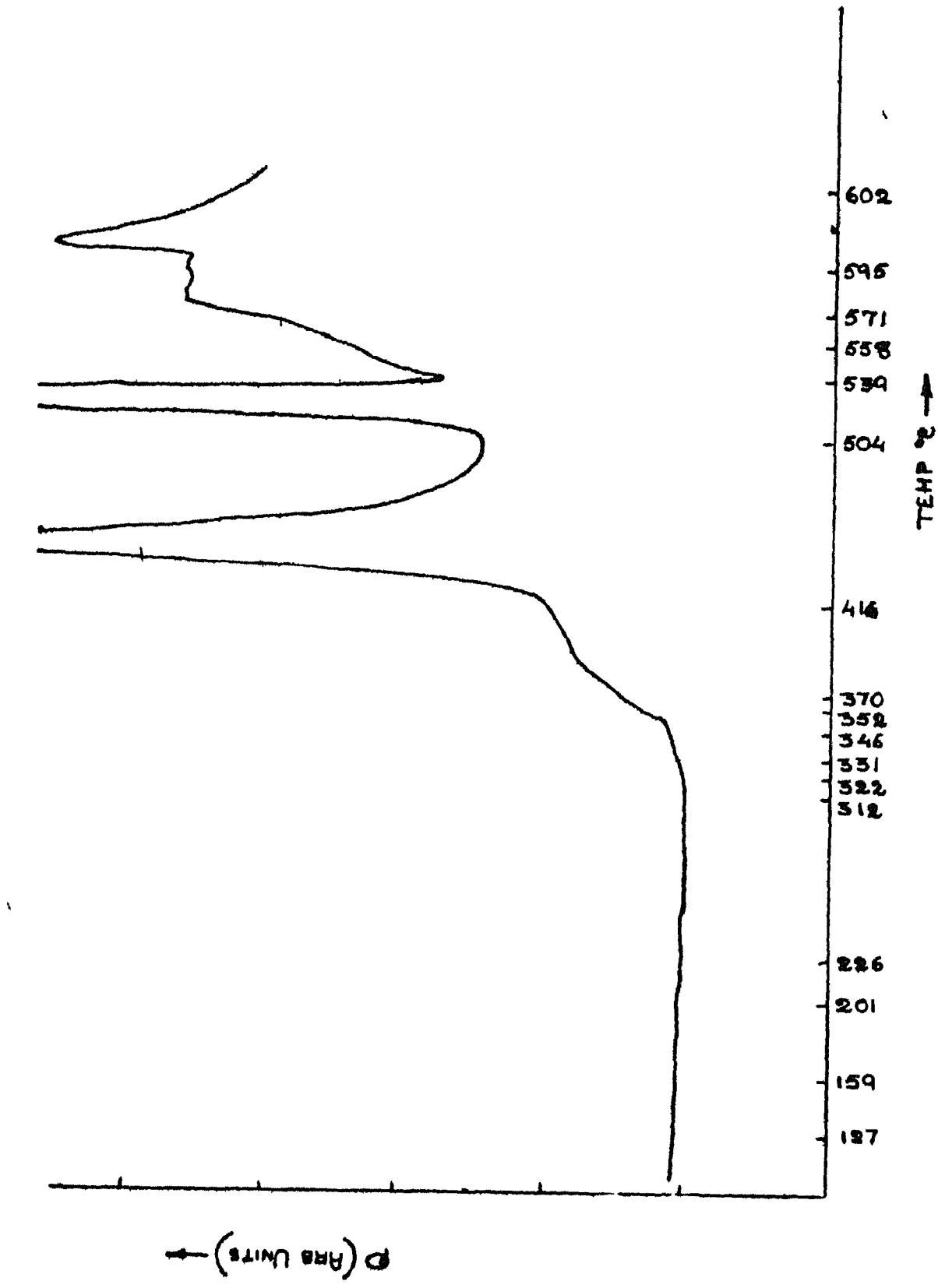

Figure 23 General DSC curve for '310°C/25 min/first run' sample

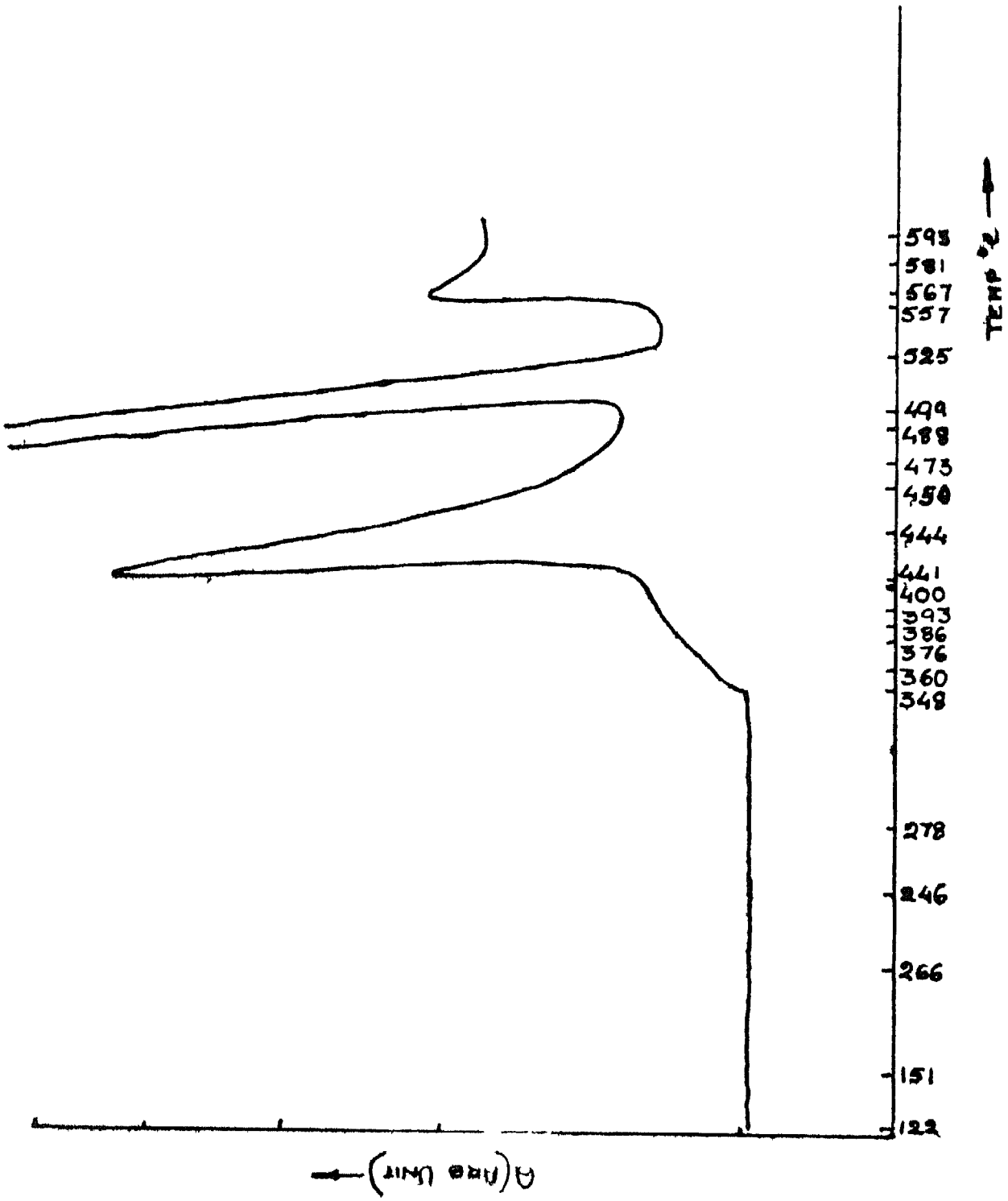

Figure 24 General DSC curve for '310°C/60 min/ fourth run' sample

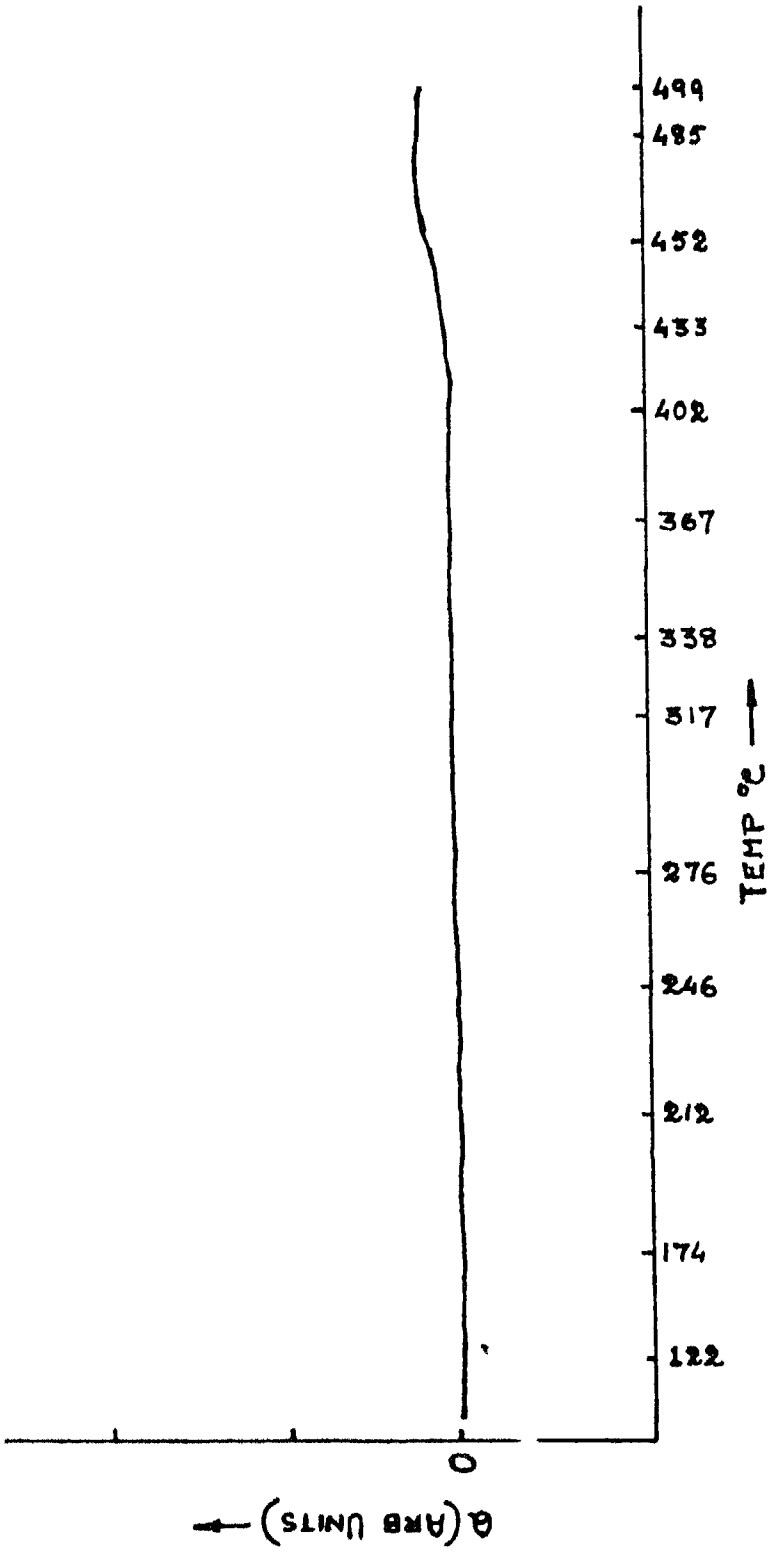

Figure 25 General DSC curve for ' 600°C/10 min/first run' sample

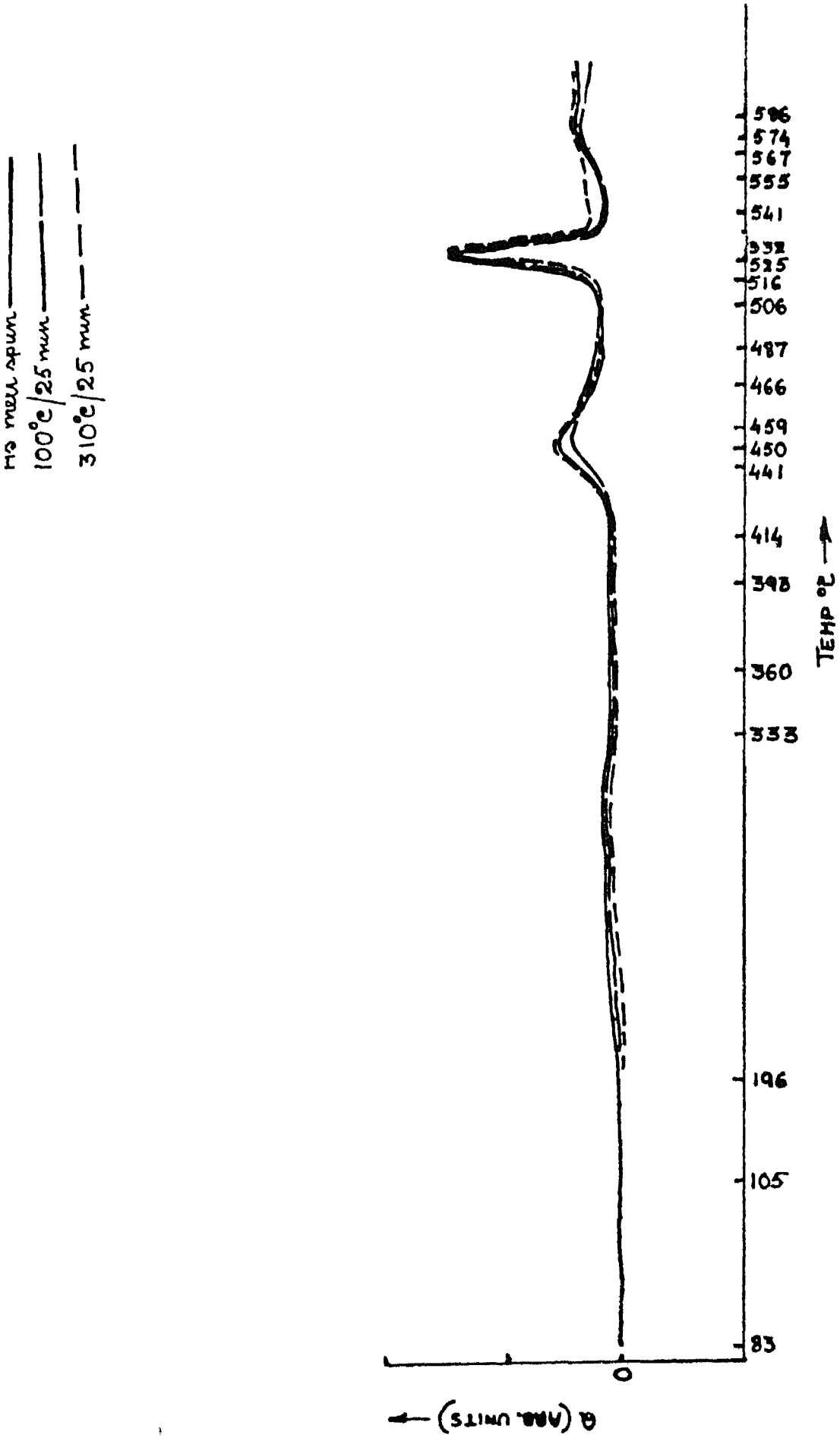

Figure 26 General comparison studies in DSC of 'as melt spun', '100°C/ 25 min', '310°C/25 min'-all first run samples

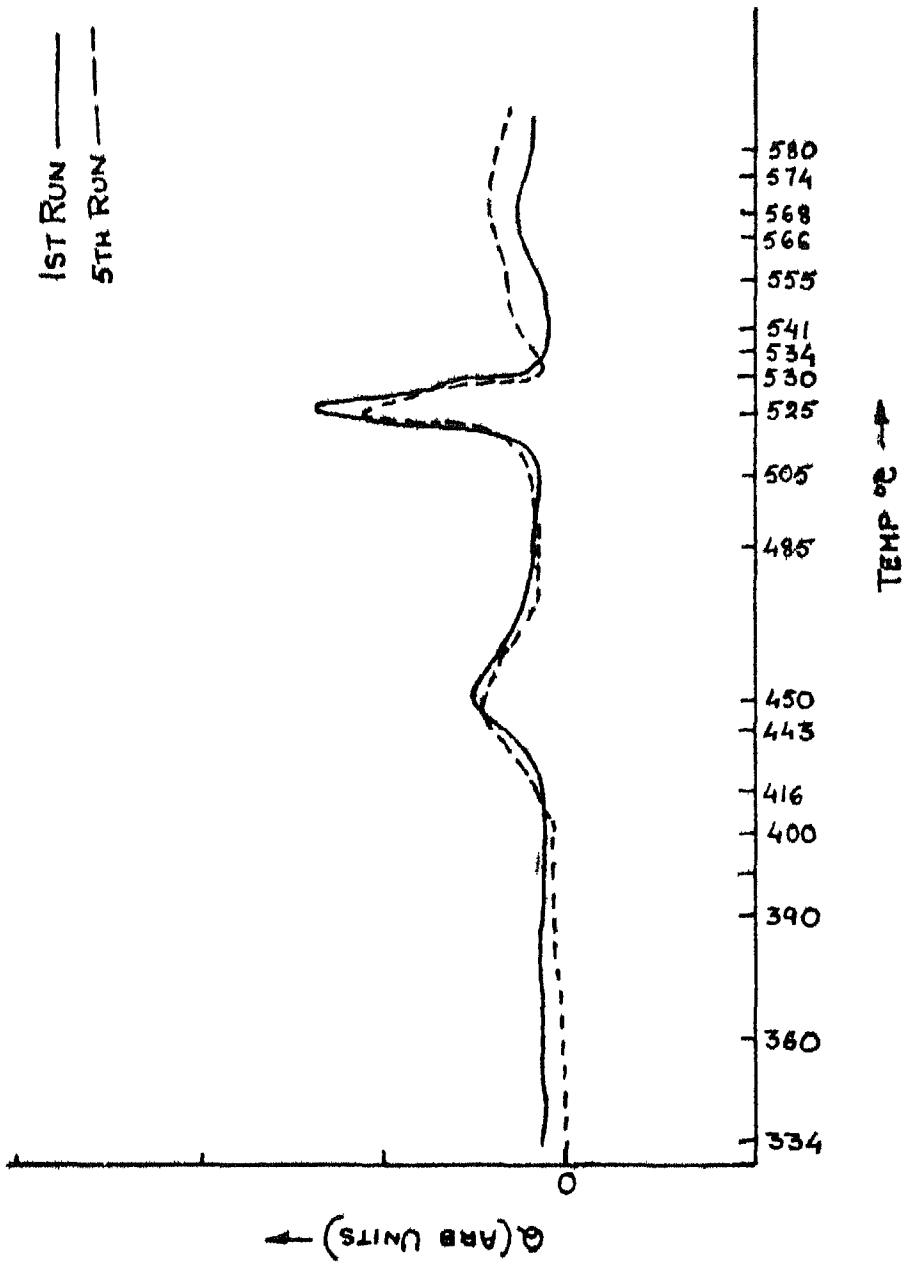

Figure 27 Crystallization comparison studies in DSC of 310°C/25 min/ 1st and 310°C/25 min/ 5th run samples

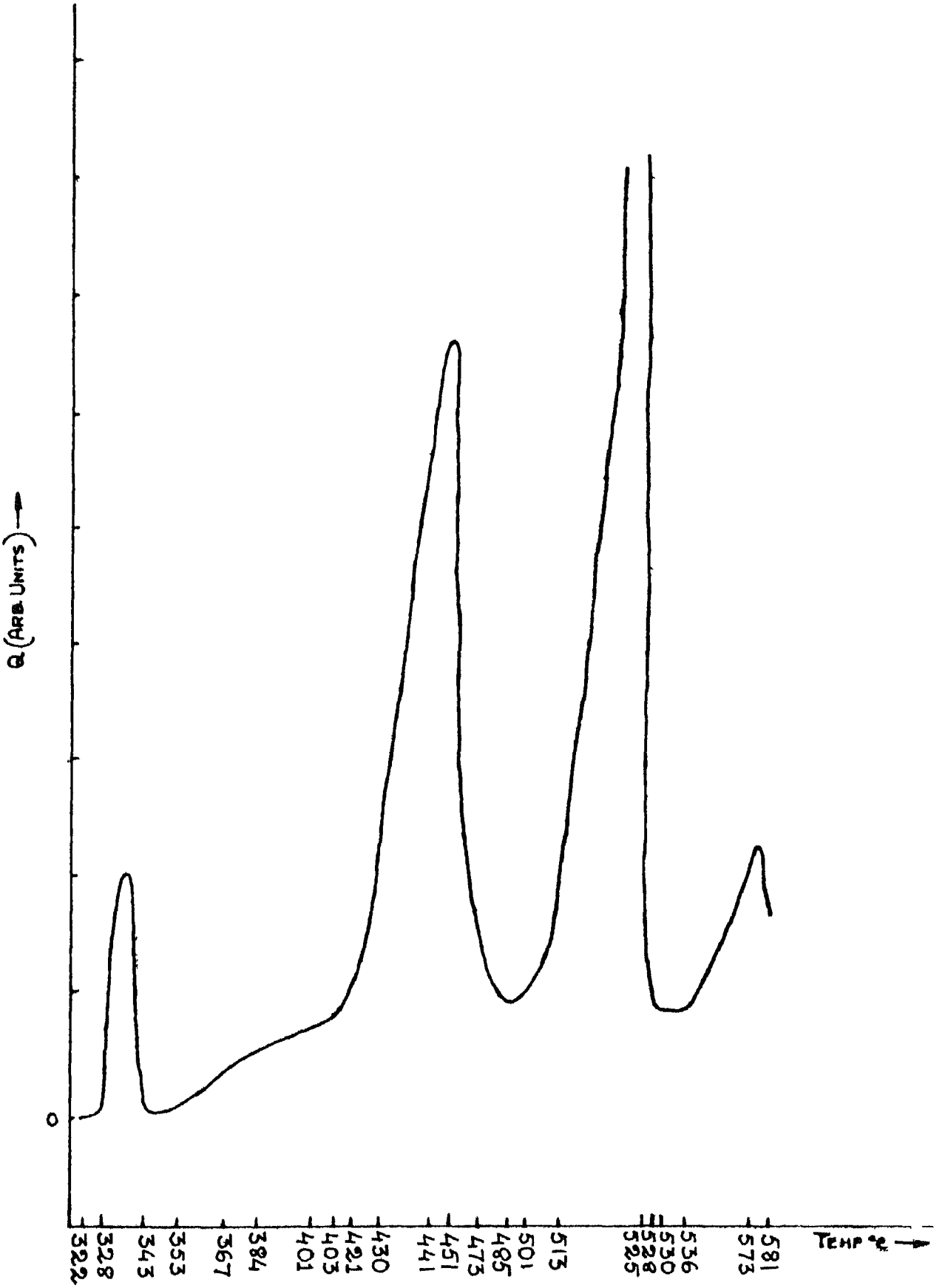

Figure 28 Crystallization studies of ' as melt spun/ 4th run' sample in DSC

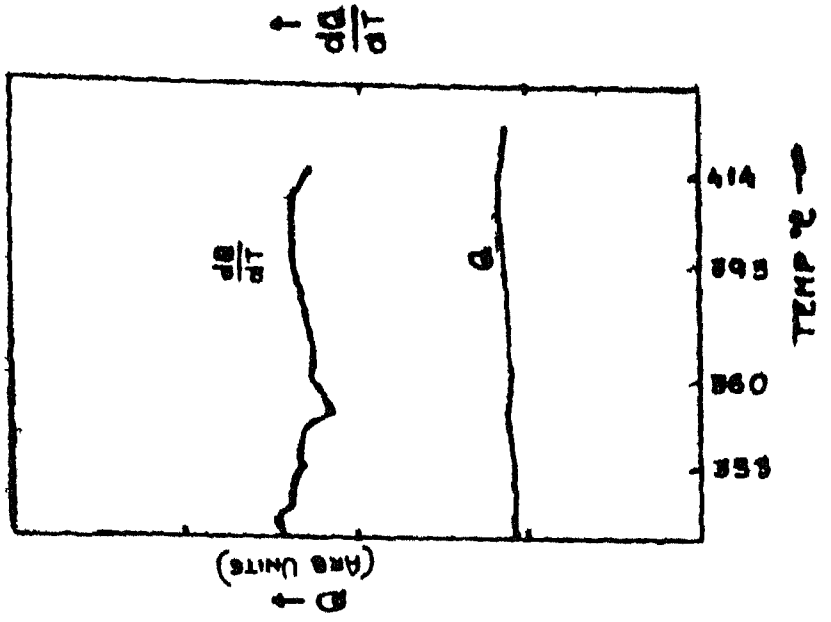

Figure 29 Crystallization studies of 100°C/25 min/1st run sample in DSC

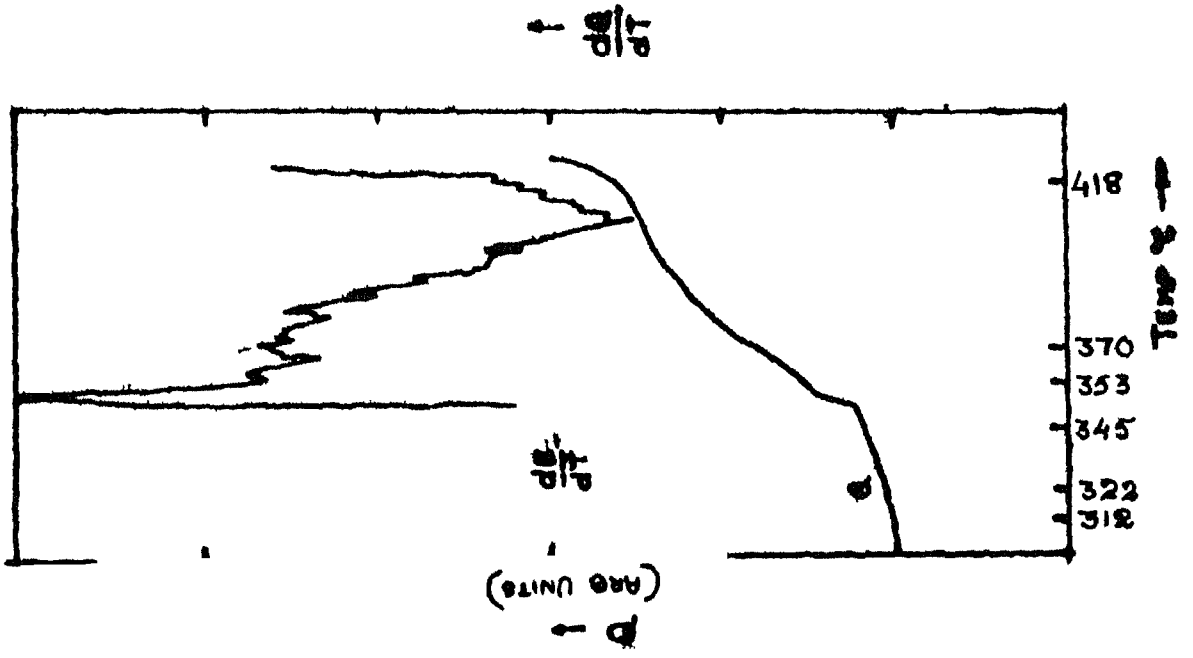

Figure 30 Crystallization studies of 310°C/25 min/2nd run sample in DSC

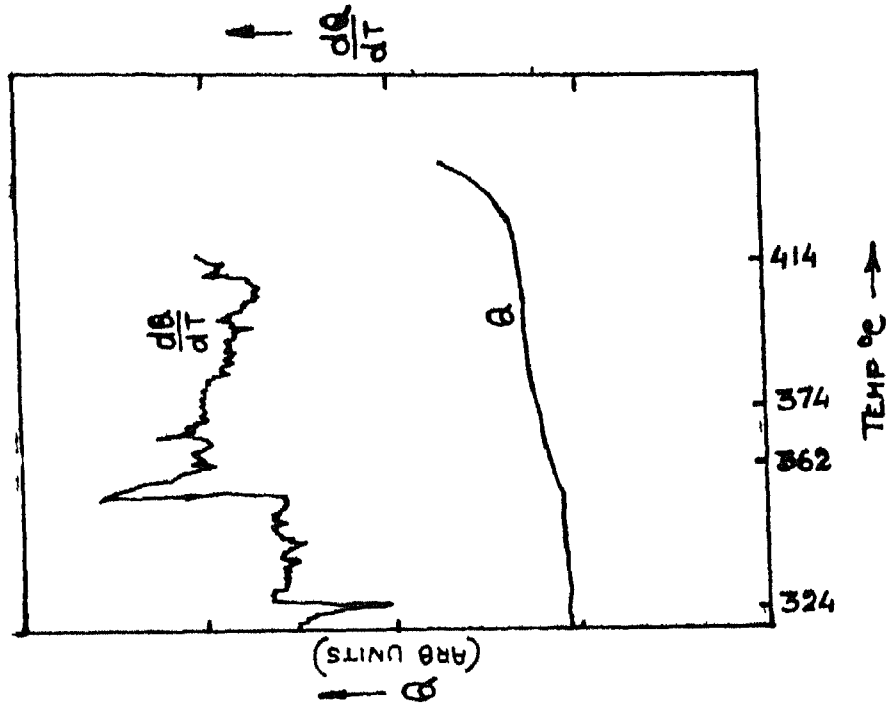

Figure 31 Crystallization studies of 310°C/60 min/1st run sample in DSC

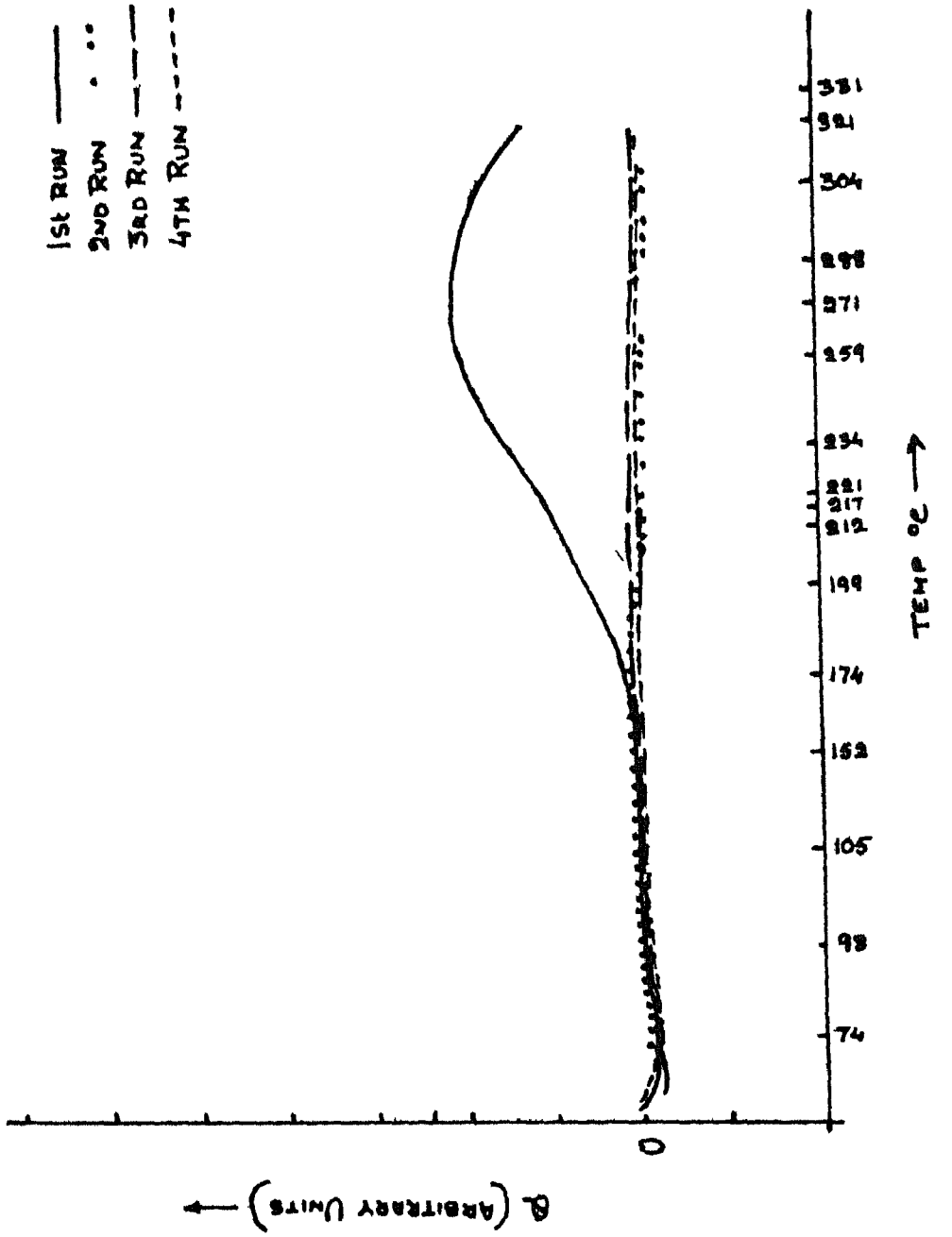

Figure 32 Structural relaxation studies of 'as melt spun/first to fourth run' samples in DSC

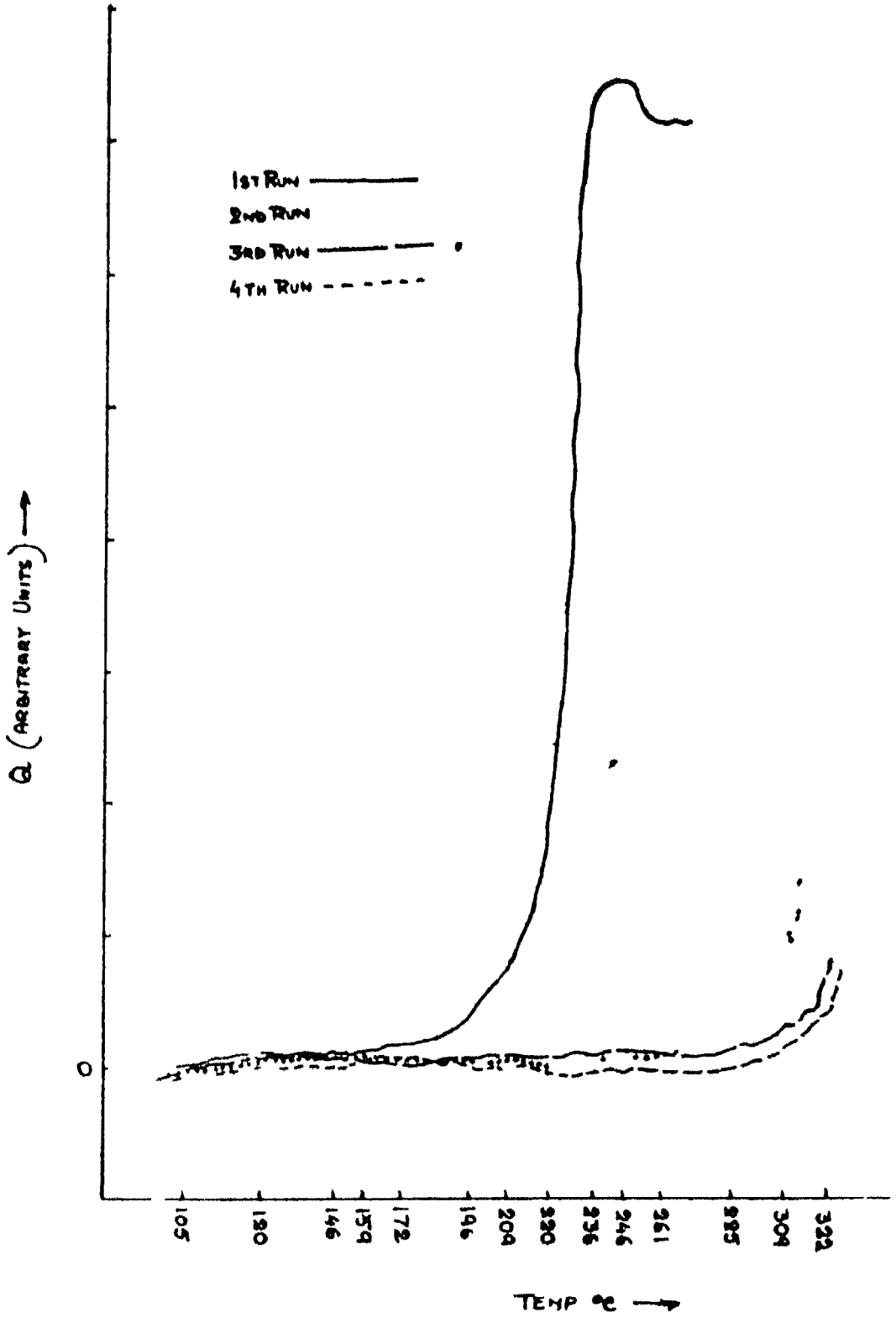

Figure 33 Structural relaxation studies of 310°C/25 min/ 1st to 4th run samples in DSC

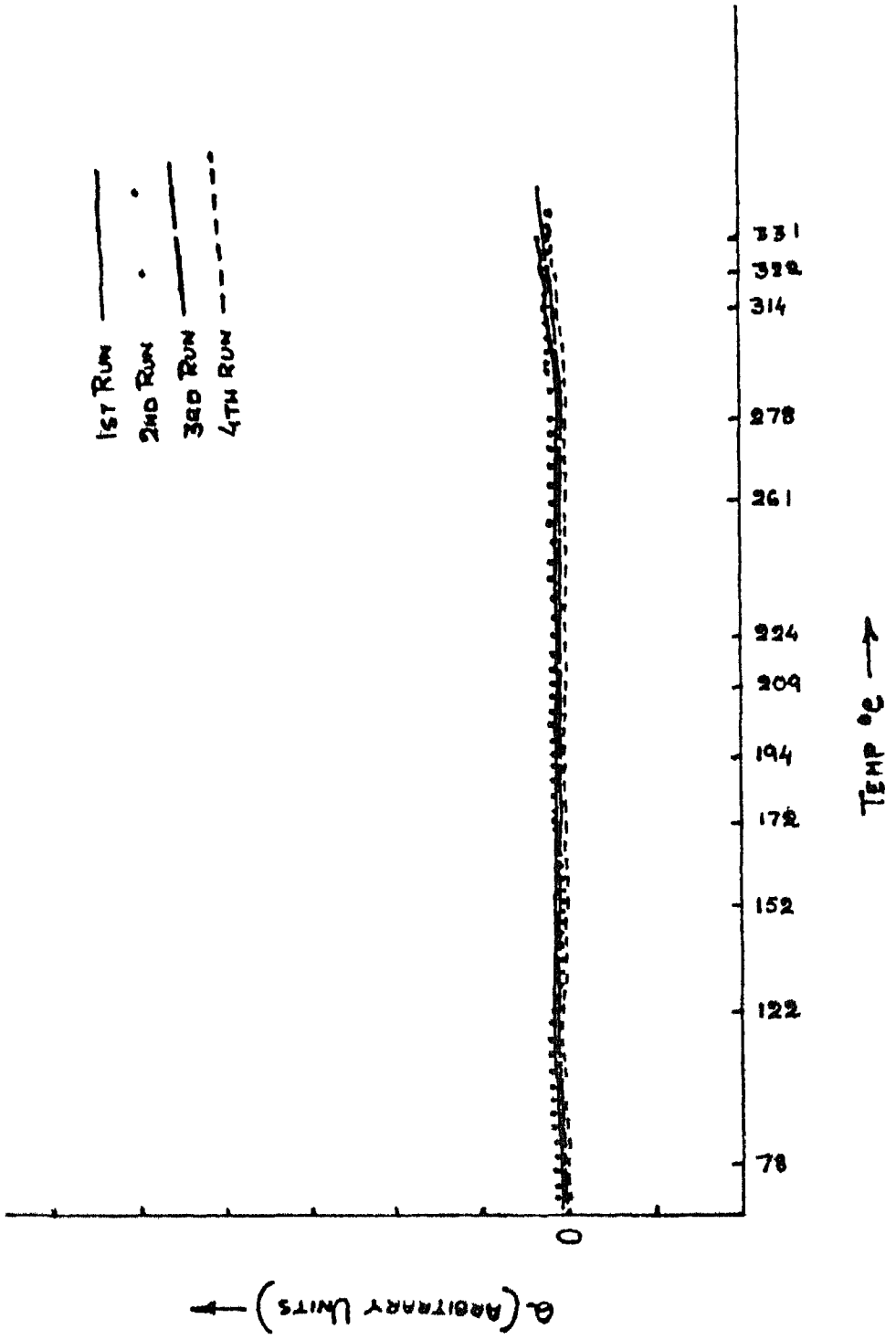

Figure 34 Structural relaxation studies of 310°C/60 min/ 1st to 4th run samples in DSC

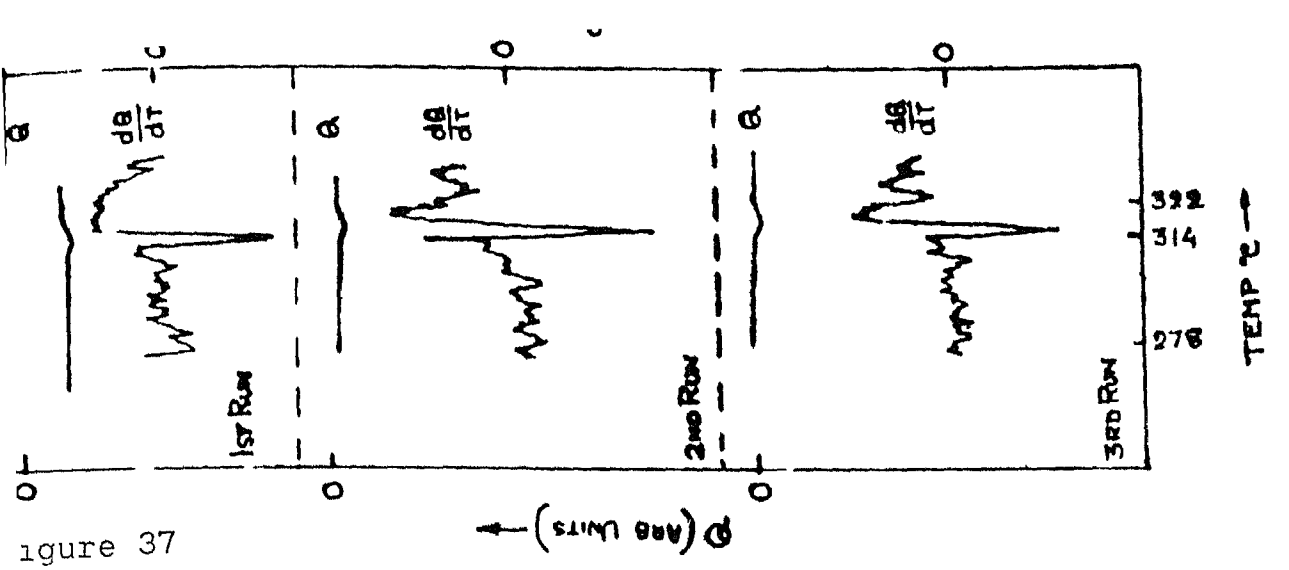

igure 37

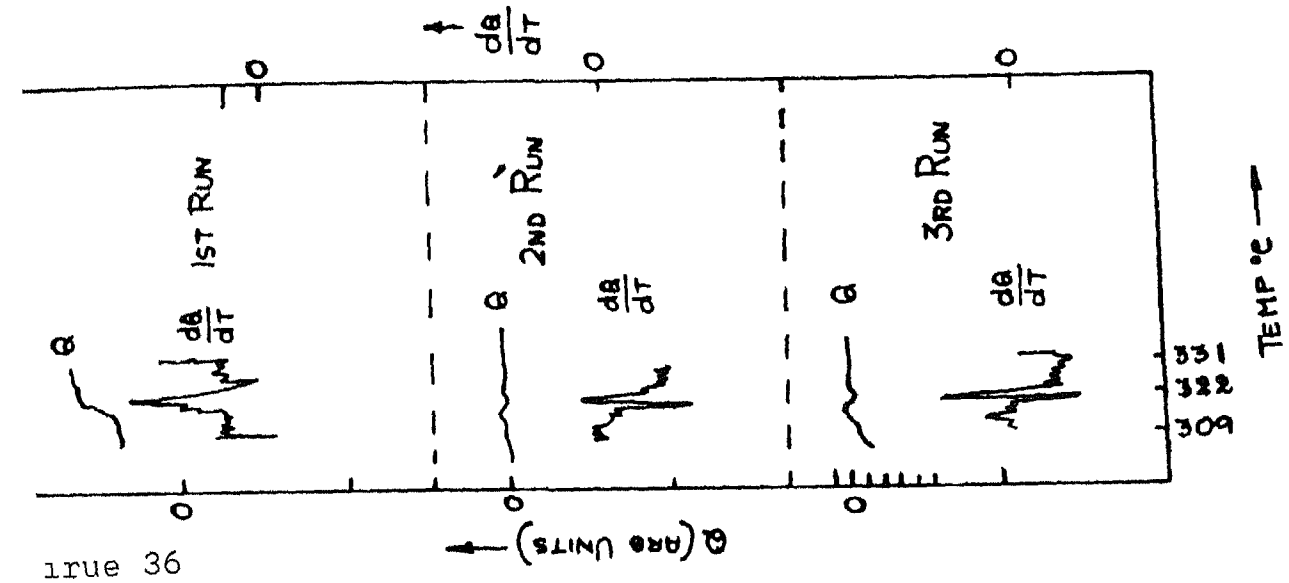

ırue 36

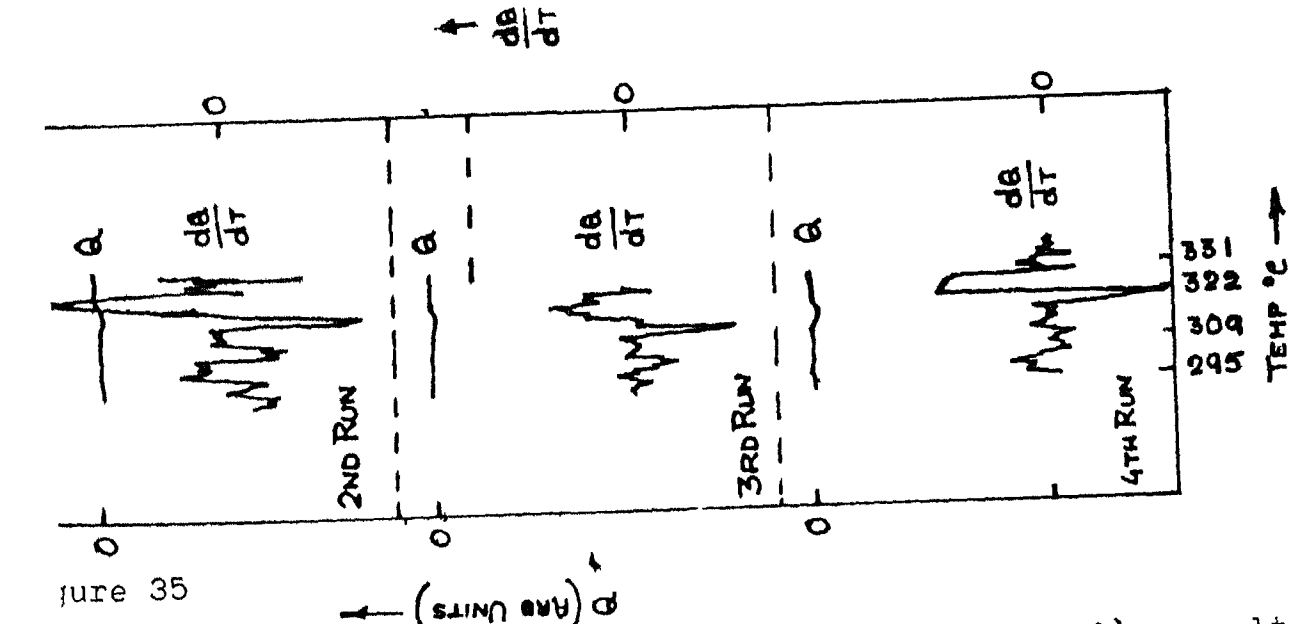

jure 35

ıures 35 to 37 First reversible change studies of a) as melt spun/
2nd to 4th run samples - Fig 35 b) 310°C/25 min/
1st to 3rd run samples - Fig 36 c) 310°C/60 min/
1st to 3rd run samples - Fig 37 in DSC

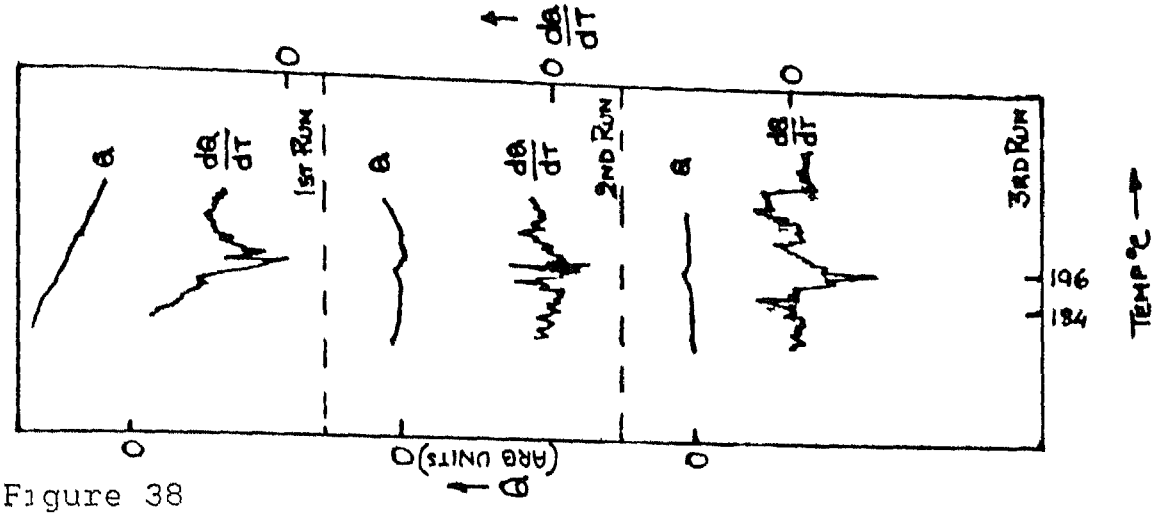

Figure 38

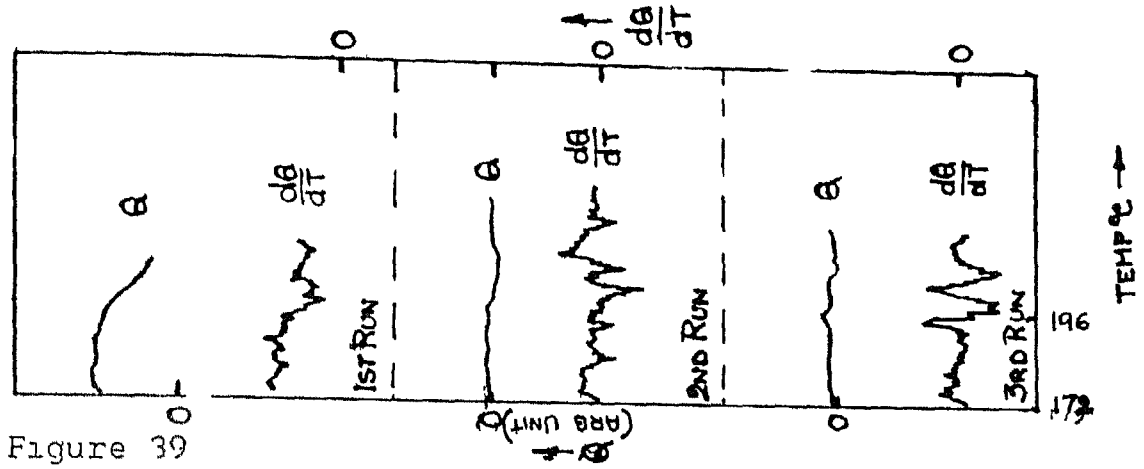

Figure 39

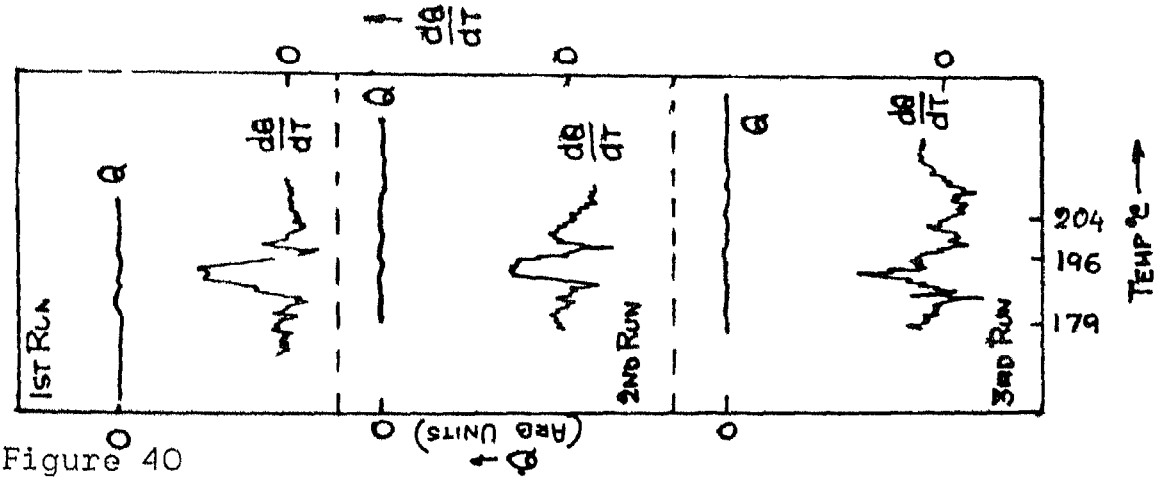

Figure 40

Figures 38 to 40 Second reversible change studies of
a) as melt spun / 1st to 3rd run samples-Fig 38
b) 310°C/25 min / 1st to 3rd run samples-Fig 39
c) 310°C/60 min / 1st to 3rd run samples-Fig 40
in DSC

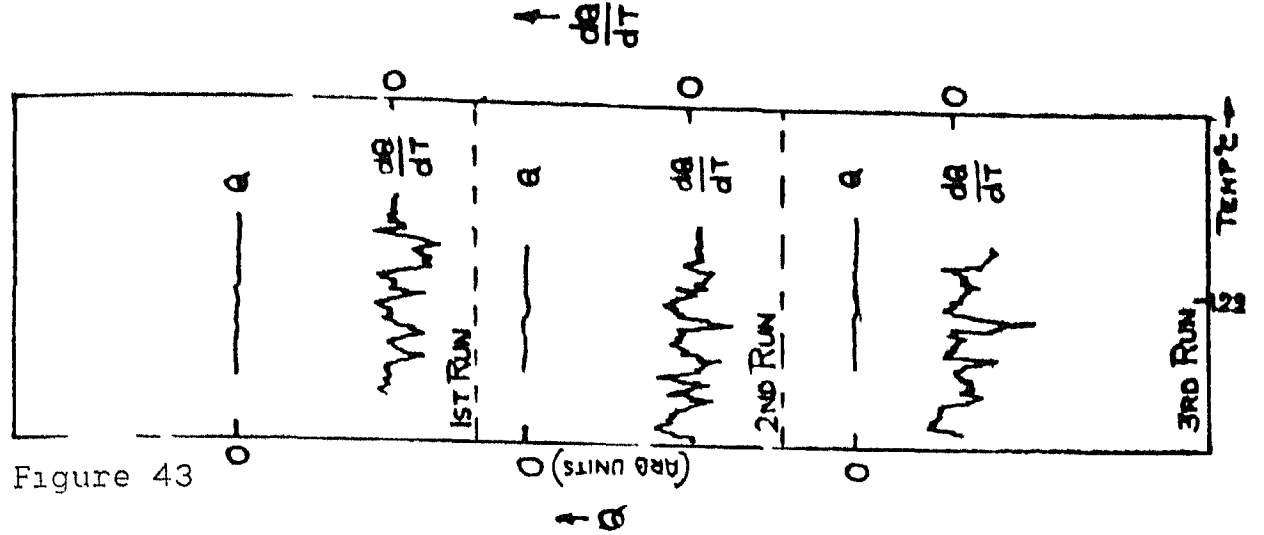

Figure 43

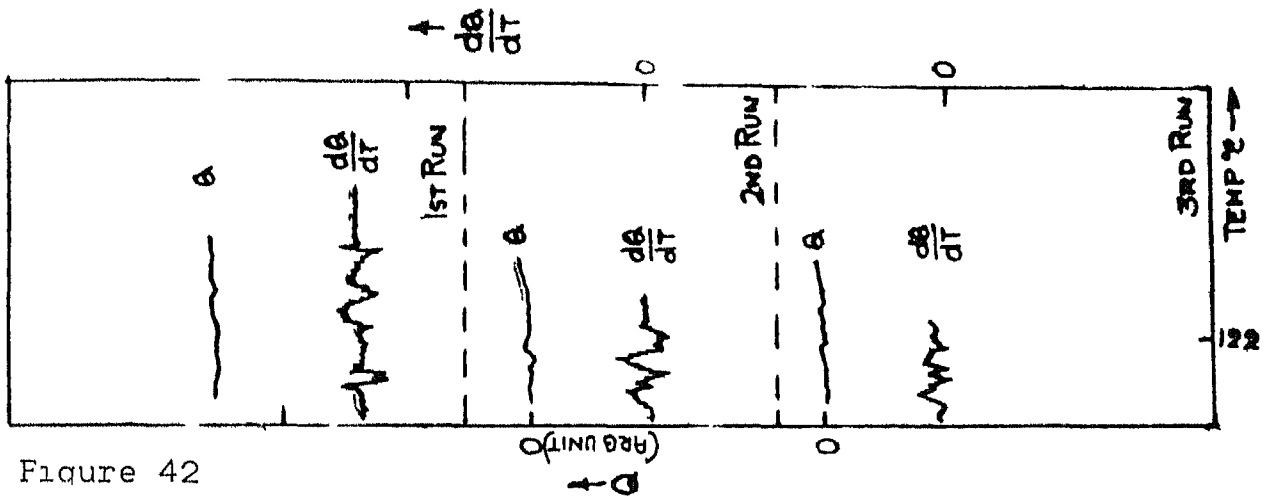

Figure 42

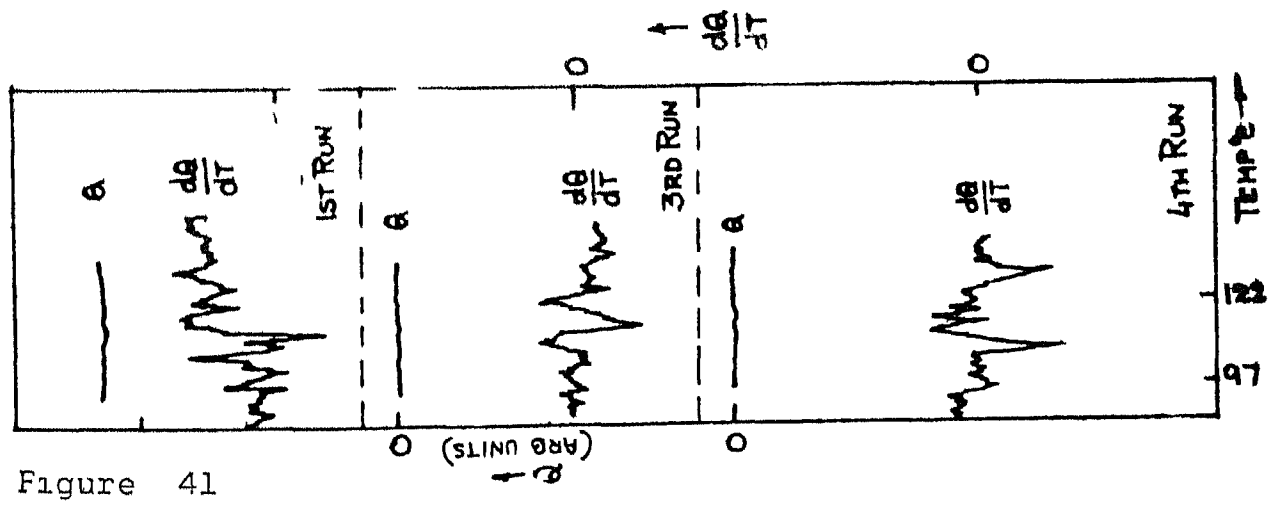

Figure 41

Figures 41 to 43 Third reversible change studies of
a) as melt spun / 1st, 3rd, 4th run samples- Fig 41
b) 310°C/25 min/1st to 3rd run samples-Fig 42
c) 310°C/60 min/1st to 3rd run samples -Fig 43 in DSC

Magnetic measurements for various samples

Curie temperature determination

Sample number and conditions	Experiment	Experimental and equipment conditions	Figure number
1) As melt spun	In single run from room temperature to 367oC	Room temperature = 22 5oC Field applied =50 Causs Weight= 0 0052 gm Moment measured in scale = EMU Full scale (X1)	44
2) As after (1)	In single run from room temperature to 380oC	same as above	45
Magnetization measurements			
3) As melt spun	-	Room temperature = 22 5oC Weight = 0 0052 gm Moment measured in scale = EMU Full scale (X1)	46
4) As after (1)	-	same as above	47
5) As after (2)	-	same as above	48

The results are plotted as follows

X axis = Temperature in oC

Y axis = $\frac{\text{Moment}(\mu)}{\text{Weight of the sample}(gm)} = \frac{\mu}{g}$

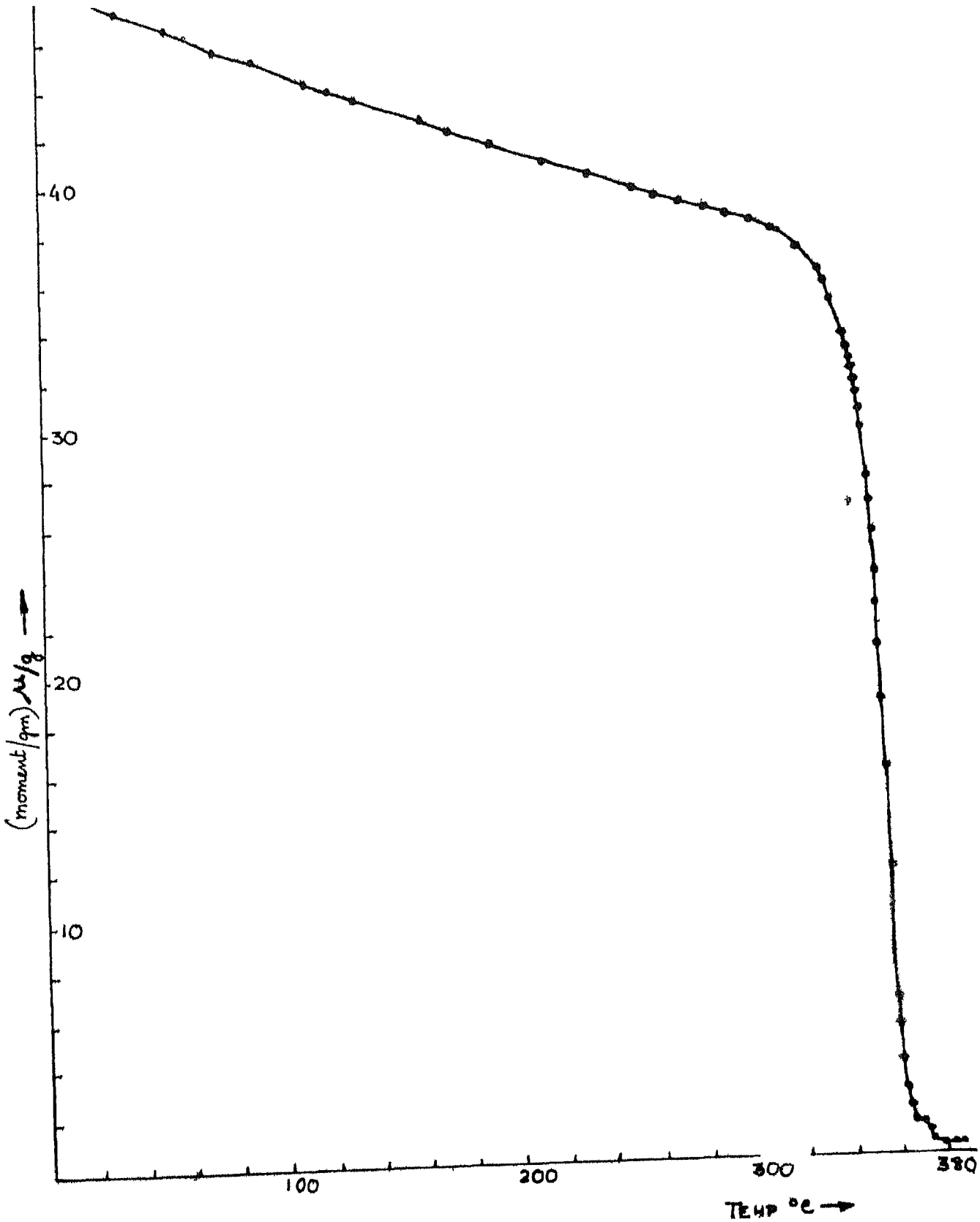

Figure 44 Curie temperature determination of 'as melt spun/ first run' sample

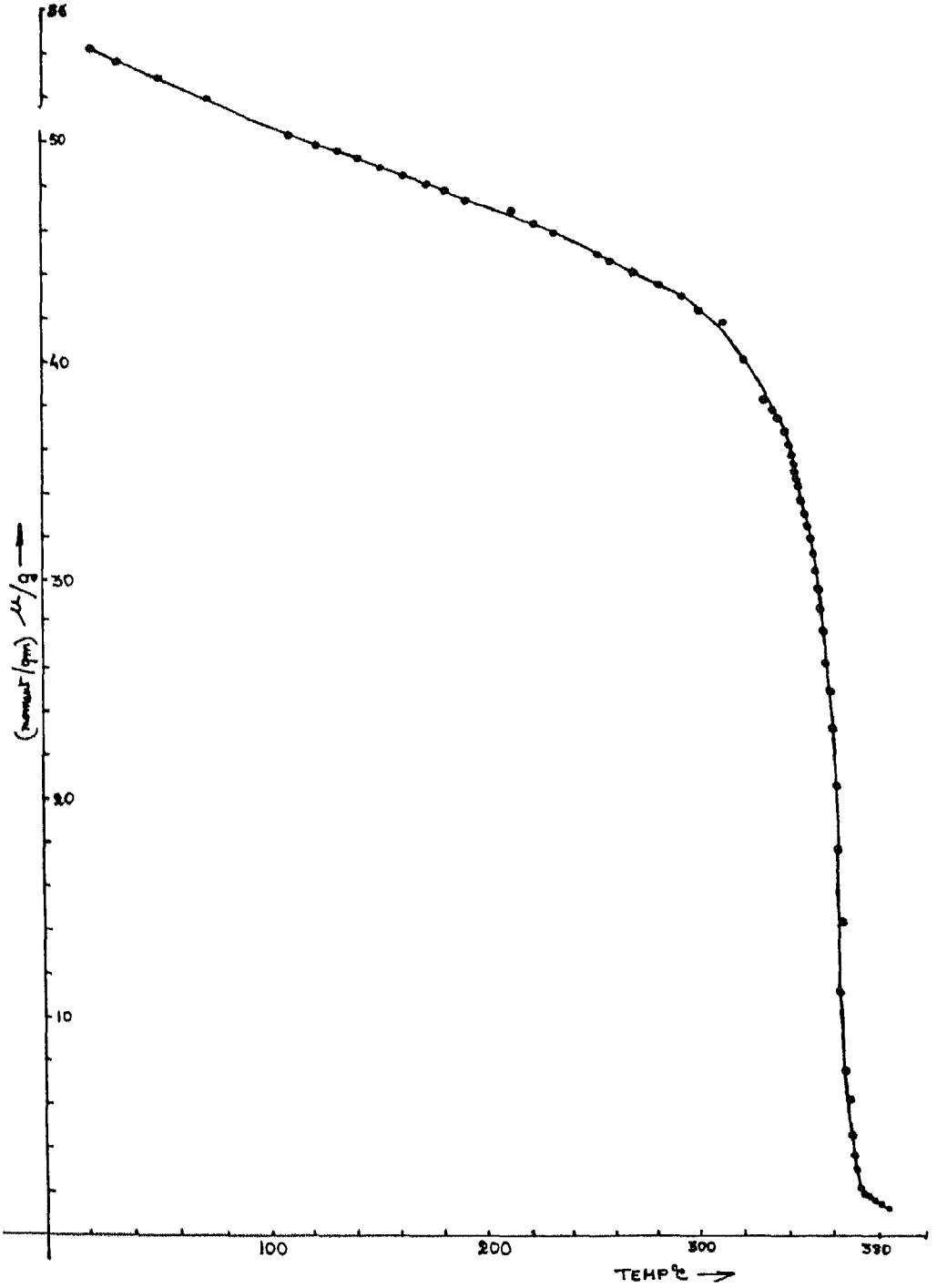

Figure 45 Curie temperature determination of 'as melt spun/ second run' sample

Figure 46 Magnetization studies of ' as melt spun' samples

Figure 47 M netization studies of ' as melt spun/' 1 rst ru)' sample

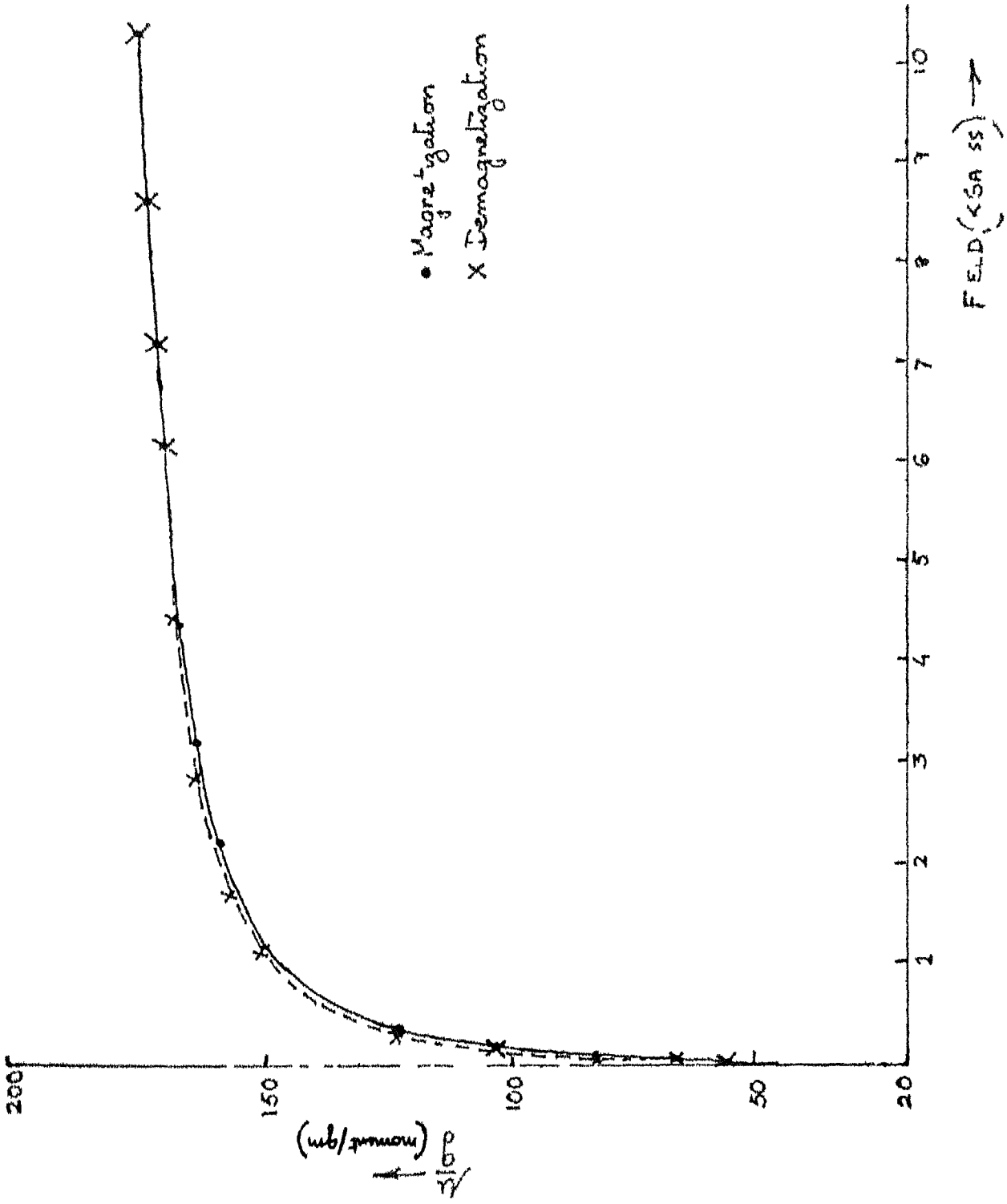

Figure 48 Magnetization studies of 'as melt spun/ second run' sample

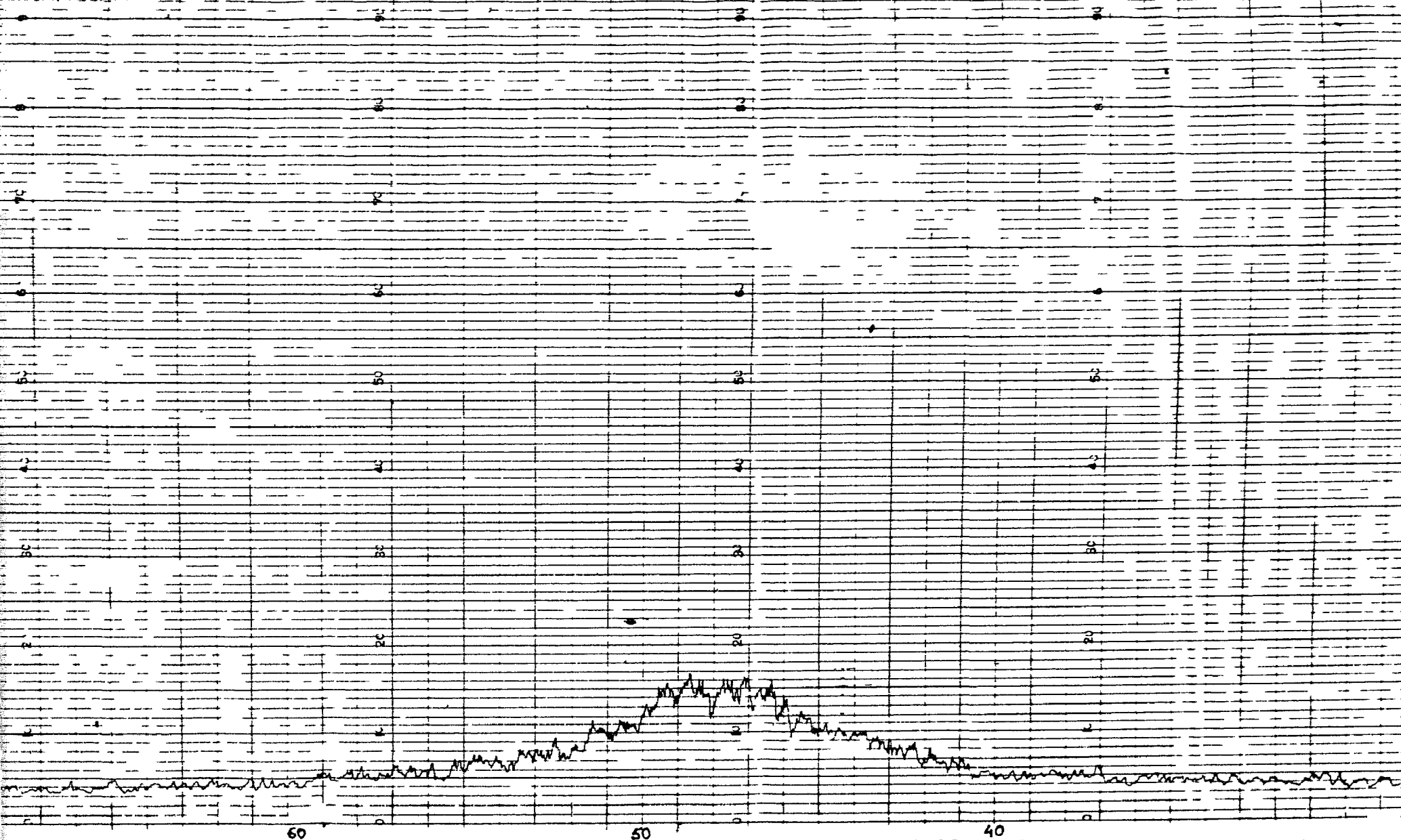

Figure 49 X-ray diffraction pattern of as melt spun metallic glass ribbon equivalent to Metglas 2605 Sc as prepared in laboratory (showing halo and port ons)

Figure 50 TEM diffraction pattern (SAD) and microstructure of as melt spun metallic glass ribbon equivalent to Metglas 2605Sc as prepared in laboratory

CHAPTER V

DISCUSSION

V 1 Fabrication of Metallic glass

To obtain an amorphous ribbon and also a deoxidized one, the time required to cool the molten metal to the final ' room temperature structure' should be as small as possible as well as the distance between molten metal and cool substrate And in the process, the important controlling parameters are the distance between chillblock and the nozzle, the amount of superheating as well as, in some cases, orifice geometry and even surface velocity of the wheel. Agarwal and Chakachary [10] hold the view that the lesser is the distance between the chill block and nozzle, the lesser is the chance of melt oxidation and freezing Our results also support this view Upto a distance of 2 mm, the chances of ribbon production without oxidation is better while at a higher distance, namely 4 mm, results in completely oxidized ribbon. However, Agarwal and Chakachary [10] proposed an optimum distance of 1 mm, while our experiments show that amorphous, deoxidized ribbons can be obtained even upto a distance of 2 mm

The fact that the path difference between the chill block and molten metal should be as small as possible also finds expression in orifice geometry In nozzle (2) (Fig.17) the orifice extends upwards thereby increasing the

distance between chillblock and nozzle That may be one of the reasons why the nozzle is not suitable for melt pinning

The results (see Chapter IV 1) show that if no superheating is applied to the material, as is evident from the case of melt cooling from the melting temperature of the alloy, partly crystalline ribbons are formed Whereas there will be some upper limit in the amount of superheat above which crystalline material again forms The results can be rationalized as follows Enough superheating is required to compensate for the cooling of the alloy during its pass age through the relatively cold part of the nozzle and the air gap between nozzle top and cold substrate On the other hand, at the highest limit, since the dwell time of the substrate is short and fixed for a fixed speed, the ribbons are not cooled below the temperature of glass formation and are ejected from the surface Thereby they will follow the natural air cooling, resulting in the formation of crystalline product.

The same rationalisation can be done when the surface speed of the cold substrate is very high. For example, the results (Table 6 in Chapter IV 1) show that at a high surface speed corresponding to 270 volts, crystalline material formation takes place.

The jet turbulence of the molten metal jet seems to be an important factor in determining whether

uniform, continuous ribbons can be obtained or not It is found that the nozzles where the angle with the horizontal (Table 2 of Chapter IV 1) is varied from 60o to 80o even edge continuous ribbon formation is taking place Whenever the angle is too low, for example 35o, or too high, for example 8°o, uneven and discontinuous ribbon formation takes place

Nozzles with serrations, i e nozzle (3), (Fig. 17 of Chapter IV 1), nozzles where the orifice does not extend full distance lengthwise i e nozzle (4) (Fig 17) probably cause turbulence, resulting in uneven ribbons having holes and cracks From the results of Table 3 (Chapter IV 1), it can be observed that there is a limit of ejection pressure below which uneven and discontinuous ribbon formation takes place However, after an upward value, no further effect of increasing pressure is observed This view is also supported by Huang (Fig 3) [11]

As is expected increasing suiface velocity results in docreasing the thickness of the ribbon produced.

The above discussion shows that the time required to cool the metal to glassy state is an important factor to determine whether a deoxidized uniform and continuous amorphous metallic glass ribbon will be obtained Also the jet turbulence probably plays an important part in determining the physical characteristics of the ribbons

However further experimentation is required to show whether the above factors do affect the ribbon formation or not and if so to what extent

V 2 Characterization

The characterization of the general nature of the as fabricated metallic glass is done in two ways First the fabricated ribbons are examined by TEM and X-ray to find whether amorphous structure has been achieved or not The presence of the hallo characteristic of amorphous materials as well as the absence of any grains in the microstructural results of TEM (Fig.50) confirms that the amorphous state has been achieved Similarly in X-ray (Fig 49) the presence of the broad peaks suggest that the ribbons examined are amorphous in nature Secondly, the thermal stability of metallic glasses so obtained is studied with different types of experiments as discussed in the Experimental Procedure (Chapter II) and the results obtained (Chapter IV) are discussed as follows

i) Structural relaxation

The literature survey shows that the as obtained Metglas 2605SC crystallizes giving rise to thermal effects in the temperature region at least above 330oC (Chapter II 2) As discussed in the literature survey, the changes occurring in the low temperature region can be considered to be due to atomic rearrangements arising out of the highly disordered

and metastable states of the amorphous alloys These changes are attributed to TSRO or CSRO (Refer II 3) Fig 32 to 34 shows the effect of one or more thermal cycling on as melt spun and heat treated specimens of the prepared Fe-B-Si-C alloy Fig 32 shows that a broad exothermic peak appears in the first run of the as melt spun sample in the range of ~160oC and ~330oC in the first heating itself But after this first run of followed by furnace cooling to room temperature is completed, subsequent runs do not show the presence of this broad exothermic peak Of the two possibilities of low temperature changes, TSRO and CSRO, only TSRO is irreversible, hence the disappearance of this peak in the second and subsequent runs suggest that the changes occurring in between ~160oC to ~330oC are due to structural relaxation of the specimen because of TSRO

The trace of Fig 33 has been obtained with Y axis (Q) ten times more sensitive than that in Fig 32 If the peak heights are considered to approximately give the intensity of thermal effect, the preheattreated specimen of Fig 33 shows somewhat less thermal effect than the as melt spun sample in Fig 32 Fig 33 also shows that the heat treated sample has no more thermal effect after the first run, as that of Fig 32 The observed small rise in the upper level of temperature in the second or subsequent runs are due to base line characteristics of the apparatus at

the high sensitivity level It is surprising that inspite of the 25 minute isothermal anneal at 310oC given to the sample of Fig 33, the specimen does not go through complete structural relaxation Whereas the same sample, after even a single thermal recycling through ~ 320oC, almost completely structurally relaxes (Fig 33) This severe effect of thermal cycling is also found for as melt spun specimens (Fig 32) The question comes to mind is why 25 minute isothermal annealing at high temperature (at 310oC) followed by very slow cooling (sample withdrawn from hot zone to room temperature in 24 hours) would not relax the sample more easily and effectively then the dynamic heating (at the rate of 10°C / min) upto ~ 320oC followed by comparatively quick furnace cooling in the DSC apparatus (approximately about three quarter of an hour to come down to 50°C) Further work is necessary in detailed to understand this behaviour

The relaxation studies of 310oC/60 minute annealed sample (Fig 34) shows that this isothermal heat treatment causes almost complete structural relaxation as the broad exothermic peak is absent in the first run itself From this result it can be qualitatively said that the effect of one thermal recycling is somewhere in between but at least greater than 25 minutes but less than 60 minutes isothermal annealing of a sample at 310oC

4) Crystallization

The crystallization behaviour of the metallic glass of present study by electrical resistance are shown in Fig. 18 and 19 The general nature of the shape of the curve obtained in the study of change in electrical resistance with temperature (Fig 18 and Fig 19) tallies well with the data obtained with Metglas 2605Sc by Bhanu Prasad et al([19] and Fig 8) but differ considerably in the temperature regions of transformations as well as in fine details The temperature regions of transformations observed in this investigation agree reasonably well with the different transformations determined by Sageusa and Moris [17,18] through Mossbauer spectroscopy Bhanu Prasad et al [19] have found that first a linear increase in electrical resistivity (Fig 8) occurs followed by a rapid and continuous decrease in electrical resistivity which starts at around 452oC The decrease in electrical resistivity is followed again by a uniform increase of resistivity starting at around 535oC The decrease in electrical resistivity from 452oC has been correlated with crystallization and the next increase in electrical resistivity from 535oC is correlated with the normal increase in electrical resistivity of the crystallized product The present results suggest that both for the as melt spun sample heated to crystallization (Fig 18) and for the as melt spun sample heated to 300oC followed by furnace cooling to room

temperature and then heated to crystallization (Fig 19), the crystallization start and finish occur at much lower temperatures (~ 390oC to ~ 500oC for the former and ~ 350oC to ~ 486oC for the latter). It is also seen that unlike the results obtained by earlier investigators [19], electrical resistance does not decrease in a continuous fashion but in steps An arrest in the decrease in electrical resistance at ~ 460oC occurs for both the samples studies (Fig. 18 and Fig 19) Moreover, an additional arrest appears in the temperature range of 383oC and 400oC for the heat treated sample (Fig 19) Crystallisation temperature range of the as melt spun first run sample correlates more closely with the start and finish of crystallization temperatures of the as melt spun alloy data reported by Sageusa and Moris [17,18] One possible reason as to why there is so much discrepency in the results obtained by Bhanu Prasad et al (19) and others on the one hand and Saegusa and Moris [17,18] and the present investigation on the other is possibly due to the presence of microscopic variations in composition, variation in the state of stress present in the material etc

Comparision of the crystallization of - melt spun sample (Fig 18) and as pre heat treated sample subjected to one thermal recycling through ~300oC followed by crystallization (Fig 19) shows interesting changes

has been found by the structural relaxation discussion of the present study (Chapter V 1), that a dynamic heating to a temperature of ~ 300oC followed by furnace cooling structurally relaxes a sample almost completely Hence the sample whose electrical resistance graph has been shown in Fig. 19 can be considered to be almost completely structurally relaxed whereas the as melt spun sample of Fig. 18 is not The enhancement of start and finish of crystallization of the former (Fig 19) by ~ 15o to ~ 35oC shows that the structural relaxation helps in enhancing the crystallization process

In interpreting their results obtained through Mossbauer spectroscopy Sageusa and Moris [17,18] have argued that the amorphous state instead of changing directly to final crystallised products passes through a series of intermediate states occuring in the temperature range of ~ 432o and ~ 457oC The present results (Fig 18 and 19) also shows a break in the electrical resistance vs temperature curve in the temperature range of ~ 436o and ~ 460oC and supports the interpretation of results of Sageusa and Moris Since no TEM and X-ray diffraction was done in the present investigation ,the product phases, however, could not be identified The thermally relaxed sample (Fig 19) also shows an additional arrest in the electrical resistance-temperature curve in the temperature range of ~ 383o and ~ 400oC The presence of this additional arrest suggest the showing up

of a finer change which was either obsecured by the rapid reaction occuring in the unrelaxed sample (Fig 18) or the occurence of a structural relaxation induced new intermediate state Further work using TEM and X-ray diffraction is necessary to throw light on the nature of this observed change

The crystallization behaviour of as melt spun specimen by DSC is shown in Fig 22 All the thermal effects (except the reversible changes discussed before) are exothermic and unlike Swartz et al ([16]and Fig 5), no endothermic reaction with a clear break in the DSC curve, due to magnetic transition of the specimen, can be seen

The first exothermic plateau occurs in the temperature region of about 316oC to 417oC and shows only a small thermal effect It is followed by an exothermic peak between $\sim$ 417oC to $\sim$ 500oC, termed as the first exothermic peak or first thermal effect and is followed by a very sharp thermal effect between $\sim$ 500oC and $\sim$ 540oC, called the second exothermic peak Finally a small thermal effect, smallest of the three and is called third exothermic peak, is observed above 540oC but it does not go to completion as the experiment was terminated at $\sim$ 600oC, the high temperature limit of the DSC apparatus. The nature of the exothermic peaks indicate that there are at least four distinct processes evolving

different quantities of heat and the reactions overlap each.

A specimen rapidly heated in the DSC aparatus within 15 to 20 minutes to 600oC follwed by 10 minutes of anneal is cooled to room temperature and then the DSC curve is traced (termed as 600oC/10 min/1st run) (Fig 25) A small thermal effect between ~433oC and ~499oC shows that complete crystallization has not occured in the sample even if it is heated to much higher temperature above the crystallization temperature Normally at a temperature higher than the crystallization temperature one should expect such a thin ribbon to crystallize completely in a short time

The nature of the DSC curves of the preheat treated specimens, 310oC/25 min/1st run (Fig 23) and 310oC/60 min/4th run (Fig 24) are very similar to the DSC curve of the as melt spun specimen (Fig 22), the exothermic peaks appear more or less at the same temperature regions However it is observed that the start of the exothermic reactions in Fig 24 appear at about 10 to 20oC lower temperatures than that observed in the other two cases (Fig 22 and Fig 23) From the discussion on structural relaxation, we have seen that annealing at 310oC for 25 minute does not relax the sample to a great extent as compared to the as melt spun/first run specimen In both the cases the temperature regions corresponding to the start and finish of each of the exothermic peaks are almost the same Hence we may

conclude that whenever two samples are more or less in the same structurally relaxed condition, as is the case of as melt spun/first run and 310oC/25 min/1st run samples, the crystallization behaviour remains more or less the same However from structural relaxation data, we have seen that the 310oC/60 min/4th run sample has complete structural relaxation When this sample crystallizes, we see that the temperature region corresponding to the start and finish of each peak is shifted somewhat to lower temperatures of approximately within 10 to 20oC This indicates that structural relaxation enhances crystallization Further evidence of this can be obtained if we compare the crystallization behaviour of as melt spun/first run (Fig 22) and fourth run (Fig 26) samples as also 310oC/25 min/1st run and 310oC/25 min/5th run (Fig 27) samples Enhancement of crystallization start temperature for completely relaxed specimen is also shown in electrical resistance data where as melt spun samples are taken to crystallization in first run (Fig 18) and second run (Fig 19) respectively The electrical resistance data also shows an enhancement of crystallization Hence comparing the structural relaxation data, electrical resistance data (Fig 18 and 19) as well as the DSC data (Fig 22 to 24), we conclude that recycling between room temperature to 320oC is more effective in enhancing the crystallization behaviour rather than isothermal annealing at 310oC for 25 minutes The most

important conclusion from these studies is that complete structural relaxation is obtained by even one cycle of heating to ~ 320oC to cause enhancement of crystallization process This also disproves the common belief that the as melt spun specimens become completely relaxed during heating before crystallization starts

In the above discussion only the gross changes observed due to different isothermal or dynamic treatments of the samples are pointed out There are certain fine changes in the DSC curves for the different samples too (Fig 26 and 27) In the DSC curves of as melt spun, 100oC/25 minute and 310oC/25 minute-all first runs (Fig 26) show that there are shoulders on the tailends of both the first and second exothermic peaks. Which indicate that the thermal effects observed are possibly not due to two single processes The discussion of crystallization behaviour of electrical resistance shows also a break in the electrical resistance in both Fig 18 and 19 at 460oC Both the electrical resistance as well as the DSC results support the view that crystallization does not follow a single or two step process but rather a multistep process Sageusa and Moris [17,18] also found by Mossbauer spectroscopy that Metglas 2605Sc is going through a series of multistep reactions during crystallization, forming metastable intermediate products and the amorphous phase continuously rearranging itself throughout the entire crystallization

process Hence the observations suggest that crystallization is a series of overlapping reactions

Preheat treatment as well as dynamic heating appears to affect not only the start and finish of crystallization but also appears to affect the shape of the peaks For example, comparison of the first exothermic reaction giving rise to a small plateu just before the first exothermic peak for the as melt spun/1st run (Fig 22) and 310oC/25 min/1st run (Fig 23) with those of 310oC/60 min/1st run (Fig.31), 310oC/60 min/ 4th run (Fig 24)and 310oC/25 min/ 2nd run (Fig 30) samples, shows that the starting of the plateu becomes more sharply defined for the heat treated specimens The fine structures in the DSC peak appear to be affected by heat treatment (Fig 26) The DSC curves of 1st and 5th run of 310oC/25 min samples (Fig 27) show some new variations in the DSC plots for structurally relaxed sample. The comparison of the as melt spun/first run (Fig 22) and as melt spun/4th run shows the presence of an additional peak in the temperature region of ~328oC to ~ 343oC This is however, not consistant with our observation of structural relaxation and its effect on crystallization. Since the completely relaxed specimen (310oC/60/min/ 4th run) (Fig 24) does not show any extra thermal effect in the corresponding temperature region, it is rather hard to explain why the as melt spun/4th run sample, which is also a completely relaxed specimen, should not have the

thermal effect Some spurious effect can not be ruled out and this is particularly suspected because this exprıment was carried out only once, whereas for all the others, the experiments were repeated at least twice From our electrical resistance plots we have seen that structural relaxation is throwing up new arrests during crystallization (Fig 18 and Fig 19) From this, we can possibly conclude that either structural relaxation is showing up clearly a reaction already present or some new reactions involving the formation of new intermediate states are taking place

One importan observation is that all the as melt spun samples, 100oC/25 min annealed samples, 310oC/25 min samples with or without one or more thermal recycling through a temperature below crystallization (<330oC) do not become brittle As the literature survey suggests (Chapter III 2) some glasses become brittle if subjected to some heat treatments below crystallization Davis [44] observed that there is a relation between the final crystallized product and the corresponding amorphous phase in the matter of brittleness Further identification with the final products in the present study may show whether the relationship extends to the present system too

iii) Reversible change

Figs 35 to 43 show three specific temperature regions of DSC thermogram for metallic glass samples with different heat treatments From both the Q and $\frac{dQ}{dT}$ plots,

it is apparent that there is a sharp and small endothermic dip in the temperature region of ~ 315oC to ~ 322oC (Fig 35 to 37) (termed 1st reversible change), another exothermic small and sharp change at a temperature region just above ~ 197oC (Fig. 38 to 40) (termed second reversible change) and most probably a third endothermic dip at a temperature region just below ~ 122oC (Fig 41 to 43) (termed third reversible change) The presence of the second and third reversible changes is also found in the electrical resistance temperature curve of the structurally relaxed sample as small decrease in electrical resistance in more or less the same temperature regions (Fig 21) These changes are reversible in nature and do not change their position when the samples are subjected to both isothermal and dynamic heat treatments and hence do not depend on the state of structural disorder (Figs 35 to 43).

There may be two kinds of reversible changes in metallic glasses One is the expected magnetic change due to Curie temperature transformation Any of the observed changes are not due to the magnetic transformation The prepared specimens show T_c of 352oC for unrelaxed samples and 368oC for relaxed samples The reason why it is not possible to observe the reversible magnetic change in DSC traces is that these values of Curie temperature falls within the temperature region where an exothermic change has been observed.

The literature suggests that the nature of the changes obtained tallies well with that of CSRO In some cases of the unrelaxed first run specimens, these changes are not shown up clearly This is probably because of the camouflage of such small changes by structural relaxation However in second or subsequent runs the changes show up more clearly The possibility of such camouflaging in electrical resistance had been suggested by Ballanzat et al and others [33] Hence they had suggested further studies by different methods particularly calorimetric tests to detect such changes. The fact that the other investigators who worked with the as obtained Metglas 2605SC [16 to 19] did not find these changes in electrical resistivity, DTA or DSC measurements may also be because of the structural relaxation The results of electrical resistance(Fig 21)also shows the changes in electrical resistance corresponding the second and third change in DSC The first change can not be detected by electrical resistance is because no such experiment has been done in that temperature narrow Whether these changes, which are occuring in very narrow temperature regions, are due to CSRO requires to be further investigated

iv) Magnetic properties

Curie temperature determination studies have been carried out with as melt spun ribbons (Fig 44) and ribbons relaxed by a cyclic heating of few degrees of centigrade per minute upto~367oC followed by furnace cooling in air in

The results show an increase in Curie temperature by about 110C for the structurally relaxed sample (Fig 45) than that of structurally unrelaxed sample T_c is 352oC (Fig 44) Since structural relaxation of specimen increases T_c and the T_c of the specimen lies in the temperature range in which crystallisation appears to have started, it is possible that the T_c of unrelaxed sample is not of the lowest limit value

The Curie temperature obtained in this investigation is considerably different from that reported by other researchers [16 to 19] Even the values of T_c given by Sagousa and Moris [17 and 18], whose results in case of crystallization is talying closely with us, is very different This probably is because of microscopic difference in composition for different samples However the general idea that structural relaxation or TSRO enhances Curie temperature is supported by the findings of present study. The magnetization and demagnetization curves obtained by the present study for as melt spun (Fig 46), as melt spun after 1st run (Fig 47) and as melt spun sample with two thermal cycles (Fig 48) show that the that the sample follows the general characteristics shown by soft magnetic materials However, they do not reach the saturation even after a high field But the structurally relaxed sample (Fig.47 and Fig 48) shows a high value of moment per gram with a small field than the structurally unrelaxed sample

(Fig 46) But onece the structural relaxation is achieved, subsequent thermal cycling do not produce any further effect as is evident from Fig 47 and 48

CHAPTER VI

CONCLUSION

The preparation an characterization of Metglas 2605Sc show the following

i) The process of preparing reasonably wide (6 to 7 mm) ribbons by single roller melt spinning process has been developed and standardized.

ii) The range of different process parameters on the preparation of ribbons has been established The time and temperature path difference between the molten metal state and the final amorphous state is important in achieving an amorphous structure and the jet turbulence of the molten metal decides the physical characteristics or the ribbon It is difficult, under existing conditions, to get an amorphous state from the liquidous temperature only and some superheat is found to be necessary

iii) The amorphous to crystalline transformation seems to be the net effect of a series of overlopping reactions The alloy is rearranging itself throughout the transformation region through a series of steps, probably precipitating intermediate products This continuous rearrangement extends not only at the finish of crystallization, but well bevond

to it

iv) Structural relaxation enhances crystallization by enhancing the start and finish of crystallization temperature It also shows up additional variations in calorimetric and electrical resistance tests indicating either old reactions camouflaged by structural disorder are showing up or crystallization takes a slightly different path for structurally relaxed sample

v) The thin metallic glass samples structurally do not relax much when compared to as melt spun samples upto an isothermal anneal of 310oC and 25 minute severity whereas an isothermal anneal at 310oC for 60 minute relaxes it completely

vi) One dynamic thermal recycling with a few degrees per minute of heating rate through a temperature near but not far below crystallization start almost completely structurally relaxes a sample Hence the effect on structural relaxation of an dynamic annealing is equivalent to an isothermal anneal at 310oC for a time not less than 25 minute but not greater than 60 minute

vii) The as melt spun thin samples do not crystallize completely even after annealing to a temperature higher than crystallization temperature for several minutes,

viii) The ductile as melt spun ribbons do not lose their ductility even after isothermal annealing (upto 310oC) for some time (25 minutes) and / or subjected to one or more

thermal cycling through a temperature below crystallization starting temperature

ix) The presence of CSRO changes in this composition has been detected The detection has been done by electrical resistivity and particularly calorimetric tests. There are more than one but two and most probably three CSRO changes in the alloy below crystallization

x) Structural relaxation enhances Curie temperature and eases magnetization process

REFERENCES

1 D Pavuna, J of Mat Sc , 16 (1981) 2419

2. S Kavesh, Metallic Glasses- American Society for Metals Metals Park, Ohio 44073, USA, 36

3 H A Davis, Phys and Chem of Glasses, (1976) 17

4 H A Davis,J Aucote and J B Hull, ' Nature'- Phys Sc 13 (1973) 246

5 H A Davis, and B G Lewis, Scripta Metall 9 (1975)1107

6 H S Chen, Acta Metall.22 (1974) 1505

7 H H Liebermann, Mat Sc Engg 43 (1980) 203

8 D Pavuna, J Non Cryst Sol 37 (1980) 133

9. D Pavuna, J Non Cryst. Sol 37 (1980) 417

10. D.C Agarwal and E A Chakachary, Bulletin of Mat Sc 7, No.2 (July, 1985) 137

11 S. Huang, Proc. 4th Int Conf on Rapidly Quenched Metals,The Japan Institute of Metals,1 (1982) 65

12. U. Koster and U Herold, Topics in Applied Physics, 46, H J. Gunterford and H. Beck ed , Springer and Verlag (1981) 225

13 S Ranganathan and S Banerjee, Metallic Glasses, T R Anatharaman ed, Trans Tech Publication (1984) 147

14. U. Herold and U Koster, Proc. 3rd Int Conf on Rapidly Quenched Metals, The Metals Society London (1978) 81.

15. U Koster and U Herold, Topics in Applied Physics, 46, H J. Gunterford and H Beck ed, Springer and Verlag (1981)253.

16 J C Swartz, R Kossowsky, J J Haugh and R F Crause, J. Appl Phys 52 No 5 (May 1981) 3324

17 N Sageusa and A H Moris, Phys Review B, 27,No 7 (April, 1983) 4027

18 N Sageusa and A H Moris, Phys Review B, 26, No 1 (July 1982) 305

19 B Bhanu Prasad, A K. Bhatnagar and R Jagannathan,J Appl Phys 54,No 4 (April 1983) 2019

20. C E Violet and D N Pipkorn, J Appl Phys 42 (1971)4339

21. M Goldstein, Modern aspectsof the vitrious state, J D Mackenji ed Buttersworth Washington (1960)Vol 3, 90

22. S E Petrie, Polymorphic Materials, ASM ed (1975) 55

23 A J Kovaes, R A Stratton and J D Ferry, J Phys Chem 6-7 (1963) 152.

24. T Egami, J of Mat Sc 13 (1978) 2587-2599

25 M H Cohen and D Turnbull, J. Chem Phys 31 (1959) 1164

26. R Madin and T Masumoto, Mat Sc Engg 9 (1972)153

27. R. Williams and T Egami, IEEE Trans Mag Mag 12 (1976)927

28. T. Sochiroda, M Kavira and T. Masumoto, J Non Cryst Sol . 21 (1976) 688

29. H.H Liebermann, C D Graham Jr and P J Flanders,IEEE trans. Mag Mag 13(1977) 1541

30. E. Ballanjat,Scripta Metall 14 (1980) 173

31. A.V.D. Boukel and S. Radelaar, Acta Metall31 (1983) 419

32. T. Egami, Mat Res. Bull 13 (1978) 557-62

33 E Ballanjat, J T Stanley, C Mairy and J Hillbert , Acta Metall 33 No 5 (1985) 785

34 J M Zimin, Phil Mag 6 (1961) 1013

35 T Egami, Mat Res Bull 13 (1978) 557

36. H S Chen, Proc 4th Int Conf on Rapidly Quenched Metals, The Japan Institute of Metals, 1 (1982) 495

37 K.F Kelton and F Spapean, Proc 4th Int Conf on Rapidly Quenched Metals, The Japan Institute of Metals, 1 (1982) 527

38 C.P.P. Chau and D Turnbull J Non Cryst Sol 17 (1975) 169

39 F E. Lubrosky, J J Backer, and R O McCary, IEEE Trans Mag Mag 11 (1975) 1644.

40. S.S. Chen, R.C Sherwood and E M Greorgy, IEEE Trans Mag. Mag 13 (1977) 1538

41. T Egami and R J Flanders, AIP Conf Proc 29 (1976)220

42. F E. Lubrosky, R O McCary and J J Beker, Proc 2nd Int Conf on Rapidly Quenched Metals,MIT (1975)

43 J.L. Waller, F Baco and F E Lubrosky, Mat Sc Engg. 24 (1976) 239

44. G Hunger, K.D Ward and H A. Davis, Zeitschrift fur Metallkunde 70 (1979) 714.

45. T. Mihara, S Otake, H Fukushima and M Doyama, J Phys F 11 (1981) 727